Synthesis of Master Batch from Modified Gum Arabica and Modified Euphorbia Trigona Mill for Development of Poly (Lactic Acid) based Bio Composite

Kasahun Tsegaye Mekonnen

A Thesis Submitted to

The Department of Chemical Engineering

School of Mechanical, Chemical & Material Engineering

Presented in Partial Fulfillment of the Requirement for the Degree of Master's

in Chemical Engineering (Specialization in Process Engineering)

Office of Graduate Studies

Adama Science and Technology University

September 2022

Adama, Ethiopia

Synthesis of Master Batch from Modified Gum Arabica and Modified Euphorbia Trigona Mill for Development of Poly (Lactic Acid) based Bio Composite

Kasahun Tsegaye Mekonnen

Advisor

Melaku Tesfaye (Ph.D.)

Co- Advisor

Mulugeta Yilma (Ph.D.)

A Thesis Submitted To

The Department Of Chemical Engineering

School Of Mechanical, Chemical, Material Engineering

Presented in Partial Fulfillment of the Degree of Master's in Chemical Engineering

Office of Graduate Studies

Adama Science and Technology University

September 2022

Adama, Ethiopia

DECLARATION

I hereby declare that this Master Thesis entitled **"**Synthesis of Master Batch from Modified Gum Arabica and Modified Euphorbia Trigona Mill for Development of Poly (Lactic Acid) based Bio Composite" is my original work. That is, it has not been submitted for the award of any academic degree, diploma, or certificate in any other university. All sources of materials that are used for this thesis have been duly acknowledged through citation.

Kasahun Tsegaye Mekonnen	_____	_____
Name of the student	Signature	Date

RECOMMENDATION

We, the advisors of this thesis, hereby certify that we have read the revised version of the thesis entitled “Synthesis of Master Batch from Modified Gum Arabica and Modified Euphorbia Trigona Mill for Development of Poly (Lactic Acid) based Bio Composite” prepared under our guidance by Kasahun Tsegaye submitted in partial fulfillment of the requirements for the degree of Masters of Science in Chemical Engineering. Therefore, we recommend the submission of the revised version of the thesis to the department following the applicable procedures.

Melaku Tesfaye (Ph.D.)	_____	_____
Major advisor	Signature	Date
Mulugeta Yilma (Ph.D.)	_____	_____
Co-advisor	Signature	Date

APPROVAL PAGE

We, the advisors of the thesis entitled **"**Synthesis of Master Batch from Modified Gum Arabica and Modified Euphorbia Trigona Mill for Development of Poly (Lactic Acid) based Bio Composite" and developed by Kasahun Tsegaye, hereby certify that the recommendation and suggestions made by the board of examiners are appropriately incorporated into the final version of the thesis.

Melaku Tesfaye (Ph.D.) _____ _____
Major Advisor Signature Date

Mulugeta Yilema (Ph.D.) _____ _____
Co-advisor Signature Date

We, the undersigned, members of the Board of Examiners of the thesis by Kasahun Tsegaye have read and evaluated the thesis entitled Synthesis of Master Batch from Modified Gum Arabica and Modified Euphorbia Trigona Mill for Development Poly (Lactic Acid) Bio Composite and examined the candidate during the open defense. This is, therefore, to certify that the thesis is accepted for partial fulfillment of the requirement of the degree of Master of Science in Chemical Engineering

_____ _____ _____
Chairperson Signature Date

_____ _____ _____
Internal Examiner Signature Date

_____ _____ _____
External Examiner Signature Date

Finally, approval and acceptance of the thesis is contingent upon submission of its final Copy to the Office of Postgraduate Studies (OPGS) through the Department Graduate Council (DGC) and School Graduate Committee (SGC).

_____ _____ _____
Department Head Signature Date

_____ _____ _____
School Dean Signature Date

_____ _____ _____
Office of Postgraduate Studies, Dean Signature Date

ACKNOWLEDGEMENT

First of all, I would like to thanks GOD Almighty, who has granted countless blessing, wisdom, peace of mind and opportunity to study my MSc. and finally, I was able to accomplish this thesis. This thesis becomes a reality with the kind support and help assistance of many people. I would like to express my heartfelt gratitude to each and every one of them. I wish to convey my profound gratitude to my advisor Dr. Melaku Tesfaye for his intellectual guidance, valuable advice on doing the experiments and preparing my thesis. I am also grateful to my Co-Advisor Dr. Mulugeta Yilma for his unfailing assistance and very valuable comments on this thesis. Thanks to my families, for the numerous times they have helped me throughout my journey in University as well as work; I believe that all of their efforts will gain something great in the near future. When times were tough, their encouragement, financial assistance, and constant prayer were much welcomed and acknowledged.

Finally, I owe particular thanks to my friends and ASTU Classmates for their help and encouragement

TABLE OF CONTENTS

List of Tables

List of Figures

LIST OF ACRONYMS AND ABBREVIATIONS

13C-NMR	13C-NMR Carbon Nuclear Magnetic resonance
1HNMR	1HNMR Hydrogen Nuclear Magnetic resonance
DSC	Differential scanning calorimeter
ETML	Euphorbia Trigona Mill latex
FTIR	Fourier Transmission Infrared Spectroscopy
F-W-O	Flynn-Wall-Ozawa
GA	Gum Arabica
HDPE	High density polyethylene
K-A-S	Kissinger-Akahira-Sunose
LA	Lactic Acid
LDPE	Low density polyethylene
OM	Optical micrographs
PBAT	Poly(butylene adipate-co-terephthalate)
PC	Polycarbonates
PE	Polyethylene
PEG	Poly (ethylene glycol)
PLA	Poly (lactic acid)
RBF	Round Bottom Flask
ROP	Ring opening polymerization
OLLA	Lactic Acid Oligomer
OLLA-g-ETML	Lactic acid grafted Euphorbia Trigona Mill latex
OLLA-g-GA	Lactic acid grafted Gum Arabica
TGA	Thermogravimetric Analysis
UTM	Universal Testing Machine

Notations

A	Pre-exponential factor
Ea	Activation energy
Eav	Average activation energy
K	Avrami kinetic constant
R	Universal gas constant
R2	Correlation coefficient
T50	Temperature at which 50% mass loss of sample (oC)
Tc	Crystallization temperature
To	Onset degradation temperature
Tg	Glass transition temperature
Tm	Melting temperature
Tp or Tmax	Temperature for maximum rate of mass loss (oC)
To	Onset decomposition temperature
Xc	Degree of crystallinity
α	Conversion of biomass (mass %)
β	Heating rate (oC min-1

ABSTRACT

Environmental pollution caused by the widespread use of petroleum based polymers brought the need to replace the petro-based polymers with bio based polymers made from renewable resources due to their degradability. Among these, Polylactic acid (PLA) is a well-known biodegradable, biocompatible and sustainable polymer, derived from renewable agricultural sources. However, its wide range of applications (packaging) is constrained by low crystallization rate, poor mechanical properties and low thermal stability. The main aim of this research was to investigate the effect of modified gum Arabica (GA), euphorbia trigona mill latex (ETML) and its master batch on PLA properties.

In this context, this work demonstrates modification of both gum arabic and euphorbia trigona mill with lactic acid oligomer by in situ condensation polymerization. Effect of different reaction conditions such as; reaction temperature, mixing ratio and reaction time on grafting efficiency and percentage solubility of synthesized bio-conjugate have been investigated and grafting reaction was confirmed by FTIR and NMR. A modified gum Arabica, euphorbia trgona mill latex and master batch dispersed PLA (PLA/OLLA-g-GA, PLA/OLLA-g-ETML and PLA/master batch) bio composite films were prepared by solution casting method. After incorporating modified gum Arabica, euphorbia trgona mill latex and master batch into the PLA matrix, the effect of modified gum Arabica, euphorbia trgona mill latex and master batch on the tensile strength, elongation at break, rate of crystallization, transmittance, thermal stability, and anti-microbial properties of PLA was investigated.

Surface morphology of different fillers loading dispersion in the PLA matrix was analyzed by optical microscopy. The ultraviolet-visible (UV-Vis) result implies that the transmittance of neat PLA, PLA/OLLA-g-GA(3%),PLA/ OLLA-g-ETML(5) and PLA/ master batch bio composite film was 55.6%,25.2,27.4 and 64.76 at 600 nm, respectively, which indicates the decrement in transmittance. The antibacterial activities of PLA/OLLA-g-GA,PLA/ OLLA-g-ETML and PLA/ master batch bio composite film were evaluated against Gram-positive bacteria (S. pyogenes and S. aureus) and Gram-negative bacteria (E. coli and P. aeruginosa) and it was observed that a higher zone of inhibition which suggests the prepared films could be used as antimicrobial packaging materials.

The tensile strength was improved by 38.31, 10.47 and 47% with the addition of OLLA-g-GA (3%), OLLA-g-ETML (5%) and master batch (OLLA-g-GA (3%) OLLA-g-ETML(5%), respectively. The elongation at break also enhanced by 20.62 and 34% with the addition of OLLA-g-GA (3%), OLLA-g-ETML (5%) and master batch (OLLA-g-GA (3%) - OLLA-g-ETML (5%), respectively.

The results from DSC showed that after introducing the nucleating agents into PLA, the crystallinity in all samples was improved. The highest crystallinity at 45.83% was obtained from PLA /master batch. Effect of annealing time on degree crystallinity was also investigated. The thermogravimetry analysis (TGA) reveals that the thermal stability PLA after incorporating modified GA and ETML increased but with addition of master batch. Thermal degradation behavior of neat PLA and PLA/master batch films was investigated using different kinetics models. The activation energies of both neat PLA and PLA/master batch were estimated using isoconversiconal Augis & Bennet, Kissiger, Frediman(FD), Kissinger-Akahira-Sunose (K-A-S) and Flynn-Wall-Ozawa (F-W-O) method, the mechanism of thermal degradation was elucidated by Coats-Redfern method. The activation energy PLA/master batch bio-composite film was lower for all model compared to neat PLA.

Keywords

Bio-composite, Euphoria Trigona Mill, Gum Arabic, Master-Batch, OLLA-g-ETML, OLLA-g-GA, Poly (l-lactide).

CHAPTER ONE

1. Introduction

1.1. Background of the study

Demand for bio-polymer such as such as poly (lactic acid) (PLA) has increased recently to produce environmentally friendly, a renewable with high-performance bio-derived materials that helps to mitigate white pollution. PLA is the 21st century polymer that synthesized on a greater scale with its excellent properties like degradability, renewability, eco-friendly and biocompatibility biopolymers to substitute conventional polymers (Balla et al. 2021,Aaliya, et. 2021). It is the most studied aliphatic polyester for biomedical and packaging applications, due to its biocompatibility, biodegradability, clarity, modulus, and facile process ability through extrusion, injection molding or casting. Thermal stability and mechanical properties of PLA is higher than that of other biodegradable polymers like polycaprolactone, polyethylene glycol, poly hydroxyalkonate, and polyhydroxybuterate. Because of the above-mentioned properties, it is widely applicable in various industries such as textiles, food packaging, drug delivery, tissue engineering, and biological scaffolding (Avinc and Khoddami 2009; Donate et al. 2020; Fattahi et al. 2019; Mullapudi et al. 2018; Tyler et al. 2016). Despite the above mentioned positive features and usage, the innate deficiencies like high stiffness, poor ductility, brittleness, slow crystallization rate and low deformation at break limited its usage in different engineering applications, and hence, it has yet to attain a strong commercial standpoint (Kaseem et al. 2017; Norazlina and Kamal 2015; Sha et al. 2016; Yiga et al. 2021).

Thus, there is the need to overcome the previously mentioned drawbacks of PLA and develop advanced materials for a variety of packaging and engineering applications by achieving durability. Different scientific approaches, such as copolymerization, polymer blending, and polymer compositing have been proposed by several research groups (Z. Q. Li et al. 2010; Sanivada et al. 2020; Su Shen, et al. 2019). Among them, the polymer compositing method, which includes the reinforcement of PLA with fillers or nanofillers to form PLA composite materials, has attracted tremendous interest as an easy and cheap method for promising materials with wide variety of applications. Accordingly, many fillers from organic (Fortunati et al. 2015; Li et al. 2013;Tesfaye et al. 2016; Tripathi and Katiyar 2016) and

inorganic (Gunasekera et al. 2016; Sayyar et al. 2017; Sinha et al. 2003)materials have been investigated to enhance the properties of PLA matrix.

Bio-fillers derived from plants and animals have attracted interest because they exhibit a variety of appealing qualities while yet meeting requirement for degradability, compatibility, availability and ease of process ability that makes them perfect for selection within the creation of green composites. From these domains of bio-fillers, cellulose, chitosan, gum, starch natural rubber and sucrose palmitate have been studied as nontoxic reinforcement for PLA matrix (Ecker et al. 2019; Gao et al. 2017; Lu et al. 2016; Masek and Cichosz 2021; Pal and Katiyar 2017b; Xie, Zhang, and Lin 2017). For example Renewable natural rubber (NR) as an effective toughening agent for PLA and its bio composites. It was found that the natural rubber significantly enhanced the tensile toughness of the PLA and the composites (Bitinis et al. 2012). Another work (Lu et al. 2016) increased the crystallization rate, and thus led to obvious enhancements of the mechanical performance and thermal stability of the PLA,by incorporating spherical nanocellulose formates (SCNFs) into a PLA matrix. Compared to pure PLA, 130% and 116% improvements for the tensile strength and Young's modulus can be obtained for the resulting nanocomposite with 10 wt% SCNFs, respectively, and the initial degradation temperature (T^0) and maximum degradation temperature (T_{max}) increased by 17.4 and 21.5^oC, respectively. PLA based composites were manufactured by combining cellulose nanocomposites (CNCs) master-batches and PLA resin using twin screw extruder followed by injection molding. Degree of crystallinity of PLA exhibited a major enhancement by 14.7% and 38.0% in solvent cast and spin-coated composites, respectively (Shojaeiarani, et.al.2018).

Polysaccharide gums are natural biopolymer, which are abundantly available in nature. These gums find tremendous industrial applications in various fields due to their renewability, non-toxicity, and biodegradability. Among polysaccharide gums, gum arabic is a naturally occurring polymer with important applications in food industry and cosmetic products. It is a non-toxic hydrophilic biopolymer in its natural form which has good emulsion and encapsulation properties (Al-akayleh et al. 2014). It can also be used as filler in polymer to produce bio- composite. However, the inability to successfully produce commercial composites due to gum arabica's low dispersibility and the low interfacial adhesion between gum arabica and PLA. Therefore some modifications in its structural is important to improve the dispersion with PLA matrix. Tripathi and Katiyar (2016) investigated the effect of lactic acid grafted-gum Arabic (LA-g-GA) on water and gas transmission rate (WTR) and (OTR) of PLA. It

was found that the reduction in WTR analysis for PLA/LA-g-GA (3%) and PLA/ LA-g-GA (5%) films was observed as 7% and 27%, respectively. A decrease of 10 fold in the OTR value was observed which was very significant improvement in the barrier property of the film, especially for using them as packaging films. Ali et al. (2010) evaluated the potential of GA in coating tomatoes for their shelf-life extension after postharvest storage. It was observed that tomato coated with 10% GA shows a significant delay in changes of weight, firmness, decay percentage, and color development compared to the uncoated fruit. The sensory evaluation proved that the above dose of GA maintains the overall quality of the vegetable during the storage period of 20 days at 20°C, without any spoilage and off-flavor. *Euphorbia trigona mill latex (ETML)* is a species of Euphorbiaceae family. Latex from Euphorbia trigona mill latex was use in antimicrobial and antifungal property (Deenen,et al. 2011). Literature survey reveals that none of the articles has demonstrated the blends of PLA and Euphorbia trigona mill latex for film preparation for packaging application. It might be due to incompatibility of neat PLA, which is hydrophobic whereas *Euphorbia trigona mill latex* is hydrophilic in nature and no examples are reported in the literature on the combination of ETML and GA on PLA films and how their synergic combination could affect the final performance of PLA films. In this study, lactic acid grafted (modified) GA and ETML were premixed in different master batches based on PLA matrix, with the aim to produce and characterize high performance PLA based bio-composites for packaging applications. Indeed, modification of both GA and ETML has been confirmed as effective solutions to improve the dispersion of these fillers in PLA and enhance the performance of resulted bio-composites. With the aim of evaluating their possible individual and synergic effects, OLLA-g-GA/PLA, OLLA-g-ETML and master batch PLA based bio-composite was prepared by solution casting method. Mechanical, optical, crystallization rate, thermal, degradation kinetics and antibacterial activity of the selected films pathogen were investigated.

1.2. Statement of the problem

Conventionally used common polymers such as polyethylene, polypropylene, polystyrene, and poly (methyl methacrylate) are non-biodegradable and recycling or reusing them is a very challenging tasks (Sohn et al. 2020). In developing countries like Ethiopia, the production rate of plastic wastes is very much exceeding the plastic degradation rate, consequently presenting an ecosystem imbalance (Woldegiorgis. 2017). In this context, in Proclamation No. 513/1999, Ethiopia bans either producing or importing of plastic bags with thickness of less than 0.03 mm or any indecomposable plastic bag. However, the wide use and disposal of plastic bags still continues while posing an environmental challenge.

Therefore, to overcome the problem, there is a need to sequentially switch or replace petroleum-based plastics with bio- plastics to minimize the reliance on fossil-based resource as well as to contribute to an easier end of life disposal (Čolnik et al. 2020). PLA has recently raised wide interest as a potential replacement for petroleum-based polymers in different applications (packaging) due to its biocompatibility, degradability and good clarity. However, its substitution to commercial synthetic polymers has some serious challenges. Primarily, due to its brittleness, low thermal stability, and slow crystallization properties (Tripathi et al.2021).

Thus, PLA based bio composites are changing the research activities carried out in the scope of material engineering because a number of beneficial properties, such as improve crystallization rate, lightweight, low energy consumption, usability, toughness. Different researcher enhanced particular properties of PLA with different type's fillers, even though all the drawback of PLA did not improved with single fillers at once. Therefore, in this thesis master batch which was prepared from modified euphorbia trigona mill and modified gum Arabica which have a synergic effect was used to fabricate poly (lactic acid) bio composite to enhance mechanical, crystallization, and anti- microbial properties of PLA films for packaging application.

1.3 Research questions (RQ), hypothesis and choice of systems

Research questions: The present research work aims to answer the following major research questions

RQ1. Is it possible to synthesizes lactic acid grafted ETML to convert hydrophilic ETML into hydrophobic, which can be applied as polymer filler?

RQ2. What would be the effect of temperature, reaction time and mixing ratio on the percentage solubility and grafting efficiency of modified GA?

RQ3. What role that modified ETML and modified GA can contribute in enhancing the properties of PLA?

RQ4. Can it be possible to synthesis OLLA-g-ETML-OLLA-g- GA /PLA based bio composite that can be ideal candidate for traditional or conventional polymers with good mechanical, crystallization and thermal properties?

From the above research questions the choice of the systems, methodology and characterization techniques are framed as follows:

- Poly (lactic acid), modified GA, ETML and master batch are selected as a base on:
  - PLA is the most extensively researched and utilized biodegradable, biocompatible and renewable aliphatic polyester that have a potential either to replace conventional petrochemical-based polymers for industrial applications or as a leading biomaterial for numerous applications in medicine, packaging fields.
  - Master batch (modified GA and ETML) selected due that fact both GA and ETML are renewable resources, non-edible and biodegradable. Modification GA and ETML by grafting with lactic acid made compatible with PLA as PLA property enhancing agent.

Thesis Hypothesis

The research is based on the scientific hypothesis that:

1. The modified gum arabic and euphorbia trigona mill latex and its master batch will uniformly disperse in the PLA matrix.
2. Incorporating modified *gum arabic* and *euphorbia trigona mill* and its master batch into PLA can improve PLA performance characteristics.

1.4. Objectives and hypothesis of the study

1.4.1. General objective

The major objective of this Research is to synthesis of master batch of modified Gum Arabica and Euphorbia Trigona Mill for Development PLA based Bio Composite.

1.4.2. Specific Objectives:

- To synthesize master batch through the modification of GA and ETML; characterize and study the effect of reaction time, temperature and mixing ratio on percentage solubility, grafting efficiency.
- To Fabricate PLA/master batch composite and study the effect of master batch on the mechanical, optical, crystallization properties of the bio composite film.
- To investigate the effect of maser batch on thermal property of PLA and study the degradation kinetic of bio composite film.
- To examine the antimicrobial properties of the PLA/ bio composite film.

1.5 Significance of the Study

Due of the poor mechanical properties, low crystallinity and thermal instability, enhancement of PLA properties were made in order to increase expand applications window of PLA. Thus, the benefit offered by this research work was improving those properties of PLA by properly dispersing modified GA, modified ETML and master batch into PLA matrix. Using OLLA-g-GA, OLLA-g-ETML and master batch improved mechanical property (elongation at break and tensile strength), degree of crystallization and anti-microbial property of PLA has synergic effect. Using a master batch made fillers to have a synergic effect. More importantly, using the developed bio composite will help to reduce environmental pollution caused by petro-based plastic. The antimicrobial property of filler can make the developed PLA/bio-composite as active package films.

1.6 Scope of the Study

The following points are used to explain the scopes of this research. This research is mainly focused on the-

- Modification of both gum Arabica and euphorbia trigona mill, based on reaction conditions such as reaction temperature, mixing ratio and reaction time.
- Study of the physical (percentage solubility, grafting efficiency and grafting percentage and chemical properties (chemical structures and thermal stability) of the prepared matrix
- Blending of modified gum acacia, euphorbia trigon mill and master batch with PLA and investigate the effect of filler on mechanical, thermal, and crystallization rate of PLA
- Study effect of maser batch on thermal degradation of PLA and study the degradation kinetic of bio composite

CHAPTER TWO

2. LITERATURE REVIEW

2.1 Poly (lactic Acid) (PLA)

Poly (lactic acid) (PLA) is a linear aliphatic thermoplastic polyester, produced from renewable resources and readily biodegradable. Its low toxicity its degradation products, namely H_2O and CO_2, that are neither toxic or carcinogenic to the human body, hence making it an excellent material for biomedical applications, along with its environmentally benign characteristics, has made PLA an ideal material for food packaging and for other consumer products (Lunt 1998; L. Yu, Dean, and Li 2006 Carrasco et al. 2010;, Rudnik and Briassoulis 2011).

It is exits in the form of polymers that are biodegradable polyesters obtained from lactic acid (LA) or 2-hydroxy propionic acid, typically obtained from agricultural crops shown in figure 2.1 such as corn, potato, molasses, tapioca, cane sugar (Ilyas et al. 2021; Madhavan Nampoothiri, Nair, and John 2010). From these renewable sources, lactic acid is basically produced by a fermentation process and used as a monomer to synthesized PLA through different polymerization routes, ring-opening polymerization (ROP), poly-condensation and other direct methods (e.g.,azeotropic dehydration and enzymatic polymerization)(Mokhena al. 2018, Anderson, and Langer 2016).

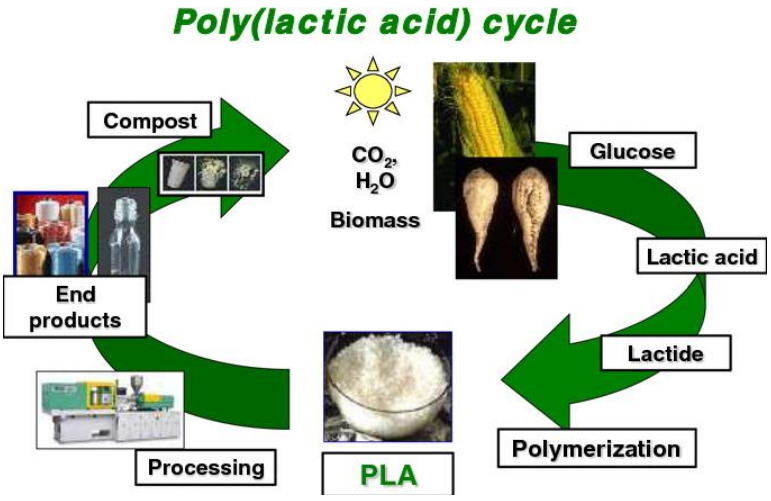

Figure 2.1: Life cycle of PLA (Maga et al. 2019)

2.2 Synthesis Routes for PLA

Starting point for the production of PLA is lactic acid (LA). Lactic acid is the most widely occurring hydroxycarboxylic optical active acid. It was first discovered in 1780 by the Swedish chemist Scheele. Lactic acid (2-hydroxypropionic acid, LA), LA is produced by fermentation of different carbohydrates (namely glucose, sucrose, lactose and maltose) obtained from renewable resources such as sugar cane, sweet potato and corn(Bajpai, Singh, and Madaan 2014). The fermentation can be performed by maintaining few important parameters such as atmospheric conditions, temperature, pH-value and agitation while conducting fermentation in batch or, in continuous process by using bacteria, fungi or yeast. Another intermediate monomer for PLA synthesis is lactide and obtained by depolymerization of low molecular weight PLA under reduced pressure to give a mixture of L-lactide, D-lactide, or meso-lactide (Figure 2.2). Lactide is also formed by the dimerization of polycondensated lactic acid. PLA can be obtained using different routes as shown in Figure 3. In generally, there are three methods which can be used to produce high molecular mass PLA of about 100,000 Daltons: direct condensation polymerization; azeotropic dehydrative condensation and polymerization through lactide formation, the ring-opening polymerization (ROP). Currently, direct condensation and ring-opening polymerization are the most used production techniques.

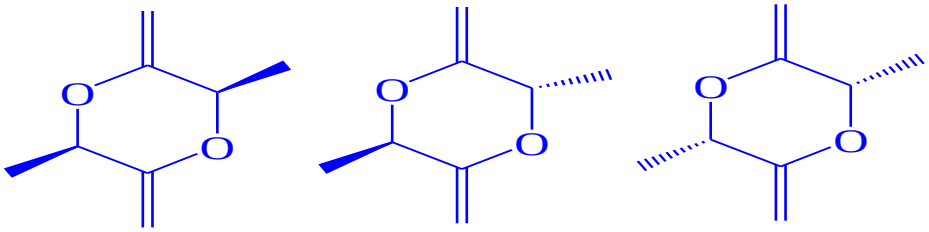

L -lactide Meso-lactide D-lactide

Figure 2.2: Chemical structures of L, L-, meso- and D,D-lactides.

Poly-condensation of lactic acid is a relatively simple process to produce PLA. Lactic acid monomers with the presence of hydroxyl and carboxyl groups can undergo self-esterification, which leads to reversible step growth polymerization and production of water as by-product. High temperatures and vacuum are used to remove produced water from bulk solution to reduce reversibility of reaction, but usually it still results in low molecular weight polymers mainly because of the presence of water and impurities. Other disadvantages of this route are the requirement of relatively large reactors and huge energy consumptions to reach high temperature and vacuum leading to expensive final product

(Maharana, Mohanty, and Negi 2009).

Ring-opening polymerization of lactide is the method used commercially. The resulting polymer is formed from an intermediate of lactic acid poly-condensation, the lactide. Lactide is a cyclic dimer of lactic acid, which is formed by removal of water from the reaction mixture during oligomerization of lactic acid. Formed lactide is the starting monomer for ROP usually using metal alkoxides as catalysts resulting in high molecular weight polyester. Most commonly used catalyst is Stannous Octanoate due to its efficiency and low toxicity, making it one of the best choices to use for production of biodegradable and environment-friendly polymers (Maharana et al. 2009).

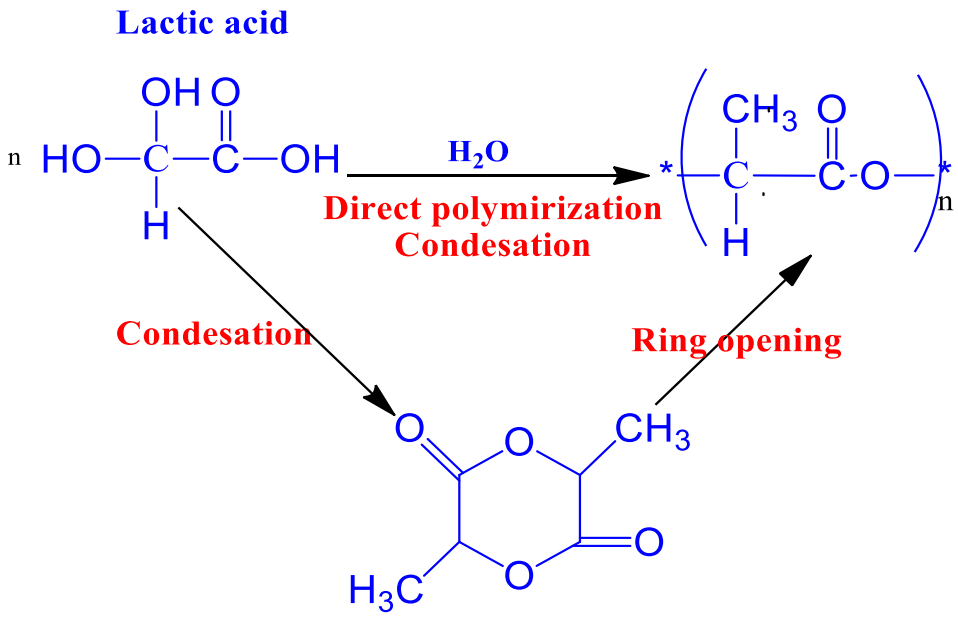

Scheme 2.1. Poly lactic acid (PLA) polymerization

Depending on the method by which PLA is synthesized, the degree of chain length can vary greatly within the polymer leading to varying property of the polymer (Machrafi et al 2012). If produced with the Ring-opening polymerization method, PLA chain lengths are generally longer than when produced via the direct condensation polymerization method (Gironet al.2016). PLA's crystalline state can vary from completely amorphous (non-crystalline) to up to 40% crystalline; many physical properties of the polymer depend on the amount of crystallinity that has occurred within the polymer.

2.3 PLA Properties and Limitations toward Engineering Applications

PLA is either transparent or exists in a yellowish glassy state at room temperature with unique properties like good appearance, mechanical strength, and low toxicity; and good barrier properties have broadened its applications. It is a crystallizable thermoplastic polymer and is categorized as synthetic linear aliphatic polyester. It has a density of 1.2–1.3 g/mm^3, crystallization temperature (Tc) of 125°C, glass transition temperature (Tg) of 45–60°C, and melting point (Tm) of 150–162°C. However, it does not necessarily achieve all of the desired technical properties (Gironi et al. 2016).due to its draw back like high stiffness (Balakrishnan et al. 2012),poor ductility (K. Zhang et al. 2014) brittleness(Dong et al. 2021) To overcome the brittle nature of PLA, plasticizer(s) such as PEG were added into the PLA. However, it results in the loss of stiffness or decreased modulus of elasticity, which is one of the desirable properties for structural applications. The low impact strength of PLA is commonly linked with the brittle nature of PLA that results in the incapability of polymeric chains to mobilize relative to each other and consequently the inability to absorb energy (Bax and Müssig 2008).Low deformation at break or elongation at break .K. Zhang et al. 2014 observed the elongation at break for PLA (Ingeo 3251D) around 4%. The ductility of the PLA was enhanced by adding renewable elastomers ethylene methyl acrylate-glycidyl methacrylate (EMA-GMA) and poly (ether-block-amide) elastomeric copolymer (PEBA). However, the addition of elastomers leads to a reduction in tensile strength and modulus. In a PLA/EMA-GMA/PEBA ternary blend, an increase in elongation at break was observed with an increase in EMA-GMA (Elvaloy) content. The PLA/EMA-GMA/PEBA of 70:20:10 wt % showed 72.7% elongation at break, which is 20 times higher when compared with that of neat PLA. Slow crystallization rate of PLA is a semicrystalline material which in XRD analysis showed a broad hollow or peak ascribed to a weak reflection peak at $2\theta = 16.8$ (Nagarajan et al. 2015). The crystallinity can be improved either by the use of nucleating agents without disturbing the inherent crystal structure or by inducing stress during polymer processing. Generally, these inherent deficiencies in PLA are the target areas that need improvement.

2.4 Modifications of PLA

PLA has several useful properties, but its brittleness, slow crystalization, and low impact resistance, are limiting factors for a wide range of commercial applications. Several methods have been developed by various researchers to overcome these shortcomings (Rasal, Janorkar, and Hirt 2010). In this area, some

of them are i) Copolymerization, ii) Mixing with others Polymers, iii) Manufacture of nanocomposites, and iv) Manufacture of mixtures and composites PLA as a performance improvement technology PLA is discussed in detail in this article. Emphasize recent developments.

2.4.1 PLA-Based Blends and Composites

PLA has currently gained a lot of attention due to its renewable-resource-based origin(Malek et al. 2021) good biodegradability (Garlotta et al. 2019; Rudnik and Briassoulis 2011) or composability (Briassoulis 2011,Maharana et al.2009),biocompatibility(da Silva et al. 2018; Yadav et al. 2021) related to other bio based plastics; better processability compared to poly(ethylene glycol) (PEG), PHA, and poly(ε-caprolactone)(PCL);low energy consumption (25−55% less than petroleum-based polymers)(Rasal, Janorkar, and Hirt 2010) and low CO_2 emissions. PLA was considered a cheap alternative to it Petroleum-based polymers with affordable performance and wide scale availability on the market. However, despite all its suitable characteristics, PLA is limited by its inherent brittle nature low crystallization ability and others. Thus, blending strategies have been widely explorer as a valid scalable process. Figure 2.3 illustrates various polymer and additive combinations for the preparation of PLA based blends and provides composites explored so far for enhancing their properties.

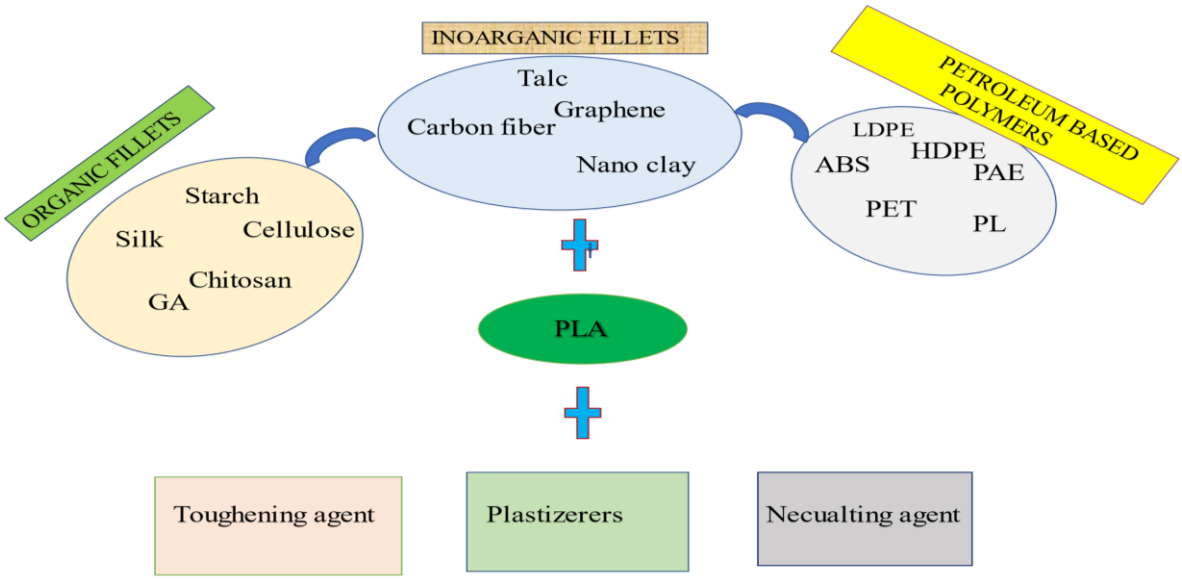

Figure 2.3: Explored research on various polymers, reinforcing agents, and additives to fabricate PLA-based materials for durable applications.

2.4.1.1 PLA-based blends and Composites for improvement of mechanical properties

Blending is probably the most extensively used methodology to improve PLA mechanical properties. The properties of PLA were improved when blended with various polymers (Rasal, Janorkar, and Hirt 2010). Formulating PLA blends or synthesizing PLA composites is one of the promising approaches for attaining durability, distinctive properties and cost competitiveness of PLA. The selection of precursor is key factor in order make the synthesized PLA blend or composite not impair environmentally friendly characteristics. Additionally, preparing a good miscible blend or composite of PLA with other polymers is a challenging task that should not hamper the toughness of the PLA. Thus, compatibilizers enhance stability by creating interactions and diminishing the interfacial tension between two or more immiscible polymers or between PLA polymer and fillers.

Plasticizer

PLA is a glassy polymer that has poor elongation at break (10%) (Rasal et al. 2010). Different biodegradable as well as non-biodegradable plasticizers have been used to lower the glass transition temperature, increase ductility, and improve processibility of PLA (Sin et al 2012.; Omar et al. 2021). Such effects have been achieved by manipulating the molecular weight, polarity, and end groups of the plasticizers being added to PLA. Lactide monomer, for instance, is a good candidate to plasticize PLA. Lactide plasticized PLA showed a significant increase in elongation at break (Tripathi et al. 2021). However, it has the disadvantage of fast migration and losses, resulting in a stiffened polymer with a sludgy surface. Thus, high-molecular-weight plasticizers, which are unlikely to migrate, remain the choice of researchers. Oligomeric plasticizers that would not tend to migrate toward the surface due to their relatively higher molecular weight have also been utilized. Many small molecule esters such as triethyl citrate, tributyl citrate, acetyl triethyl citrate, acetyl tributyl citrate (Tributyl O-acetylcitrate), diethyl adipate, dioctyl adipate (Bis(2-ethylhexyl) adipate (DEHA)),diisodecyl adipate, glycerin triacetate (triacetin), glyceryl tribenzoate (Koh et al 2018) as successfully been used to plasticized PLA and consequently increase its ductility and toughness. Cardanol (CD), which is derived from renewable natural cashew nutshell liquid, has been used as a new plasticizer for poly (lactide) (PLA). CD significantly decreased the glass transition temperature and enhanced the crystallization ability of PLA, demonstrating good plasticizing efficiency with PLA. At 10 wt% CD, ultimate elongation and impact toughness increased to 472% and 9.4 kJ m^{-2}, respectively, which represented improvements of 31-fold and 2.6-fold over the corresponding measurements for neat PLA (H. Kang et al. 2018). PLA was

plasticized with PEGs (Mw ~0.4–0.75 kDa) having hydroxyl and ether end groups. The thermal and mechanical properties were significantly dependent on PEG composition, while the PEG end groups had very little effect. It was demonstrated by DSC that the mobility gained by PLA chains in the plasticized blends yielded crystallization. The grafting of a fraction of PEG into PLA did not affect this process. However, DSC results obtained after the second heating showed an interesting effect on the Tg when 20 wt.% PEG were melt blended with neat PLA. In the latter case, the Tg displayed by the reactive blend was shifted to even lower the Tg of neat PLA and PLA blended with 20 wt% PEG was around 60 and 23 ^{o}C, respectively. Karanja oil has been epoxidized and further used as bio-based plasticizer to improve some properties of poly (lactic acid) (PLA). Melt extrusion was used to plasticize PLA with different EKO amounts in the 0-10 wt%. The formulations with EKO decrease the glass transition temperature as the EKO content increases and in addition, generates an increase in elongation at break by 77%, using a relatively small concentration of plasticizer (Arrieta and Samper 2020).

Bonilla et al. (2013) studied the plasticization effect of oligomeric lactic acid (OLA) in poly (lactic acid) (PLA) films. The films were prepared by melt-blending PLA and OLA at different concentrations between 15 to 25 wt%. The aging of the film was also studied bystoring the films for 3 months under ambient controlled conditions. From the results it was observed that, the incorporation of OLA into PLA film resulted in decrease in elastic modulus and oxygen barrier property but increase in elongation at break. OLA proved to be efficient plasticizer for PLA which significantly decreased glass transition temperature and considerably improved ductile properties. Among the different concentration films, PLA-20 wt% OLA proved to be the only one which maintained amorphous state with adequate properties required for manufacturing flexible films. High compatibility of OLA with PLA was also observed as no phase separation was detected till 25 wt%.

- **Non-biodegradable polymer/filler blends and composites**

Blending of PLA with non-degradable polymers has not been as extensively studied as blending with degradable or renewable resource polymers. Nevertheless, blending PLA with commodity polymers, in particular, can be very useful in terms of improving process ability, lowering costs and controlling the biodegradation rate. PLA blended with low density poly (ethylene) (LDPE) to improve the toughness. PLA crystallinity was found to significantly impact the blend toughness (Balakrishnan, et.al 2010) the analysis shows that, the melt blending of LLDPE had improved the impact strength of PLA with the

sacrifice of stiffness and strength. From the mechanical properties, the optimum loading of LLDPE in the PLA/LLDPE was found to be 10 wt%. The impact strength of PLA improved 53% with addition of LLDPE up to 10 wt%. However, the tensile and flexural strength decreased with increasing content of LLDPE and further blending of LLDPE also decreased the Young's and flexural modulus of PLA/LLDPE. Also, High Density Polyethylene (HDPE) and Polyethylene graft maleic anhydride (PE-g-MAH) enhanced biodegradation in soil, thermal stability, tensile strength, tensile strain of PLA. Compared with neat PLA (tensile strength of 50 MPa at 167 ^{o}C and tensile strain of 0.02263 mm/mm at 161^{o}), the blend observes high tensile strength of 67.8 MPa at 167^{o}C and tensile strain of 0.0323 mm/mm at given temperature. Polylactide (PLA) was melt blended with either polypropylene (PP) or a polypropylene-based elastomer (PBE, Vistamaxx) in an effort to improve its mechanical properties. An ethylene−glycidyl methacrylate−methyl acrylate terpolymer (PEGMMA,Lotader) was utilized as compatibilizer through coupling to the end groups of PLA (Y. Xu et al. 2015) the morphological, mechanical, and rheological properties of the PLA/PP compatibilized blends were investigated, and the blends exhibited substantial improvement in elongation at break and tensile toughness as compared to the corresponding binary blends. Balakrishnan et al. (2010) studied also focused on blending PLA with LLDPE; however, instead of adding LLDPE only, they added organophilic modified montmorillonite (MMT). The composition of LLDPE was fixed at 10 wt%, while the amount of MMT was varied at 2 and 4phr. The researchers found that with the increasing amounts of MMT in the PLA/LLDPE blend, Young's and the flexural modulus increased with a sacrifice in tensile and flexural strength. This shows that MMT is effective in increasing the stiffness of the blend. There is transmission electron microscope (TEM) and X-ray diffraction (XRD) proof that the intergallery spacing of MMT increases in the blend, forming an intercalated nanocomposite system. Yang et al. (2010) found enhancement of mechanical strength (tensile and impact, 40 MPa and 80 J·m−1, respectively) by the addition of grafted ABS (G-ABS) and grafted styrene acrylonitrile grafted glycidyl methacrylate copolymer (SAN-GMA) in a 50:50 blend of ABS and PLA.

- **Biodegradable/renewable-resource polymer blends**

PLA–non-biodegradable polymer/filler blends and composites are not as extensively studied as PLA–biodegradable polymer blends, probably due to the incorporation of non-biodegradable component into the blend. However, PLA blends with biodegradable polymers have been extensively investigated

because they offer property improvements without compromising biodegradability (Rasal, Janorkar, and Hirt 2010).

PLA with Cellulose

Gu and Catchmark (2013) reinforced mechanical performance of PLA using cellulose fiber using milk casein protein as dispersant. The dispersion of CNWs in PLA was improved when casein was present. Compared to pure PLA, the PLA composites had higher young's modulus. Cellulose nanofibers were synthesized from flax yams via acid hydrolysis and different weight loadings (2.5 and 5.0 wt%) of flax cellulose nanofibers (FC) were reinforced in the PLA matrix by solution casting approach (Liu et al., 2010). The incorporation of FC in the PLA showed good improvement in terms of tensile strength as well as tensile modulus with respect to loadings. As compared to neat PLA, PLA/5wt% FC nanocomposite showed ~59% and 47% enhancement in the tensile strength as well as tensile modulus, respectively. The effect of the novel nano fibrillated celluloses (NFCs) on the mechanical, thermal, morphological, and crystallization properties of non-plasticized and green plasticized PLA composite was studied by (L. Xu et al. 2021). The analysis reveals that the addition of NFCs not only enhanced the strength and toughness remarkably, but it also improved the thermal stability of PLA composites. The maximum tensile strength, modulus, elongation, and impact strength values (4 wt% NFC content) increased by 37%, 21%, 126%, and 78% compared with neat PLA, respectively.

PLA with Starch

Starch is blended with PLA by various research groups in order to improve the properties. Yiga et al. (2021**)** studied on an optimization of tensile strength of fiber-reinforced polylactic acid (PLA) composites using Box-Behnken design (BBD). Rice husk fiber and clay filler were used to enhance tensile properties of PLA. Fiber-reinforced PLA composites were prepared using compression molding. Five factors, namely, clay filler loading (1−5 wt.%), rice husk fiber loading (10−30 wt.%), alkali concentration (0−4 wt.%), rice husk variety (K85, K98), and alkali type (NaOH, Mg(OH)2) were varied with 68 individual experiments. Malek et al.2021 have compatibilized PLA/starch blends with bio based epoxy functional compatibilizer, and the result showed a significant increase in impact strength, tensile strength, and elongation at break. Hu et al.(2020) prepared poly (lactic acid) (PLA)/starch blends through reactive by using vegetable oil polyols, polyethylene glycol (PEG), and citric acid (CA) as additives. Results showed that the elongation at break and impact strength of the

PLA/premixed starch (PSt)/PEG/CA blend were 140.51% and 3.56 kJ·m−2 which were 13.4 and 1.8 times higher than those of pure PLA, respectively. Polylactic acid (PLA) composite materials PLA using as a matrix material and TPAS as a modifier. Analysis of the mechanical, of the PLA/TPAS composites shows that with an increase in the TPAS content, the toughness of the PLA/TPAS composites significantly improves. When the amount of TPAS added is 40% by weight, the elongation at break is increased 4 times (M. Yu, Zheng, and Tian 2020). The effect of wood flour contents on interfacial compatibility, thermal properties, mechanical properties, rheological properties and water absorption rate of composites were studied. Result shows that, with the increasing of wood flour contents, the tensile strength and bending strength of wood flour-starch/PLA composites first increase then decrease, and reaches the best values at 40.65 MPa and 60.91 MPa with 18wt% wood flour content.

- **Others renewable-resource polymer blends**

Table 2.1: Summary of literatures for renewable-resource polymer blends for enhancing mechanical properties of PLA.

Composite /blends	Method	Effect of fillers	References
PLA/ PLA-g-ABS	Injection molding	Increase percent elongation and crystallinity Extremely flexible and tough	(Chaikeaw and Srikulkit 2018
PLA/ PBS	Injection molding and extrusion	Improve Crystallinity, mechanical properties and thermal stability, and dyeing properties	(Čolnik et al. 2020), (Tripathi and Katiyar 2016
PLA/PCL, NA, PEG	Extrusion	Significant decrease in tensile strength and almost total eradication of the elongation at break of PCL matrix, ey after PEG and NA addition and increase in the flexural modulus of the blend	(Glycol 2015)

PLA/ gum rosin (GR) and pentaerythritol ester of GR (PEGR)	Injection molding	Had a lubricating effect in PLA polymeric chains, increase of and in melt flow index	(De La Rosa-Ramírez et al. 2020)(De La Rosa-Ramírez et al. 2020)
PLA/ liquid epoxidized natural rubber (LENR)	Melt blending	Significantly enhances the flexibility	(Syed Mustafa et al. 2020).
PLA/hydrophilicnanoclay, Nanomer PGV	Melt blending	Improve impact strength	(Eng et al. 2013)
PLA/Chitosanand epoxidized natural rubber	Solution casting approach	The tensile strength of the composites was improved by ~33%	(Ravi,etal 2015)

- **Master batches with PLA**

Poly (lactide)-graft-glycidyl methacrylate (PLA-g-GMA) copolymer was prepared by(Liu, et al 2012) by grafting GMA onto PLA using benzoyl peroxide as an initiator. PLA-g-GMA copolymer was used as a compatibilizer for PLA/starch blends. The structure and properties of PLA/starch blends with and without PLA-g-GMA copolymer were characterized by SEM, DSC, tensile test and medium resistance test.

In master-batch approach, a selective polymer (PLA) is employed as a carrier for various fillers. The polymer can be either the same or different than the host polymer in the nanocomposite (J.Shojaeiarani2018). A PLA-grafted maleic anhydride (PLA-g-MA) master batch containing 10 wt% PLA-g-MA was obtained by reactive extrusion and was further used, after dilution, as a coupling agent, the use of the PLA-g-MA, and helped to boost the hybrid material properties (Mihai 2017). PLA based composites were manufactured by combining CNCs master batches and PLA resin using twin screw extruder followed by injection molding. Degree of crystallinity of PLA exhibited a major enhancement by 14.7% and 38.0% in solvent cast and spin-coated composites, respectively (Shojaeiarani, et.al.2018). In similar investigation cellulose nanofiber (CNF) reinforced polylactic acid (PLA) by twin screw extrusion. Nanocomposites were prepared by premixing a master batch with high concentration of CNFs in PLA and diluting to final concentrations (1,3,5wt%) during the extrusion. The tensile modulus

and strength increased from 2.9 GPa to 3.6 GPa and from 58 MPa to 71 MPa, respectively, for nanocomposites with 5 wt% CNF (Jonoobi et al. 2010). The compatibility between PLA and starch with vegetable oil-based additives based on tensile results, it can be stated, that the strength could be improved for 70/30 and 60/40 blends in both unconditioned and conditioned cases, regardless of vegetable oil, while no advantageous change in impact strength was obtained with PLA-g-MA (Nagy, Miskolczi, and Eller 2021).

2.4.1.2 PLA-based blends and Composites for improvement of crystallization rate

PLA with a certain amount of crystallinity is required for commercial application. On the other hand, the mechanical properties and biodegradability of PLA are strongly dependent on the crystal morphology and structures, whereas, it is challenging to develop high crystallinity. Thus numerous approaches and techniques like block copolymerization, chemical modification, nucleation, plasticization and blending with suitable polymers (F. Rahmafitria 1999; Jiang et al. 2016; Zeng, et al. 2015 ; Nagarajan et al. 2015) have been explored to increase the crystallization and toughness of PLA. The crystallinity of PLA can be increased by the addition of nucleating agents, which increase the crystalline and rigid amorphous fractions. This can impede the chain mobility of PLA, and thus enable it to resist heat-induced distortions, which leads to improved heat resistance (Jin, Hu, and Park 2019). In addition, a better understanding of the crystallization behaviors of PLA and of its effect on the mechanical properties is a critical step in order to extend the application of this polymer. Several studies have been reported, aimed at understanding and controlling PLA crystallization by the use of proper nucleating agents, coupled with specific processing conditions. The addition of adding nucleating agent (NA), which can reduce the surface free energy barrier towards nucleation, and induce PLA to crystallize at higher temperature. NAs for PLA are commonly divided into three categories (Jiang et al. 2016), i.e. inorganic NA (I-NA), organic NA (O-NA) and macromolecular NA (M-NA). I-NAs like clay, talc and sepiolite are rich in sources with low prices (Feng et al. 2017), but the incorporation of I-NAs usually reduces the mechanical properties of PLA, due to the poor compatibility with PLA matrix.

- **Non- biodegradable polymer/filler blends and composites**

The presence of nucleating agents in a virgin polymer can have a positive effect on crystallization kinetics and morphology by offering nucleating sites for initializing the crystallization process. Aliotta

et al.(2017 studied the effect of nucleating agents LAK301, an aromatic sulfonate derivative, and PDLA on the crystallinity and properties of PLA. Their results indicated that the crystallinity and mechanical properties of PLA improved slightly with increasing nucleating agent content. Homklin and Hongsriphan 2013 investigated the influence of nucleating agents (nanosized calcium carbonate and sodium benzoate) on the mechanical and thermal properties of PLA/poly(butylene succinate) co-continuous blends. Li et al. (2015 investigated the crystallization behavior and morphology of PLA using N-amino phthalimide (NA-S) as the nucleating agent. DSC results exhibited that with the addition of NA-S, the induction crystallization time of PLA decreased, whereas its crystallization rate and nucleation density increased. Layered metal phosphonate reinforced PLLA composites were fabricated, and their crystallization behavior and mechanical properties were investigated. The incorporation of PP Zn significantly accelerates the crystallization of PLLA. With the addition of 0.02% PPZn, PLLA can finish the crystallization upon cooling at 10 °C/min, and the crystallization half-time decreases greatly (Pan et al. 2009). Song et al. (2017) found that the non-isothermal and isothermal crystallization rates of PLA increased with zinc citrate complex nanoparticles (ZnCC) content. Refaa et al (2019).studied the synergistic effects of shear flow and nucleating agents on the crystallization mechanisms of PLA. Their results indicated that the crystallization of PLA improved in the presence of shear flow and talc because of a supplementary nucleation induced by the synergistic effect of the talc particles and shear flow. Wen-Dong et al. 2021 investigated the effect of reactive compatibilization on the crystallization properties of PLA/PP blends were by means of differential scanning calorimetry (DSC). The nucleation capability of PLA in PLA/PP blends will increase after reactive compatibilization by using reactive extrusion method. Organically modified layered silicates (organoclay) acted as nucleating agents at low content by increasing (>5 wt %) the crystallization rate of PLA and as the organoclay content increased they became physical hindrance to the chain mobility of PLA because of the increased interaction sites (Di et al. 2005). Basalt microfiber reinforced poly (lactic acid) (PLA) composites filled with talc nanoplatelets (2D) and sepiolite nanofibers (1D). Thermal analysis results show that crystallinity of amorphous PLA can be enhanced up to 24% by adding basalt and talc (Zotti et al. 2018).

Wen-Dong et al.(2021) study on improvement of PLA crystallization property by blending with polypropylene. The researcher use used ultraviolet (UV)-induced reactive extrusion process to prepare PLA/PP blends to improve the crystallization rate of PLA by interface-assisted nucleation,

trimethylolpropane tri-acrylate (TMPTA), was adopted into PLA/PP blends to form PLA-TMPTA-PP copolymers which can improve the compatibility of PLA/PP blends. The analysis showed the nucleation capability of PLA in PLA/PP blends will increase after reactive compatibilization compared when with neat PLA.

- **Biodegradable/renewable-resource polymer blends**

Blending of renewable polymers is an alternate economical and effective way of achieving new materials with desired crystallinity (A. Ibrahim and M.Kadum 2010). To date, the various types of fibers that have been used for the reinforcement of PLA include natural plant fibers (hemp, sisal, linen, kenaf, bamboo, coir, and wood fibers), natural animal fibers (silk fibers), mineral fibers (basalt fibers), and chemical fibers (carbon and glass fibers).

Cellulose

Renewable cellulose-derived carbon nanospheres as the nucleating agent for PLA. Their results indicated that the crystallization rate of PLA increased by 1.4 times on the addition of the carbon nanospheres (Gneshin, et al 2008). The addition of cellulose nanofibers can be an efficient solution to enhance PLA crystallinity and stiffness, maintaining the transparency and biodegradability, which are mandatory for various applications. Frone et al. (2016) investigated the effect of cellulose nanofibers on the crystallinity and nanostructure of poly (lactic acid) composites. The ability of CN to act as nucleating agents was highlighted by DSC and XRD, both methods pointing out similar trends of crystallinity variation. Higher crystallinity was observed after annealing, 59 % instead of 40 % for PLA, 67 % instead of 48 % for PLA-CN and 57 % instead of 39 % for PLA-SCN, respectively. The transformation of the grained structure specific to amorphous PLA into a crystalline lamellar structure (average lamellar thickness of about 22 nm) after annealing was detected by Peak Force QNM.

Adriana Nicoleta Frone et al (2019) tried to improve the 3D printing behavior of polylactic acid (PLA), poly(3-hydroxybutyrate) (PHB) and cellulose nanocrystals (NC) by a single step reactive blending process using decimal peroxide (DCP) as a cross-linking agent. The addition of DCP improved interfacial adhesion and the dispersion of NC in nanocomposites. NC and DCP showed nucleating activity and favored the crystallization of PLA, increasing its crystallinity from 16% in PLA/PHB to 38% in DCP cross-linked blend and to 43% in cross-linked PLA/PHB/NC nanocomposite. Novel TEMPO-oxidized bacterial cellulose (TOBC) reinforced the mechanical and crystallinity of polylactic

acid (PLA). It was found that the addition of a small amount of TOBC could effectively improve the mechanical properties and crystal properties of PLA. DSC and XRD analysis results of nanocomposites show that TOBC can be used as nucleating agent to promote the crystallization of PLA matrix and improve the crystallization rate of PLA. The crystallinity of the composite materials containing 1.5% TOBC is 2.16 times higher than that of PLA.L. Li et al. (2019), Lu et al. 2016 study the effect of nanocellulose formates (SCNFs) PLA matrix. The addition of well-dispersed SCNFs significantly increased the crystallization rate, and thus led to obvious enhancements of the mechanical performance and thermal stability of the PLA. Compared to pure PLA, 130% and 116% improvements for the tensile strength and young's modulus can be obtained for the resulting nanocomposite with 10 wt% SCNFs, respectively, and the initial degradation temperature (T^0) and maximum degradation temperature (Tmax) increased by 17.4 and 21.5^{o}C respectively. Thermal annealing as an additional polymer processing step or post-treatment processing step enables the structural changes of amorphous parts into crystalline parts. The values of the degree of crystallinity and lamellar thickness determined by wide-angle-X-ray scattering showed that the thermal annealing of PLA samples modified with nucleating agents was an efficient processing step to increase the final crystallinity of PLA (Pastorek and Kovalcik 2018).

Starch

The effect of starch, an interesting biopolymer, on the crystallization of PLA was investigated as well. Ke and Sun reported that the $t_{1/2}$ of PLA was reduced from 14 to 3.2 min with the addition of 1 wt% native starch while the crystallization rate was increased slightly when the native starch content was increased from 1 to 40 wt% (Ke and Sun 2003). To increase the nucleation efficiency, thermoplastic starch (TPS) was applied instead of native starch (K. S. Kang et al. 2008) studied the effect of chemically modified thermoplastic starch (CMPS) on the thermal properties and isothermal crystallization kinetics of PLA. DSC results showed that the Xc and crystallization rate of PLA were enhanced by the addition of CMPS. The crystallinity and crystallization rate of PLA were considerably enhanced by addition of CMPS, even at 0.1% content, and the amount of the CMPS had little effect on the thermal properties and isothermal crystallization kinetics of PLA. The interfacial adhesion in preparing PLA/starch blends improved by Maleic anhydride (MA) and maleated thermoplastic starch (MATPS) as reactive compatibilizers (Jang et al. 2007). DSC studies reveal that the crystallinity of blends increased with increasing starch content. In particular, MA compatibilized blends showed

highest crystallinity amongst the three types of blends due to the dual effects of nucleation by starch and plasticization by MA.

- **Others renewable-resource polymer blends**

Table 2.2: Summary of literatures for renewable-resource polymer blends for enhancing crystallization properties of PLA.

Composite /blends	Method	Effect of fillers	References
PLA/EMA-GMA: PEBA	Extrusion	• Increase percent elongation and crystallinity • Extremely flexible and tough	(Nagarajan et al. 2015
OXA ≈ TMC306 > TALC >> PLA/OXA, TMC306, TALC >> TMP-5, LAK-301 and OA	Melt blending	• Increase the rate of crystallization in the order of nucleation effect OXA ≈ TMC306 > TALC >> TMP-5 ≈ LAK-301 ≈ OA	(Čolnik et al. 2020), (Tripathi and Katiyar 201
PLA/polyhydroxybutyrate rubber	Extrusion	• An effective nucleating agent to accelerate PLA crystallization and performs as a dynamic plasticize	Chee et al. 2020
PLA/ Natural rubber (NR) and epoxidized natural rubber (ENR)	Melt blending	• Improve crystallization properties of PLA	(Pongtanayut, et al 2013)
PLA/poly(hydroxyoctanoate) (PHO) and talc	Solution casting	• Enhance the nonisothermal cold crystallization behaviors of poly	(Alhaddadel.et .al 2019)

		(lactic acid)	
PLA/ wood flour and kaolin	Melt blending	• The tensile strength composites were improved by ~33%.	(Ravi,etal 2015)

2.4.1.3 PLA-based blends and Composites for improvement of thermal properties

- **Non-biodegradable polymer/filler blends and composites**

The glass-transition temperature (Tg) of pure PLA is little affected by the incorporation of organoclays (Mclauchlin and Thomas 2012). Addition of zeolite enhanced the thermal property of PLA has rendered PLLA more thermally stable, requiring higher Ea values for thermal degradation (Y. Hao and Huang 2018). H. Zhang et al. 2015 prepared PLA/TiO_2 nanocomposites through a vane extrude. These nanoparticles are inhibited, to some extent, for the cold crystallization process. The cold crystallization temperature of nanocomposites shifts to a maximum value at about 106°C with low TiO_2 loadings (0.5 or 1 wt%). The addition of TiO_2 enhanced the thermal stability of the nanocomposites, which is evident in dynamic TGA analysis. Similarly, CNT– aluminum hypophosphite improves the thermal stability of PLA (Basu et al. 2017). X. Hao et al. (2015) investigated the rheological and thermomechanical properties of PLA/PMMA blends. DSC results indicated a broad glass transition range and that Tg had increased with the addition of PMMA to PLA. The impact and heat resistance of PLA/polycarbonate (PC) blends was improved by coupling molecular chains at the interface between PLA and PC. After incorporating the chain extender, the interfacial strength between the PLA matrix and the PC phase increased, and consequently, the impact and heat resistance of PLA improved significantly (Lin, Deng, and Wang 2015). The analysis revealed that most suitable morphological structure for achieving PLA/PC-based blends with high impact strength and heat distortion temperature was obtained.

- **PLA-biodegradable/renewable-resource polymer blends**

Starch

Self-suspended starch fluids composed of modified granules as the core and polyethylene glycol-substituted tertiary amines. The starch flied incorporated into a poly (lactic acid) matrix to produce fully biodegradable composites with desirable performance. At a loading level of 10 wt%, starch fluids

exhibited simultaneous enhancements in elongation at break (increase of 164.7%) and thermal conductivity (increase of 119%) of PLA composites compared to pure PLA

Cellulose

Khoo and Chow (2016) investigated the effect of nanocellulose on the thermal and morphological properties of Poly (lactic acid). PLA/CNC nanocomposite was prepared using solution casting technique. The thermal properties (i.e., glass transition temperature, melting temperature, degree of crystallinity, thermal decomposition) of the PLA/CNC nanocomposites were characterized using differential scanning calorimeter (DSC) and thermogravimetry analyzer (TGA). DSC analysis showed that CNC (up to 5wt %) is capable of acting as nucleating agent for PLA. TGA analysis showed that the of decomposition temperatures PLA/CNC nanocomposites were higher than that of pure PLA. Ruz-Cruz et al. (2022) prepared PLA-based multiscale cellulosic bio composites and examine effect to incorporation of cellulose nanocrystals (CNCs) on the PLA bio composites reinforced with cellulose microfibers (MFCs) on thermal and mechanical properties of PLA. The result revealed those thermal properties and n flexure increase in the order of 40% and the storage modulus increases in the order of 35% at room temperature.

Others renewable-resource polymer blends

Lee et al. (2020) prepared the PLA/talc composites by using melt blending method and compressed into thin sheet for characterization test and investigated the effect of talc content on the thermal properties and tensile performance of the PLA. Nair and Nampoothiri (2012) prepared poly (L-lactide) blends and biodegradation by Lentzea waywayandensis. With the dual aim of improving its properties and biodegradability, PLA was blended with other polymers such as gum arabic, thermoplastic starch, and microcrystalline cellulose. The incorporation of relatively cheap and eco-friendly polymer such as thermoplastic starch, to PLA enhances its biodegradability to 98% when tested over 4 days. Results showed that the addition of talc ranged from 5 to 30wt% can enhance the young's modulus and thermal stability of the composites but there is no improvement in tensile strength and elongation at break due to poor interfacial adhesion. The researcher concluded that from overall tensile and thermal properties results, the optimum formulation for talc filled PLA bio-based polymer composite is 5 wt% talc with an improvement in Young's modulus of 1358 MPa and highest onset degradation temperature at 309°C. Abdullah et al. (2019) to investigate the effect of ENR and graphene loading on PLA matrix on the thermal, morphology and toughness properties. The TGA curve of PLA/ENR and PLA/ENR/G bio-

nanocomposites shows a single step of thermal degradation. As increasing the loading of graphene, degradation temperature (Tdeg) was increase where graphene act to slow down the rate of degradation. Graphene has enhanced the thermal stability of PLA/ENR/G bio-nanocomposite. Numerous numbers of researchers studies on the blending of PLA with various plasticizers (e.g. citrate ester, triacetine, polyethylene glycol or PEG) were aimed to modify its inherent thermal and brittle behavior. Kamthai and Magaraphan (2015) studied the effect of an isosorbide diesters plasticizer on thermal properties of PLA and bagasse carboxymethyl cellulose (PLA/CMCB) composites. PLA was blended with CMCB at 1%wt using various contents of isosorbide diesters (5, 10, 15 and 20%wt of PLA). The differential scanning calorimetric (DSC) and thermogravimetric (TGA) analyses indicated that the increment of isosorbide diesters concentration resulted in decreasing glass transition, melting and decomposition temperatures approximately 20–57 ºC, 93.6–100.8 ºC and 130.5–135.9 ºC (with melting enthalpy (ΔHm) of 28.1-37.7 J/g), respectively.

De La Rosa-Ramírez et al.(2020) modified PLA by melt compound with gum rosin (GR) and pentaerythritolester of GR (PEGR) and investigated thermal performance. Thermogravimetric analysis reveals that PEGR led to delayed PLA degradation/decomposition process to higher temperature, increasing the onset temperature (T5%) in more than 7^{o}C for PLA with 15 phr PEGR. Meanwhile, GR accelerated the thermal degradation by reducing the onset temperature (T5%) in more than 30^{o}C (PLA) with 15phr GR.

2.5 Polysaccharide gums

The natural polysaccharides have many advantages over synthetic polymers such as cost, easy availability, nontoxicity and biodegradability. Natural gums are polysaccharides consisting of multiple sugar units linked together to create large molecule (Hindi et al. 2017). Gums are frequently produced by higher plants as a result of their protection mechanisms following injury. They are heterogeneous in composition. Upon hydrolysis they yield simple sugar units such as arabinose, galactose, glucose, mannose, xylose or uronic acids, etc. Among the different polysaccharides, gums have tremendous applications in many fields due to its emulsifying and stabilizing properties,and are used in beverages, paints, cosmetics and pharmaceuticals (Nz-j 2012).

2.5.1 Gum Arabic

Among the various polysaccharides, GA is a natural, biocompatible and biodegradable complex polysaccharide derived from an exudate of Acacia trees namely *Acacia senegal* and *Acacia seyal* (Dünnhaupt et al. 2015). *Gum Arabic* is a neutral or slightly acidic salt of complex polysaccharide containing Ca, K and Mg cations. The GA molecule has been mainly divided into three main fractions namely arabinogalactan (AG), arabinogalactan-protein (AGP) and glycoprotein (GP) components, which differ mainly in molecular mass and protein content. GA has been used in a wide range of applications such as lithography, ceramics, textiles, cosmetics, pharmaceuticals and in food, etc. It is used as a thickener, emulsifier and as a stabilizing agent in food industries (Ali et al. 2010; Tumeh et al. 2014). It can also be used as filler with some modifications in its structural properties for decreasing the gas-transport through the films.

2.5.2 Polysaccharide gum-based biopolymers

Chen et al. (2019) prepared the bio films using peanut protein isolate (PPI) which were glycated with gum arabic. The prepared film was compared with neat PPI, PPI-gum arabic mixtures and glycated PPI-Gum arabic conjugate films. The PPI and gum arabic conjugates were prepared initially by mixing in water in 1:1 weight ratio and the pH was adjusted to 7.0. Then the solution was lyophilized at -70 °C. The mixture was then incubated at 60 C and 79% relative humidity for 3, 6, and 9 days. The three types of films namely neat PPI, PPI-gum arabic mixtures and glycated PPI-Gum Arabic conjugate were prepared by dissolving the components with 10 % (w/w)deionized water. The plasticization effect was imparted by 25% glycerol in each solution. The cross-linking of PPI with gum Arabic resulted in 2 -2.5 fold reduction in water vapor permeability with respect to neat PPI films. After 3 days of glycation, increase in tensilestrength was observed but decrease in water vapor permeability. However, reduction in elongation was observed. It was concluded that different degree of glycation has significant effect on properties of the film.

Suleiman et al (2013), developed and characterized a bio-composite from rice husk/gum Arabic for particle board using compression molding, by keeping the weight of the rice husk constant (150gm) and varying mass of the binder in a ration 150:15 to 150:30 at interval of 5g. The result outcome demonstrated that the sample with 30g binder emerge the best with 50% water absorption and highest modulus of elasticity of 150 Gpa. The percentage of water uptake expanded with increasing the weight

of the GA. The uniform dispersion of the particles and the binders in the microstructure of the board composites is the main consideration responsible for the enhancement in the properties.

Gutierrez et al. (2014), designed a novel functional nanostructured polymeric blend using gum rosin. The thin films were prepared by dissolving S4VP and GR in a one-step pathway using spin-coating at 2000 rpm for 120 s. Gum rosin was used to fabricate novel polymeric blends with long range order nano patterns using poly (styrene)-*block*-poly(4-vinylpiridine) S4VP block copolymer as Nano structuration agent.

Ali et al. (2010) prepared coating of GA for tomato fruit to enhance the shelf life and postharvest quality. The coating solutions were prepared by dissolving *gum arabic* in purifiedwater at 5, 10, 15 and 20% (w/v). The solutions were stirred magnetically at 40°C for 60min. After cooling, glycerol monostearate (1.0%) was added as plasticizer to impart flexibility and strength. The fruits were then dipped into the solutions for 2-3 min. Thereafter, the fruits were air dried packed and stored in 20°C and 80-90 % RH. From the results it was observed that 10% GA which was used as an edible coating delayed the ripening process as well as the storage life of tomatoes was extended up to 20 days without any off-flavor or spoilage.

2.6 Latex Bearing Plants

Higher-level plant families can produce latex that is a sticky aqueous milky-like substance. Plant latex is produced at a plant part known as a laticifer and excluded as a result of tissue damage. There are different plant families that produce latex for their own purpose may be as a defense mechanism. The chemical composition of latex and the structure of the laticifer is known to be dependent based on plant origin, anatomy, and geographical distribution. It has been found that over 20000 species from about 40 families of angiosperm plants could exude latex which is 8.9% of all angiosperm plants (Hua et al. 2017; Konno 2011). From those many plant families Euphorbiaceae is one which contains many species.

2.6.1 Plant Latex

Plant latex is milky-like sap that is produced by angiosperm plant families in a body part known as laticifier. It is a milky fluid made up of tiny droplets of organic matter suspended in an aqueous medium (a sort of natural colloidal suspension). There are many subtypes of latexes based on their

physicochemical properties, but the most well-known are rubbery latexes, in which polymeric micro-particles can account for more than half of the latex weight. Several studies have proved that plant latex production is phenotypically plastic (that is, responsive to environmental conditions). Furthermore, it is known that plant latex contains a great variety of proteins and specialized products including alkaloids, terpenoids, cardenolides, and many other components, most of which showed obvious toxicity insects and pathogens (Hua et al. 2017). Now in a day, the research world is giving attention to secondary metabolites as they have a diversified role in the field of bio-based material synthesis and also in the field of medicine with accepted medicinal value. Plant secondary metabolites are classified into three major groups based on their biosynthetic origins:

(i) flavonoids and related phenolic and polyphenolic compounds,(ii) terpenoids, and (iii) nitrogen-containing alkaloids and Sulphur-containing compounds (Crozier et al. 2007).

2.6.1.1 Euphorbia Trigona Mill plant (Cathedral cactus African milk tree Kulkual)

Euphorbia trigona (kulkual) is a plant that belongs to the *Euphorbia* genus and *Euphorbiaceae* family consisting of 2008 species. Lasting plant, beginning from Central Africa, with more popular names as the African drain tree, cactus cathedral or cactus-candle. The plant incorporates a straight, thick stem, 3-4 lined, somewhat branched, dark green with lighter green and V-shaped pattern(Yener et al. 2018). The well-known latex producing plant family Euphorbiacea is known to be a source of bio-active compounds that have both pharmaceutical and bio-technological application. Proteins from *Euphorbia trigona mill latex* were extracted and found to have various medicinal application like potent antifungal inhibition (v.Deenen, et al 2011), ribosome inactivating (Villanueva et al. 2015). The well-known latex producing plant family Euphorbiacea is known to be a source of bio-active compounds that have both pharmaceutical and bio-technological application. Proteins from Euphorbia trigona mill latex were extracted and found to have various medicinal application like potent antifungal inhibition (van Deenen et al. 2011), ribosome inactivating (Villanueva et al.2015). The antifungal activity of the latex lectin can be determined by inhibition of fungal conidiospores germination rate and hyphal growth of the filamentous fungi through in vitro analysis. Similarly,Nashikkar et al. (2011) revealed the anti-swarming mortality, biofilm formation and virulence factor of Euphorbia trigona mill latex extracts towards urinary tract infecting bacteria's. In our country Ethiopia *Euphorbia trigona mill* latex is

known as a medicinal plant and is being investigated for its bio-active compounds for utilization of drug synthesis based on its medicinal use by local herbalists (Enyew et al. 2014).

Figure 2.4: Euphorbia Trigona Mill plant

2.7 Copolymerization

Copolymerization Copolymers generally possess a different composition than that of the initial monomer mixture. The chain composition depends on the ratio between the reactivities of the two monomers and the concentrations of growing ends. In copolymerization, the more reactive monomer will polymerize preferentially: its consumption, however, means that the remaining monomer mixture will become deficient in this monomer, so that the copolymer that is formed at the end of the reaction exhibits a different composition than that produced at the beginning. The composition of the copolymer is equal to the initial mixture composition only at a specific combination of reactivity and concentration (Ai and Della 2003)

2.7.1 Graft copolymers

Graft copolymers are composed of a main backbone polymer chain that is joined to one or more side chains by covalent bonds to produce branches. In most instances, the branches and the backbone have different chemical properties and compositions (Bhattacharya and Misra 2004). Normally, branches are arranged randomly along the backbone, but recent improvements in synthetic techniques have enabled the creation of more clearly defined structures. Two major types of grafting may be considered: (i) grafting with a single monomer and (ii) grafting with a mixture of two or more monomers. The first

type usually occurs in a single step and the second may occur with either the simultaneous or sequential use of the two monomers (N.Hadjichristidi 2003).

2.7.1.1 Lactic acid Oligomer Grafted Biopolymers

Lactic acid oligomer grafted gum: Growing of lactic acid oligomer on *gum arabica* backbone takes place due to the presence of free amino groups of gum and hydroxyl group of lactic acid through Maillard-type reaction Tripathi and Katiyar 2018. Neelima Tripati and Vimal Katiyar observed that the percentage grafting and grafting efficiency decrease from 1287 to 174 % and 65 to 35% while the mixing ratio is increased from 5 to 20%. According to their study, the reaction is highly facilitated by microwave energy. When heating is done on microwave hydrophilic gum was grafted by lactic acid oligomer through in-situ polycondensation reaction so that the grafted gum dispersed uniformly in OLLA (oligomer L lactic acid) due to the formation of a chemical bond between the amino group of amphiphile gum and the hydroxyl group of OLLA chain.

Kaitha et al (2010) was studied the grafting of *gum arabic* and methacrylic acid. The copolymer was synthesized in the presence of potassium persulfate as initiator by free radical polymerization. The three-dimensional cross-linked structure of the copolymer was achieved by using hexamethylene tetramine which acts as a crosslinker. The reaction has been carried out in vacuum between 250-550 mm Hg for 120-360 min. It was observed that the produced copolymer was temperature and pH sensitive and exhibited salt-resistant swelling. It has wide applications in drug delivery devices and water treatment industries.

Lactic acid oligomer grafted chitosan: Growing of lactic acid oligomer on chitosan backbone takes place due to the presence of free amino function and the hydroxyl group of chitosan and the hydroxyl group of lactic acid without a catalyst. Bhattarai et al.(2006) were developed lactic acid-grafted chitosan for high drug loading and prolonged drug release. By using bovine serum protein, A drug encapsulation efficiency is 92% and a release rate of 28% from chitosan nanoparticles over 4 weeks were confirmed with and the lactic acid-grafted chitosan nanoparticles demonstrated a drug encapsulation efficiency of 96% and a protein release rate of 15% over 4 weeks. The drug release rate increased and drug encapsulation efficiency decreased because of the increased protein concentration. The chitosan amended with lactic acid oligomer prepared from solutions of neutral pH, proposing an additional advantage of allowing drugs or drugs to be uniformly incorporated in the matrix structure with insignificant or no denaturation that is not the behavior of chitosan which is generally soluble only

in acid solution (Bhattarai et al. 2006).

Lactic acid oligomer grafted cellulose: Lactic acid oligomer grafted untreated bacterial cellulose (PLA/OLLA-g-BC) bio-nano composites were successfully prepared by (Rahul Patwa et al.2019) using solvent casting technique and they tried to demonstrate the synthesis of (OLLA- g- BC) by in situ condensation polymerization. During the synthesis of OLLA-g-BC, hydrophilic BC was converted into hydrophobic due to structural grafting of OLLA chains with BC molecules increased and compatibilization between hydrophobic poly (lactic acid) (PLA) and hydrophilic BC, thus enhancing various properties of PLA based bio nanocomposites (Patwa, et al. 2019). The degradation temperatures for bio-nano composites films were above PLA processing temperature showing that bio-nano composite processing can be industrially viable. Bionanocomposites films displayed ~20% improvement in elongation with 10 wt % fillers and a decrease in glass transition (Tg) indicating towards plasticization of PLA. PLA/OLLA-g-BC films showed that excellent UV-blocking characteristics but a slight reduction in optical transparency. Furthermore, dispersed BC acts as hindering agents within the PLA matrix, reducing the diffusion through the bio-nano composite film.

Extensive literature survey revealed that very fewer efforts were made to improve different properties of PLA simultaneously by using different fillers for packaging applications. Like Gum Arabica, it was observed that the euphorbia trigona mill were not compatible with PLA due to its hydrophilic nature. Hence, grafting techniques was used to avoid such limitations.

Based on the literature survey, it was observed that no work has been published on: synthesis of master batch from modified gum Arabic and modified euphorbia trigona mill for development of PLA based bio composite films for packaging.

CHAPTER THREE

MATERIAL AND METHODS

This chapter aims to present the material required, sample preparation methods, and proper characterization techniques that needed to be followed for various experiments in this research work. For simplicity, the required materials, experimental protocols, and characterization techniques were categorized into two sections. The first section describes the parameter optimization of Lactic acid oligomer grafting of Gum Arabic(OLLA-g-GA),euphorbia trigona mill latex (OLLA-g-ETML) and characterization techniques of the grafted bio conjugate which is used as Poly(lactic acid) property enhancer; The second section describes the synthesis protocol and characterization techniques for the development of Poly(lactic acid)/-(OLLA-g-GA),Poly(lactic acid)-(OLLA-g-ETML) and of Poly(lactic acid)/ (OLLA-g-GA)- (OLLA-g-ETML) bio composite films. Finally, the effect of synthesized fillers on optical, antibacterial, mechanical properties, rate of crystallization and thermal property including degradation kinetics property of developed PLA based bio-composite films were examined.

3.1 Materials and Reagents

Reagents: For modification GA and ETML and analysis of modification, preparation of PLA bio composite films different reagents were used: all the chemicals such as, ethyl acetate (99.5%, Loba chemie Pvt Ltd chemical manufacturer in Mumbai, India), chloroform (99.99%, Fisher chemicals scientific UK), L-lactic acid (88% aqueous solution, analytical-reagent grade, Loba chemie Pvt. Ltd chemical manufacturer in Mumbai, India), *Gum Acacia (gum Arabic)* was purchased from Sisco research laboratories Pvt.Ltd, Maharashtra, India), distilled water, were analytical grade and they were purchased from the local markets except film grade PLA beads whereas, PLA beads purchased from Aturker trade Istanbul Turkey and *euphorbia trigona mill* collected from Adama city, Ethiopia.

Materials: Some of the materials or equipment's which were used: Cutting knife, collecting cup, horizontal condenser, RBF, petri dish, chiller, measuring cylinder, temperature controlled reactor/oven, hot plate with magnetic stirrer, rod, petri dishes, measuring balance, DSC, TGA, FTIR, NMR, UV-Vis, UTM (universal tensile measurement).

3.2 Methods

3.2.1 Design experiments

The work focused on studying the effect of three factors (reaction temperature, mixing ratio and reaction time) on the grafting of *gum Arabica.* The response to be studied was percentage solubility and grafting efficiency. Levels of the factor are tabulated in the Table 3.1 and levels of factors were determined after preliminary investigation.

Table 3.1: Level of each factor Gum Arabica modification

S. No	Factor	Unit	Level	
			Low	High
1	Temperature	^{o}C	150	200
2	Time	hr.	2	3
3	Mixing ratio	Wt/Wt%	5%	15%

Design Expert® version 11.1.0.1 software was used for the randomized design of the experiment and analysis of variance (ANOVA) was used for the statistical significance of the experimental data. Box-Behnken method design was used to design the experiment. The experimental design involved 3 factors with 2 levels temperature, reaction time, and mixing ratio was chosen as independent variables.

3.2.2 Graft co-polymerization of lactic acid with Gum Arabic and euphorbia trigona mill.

3.2.2.1 Synthesis of lactic acid oligomers

Oligomers of lactic acid (OLLA) were synthesized by poly-condensation reaction. Oligomerization of lactic acid through poly-condensation was performed using temperature-controlled reactor. To carry out the reaction, 50 mL of lactic acid were initially charged to RBF reactor and reaction maintained at temperature of 150^{o}C for 150 min (Harshe et al. 2007).

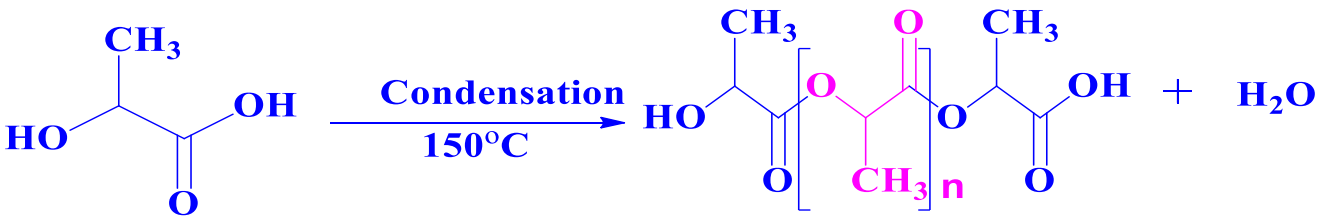

Scheme 3.1: Production of OLLA

3.2.2.1 Graft copolymerization of lactic acid (OLLA) oligomer with gum Arabic (OLLA-g-GA) and euphorbia trigona mill copolymer (OLLA-g-ETML).

The synthesis of OLLA-g-GA conjugate was developed based on a method reported by (Tripathi and Katiyar 2018). Experimental runs are tabulated in the Table 3.2 below with different mixing ratios and this ratio is determined by doing a preliminary experiment, in each experimental run specific amount of lactic acid and gum Arabica (according to design experiment were mixed in round bottom flask and mixed manually as shown in Figure 3.1. The RBF reactor was maintained at the specified temperature and time as given in Table 3.2 in temperature controlled reactor. Thereafter, the reactor was opened up, and cooled to collect the formed bio-conjugate, then taken into beaker washed with distilled to remove homo-polymer (unreacted lactic acid). Finally, the synthesized material *OLLA-g-GA* was converted into high viscous liquid form upon cooling which was kept on sealed container for further analysis.

Table 3.2: Grafting efficiency and percentage of solubility of modified gum at different condition

Sample	Mixing ratio (wt/wt%)	Time(hr)	Temperature(^{o}C)	(%)Solubility	G.efficiency(%)
GA-LAC	5	2.5	150	-	-
GA-LAC	10	2	150	-	-
GA-LAC	15	2.5	150	-	-
GA-LAC	10	3	150	-	-
GA-LAC	10	2.5	175	-	-
GA-LAC	15	2.5	175	-	-
GA-LAC	5	2	175	-	-
GA-LAC	5	3	175	-	-
GA-LAC	15	2.5	175	-	-
GA-LAC	10	2	200	-	-
GA-LAC	5	2.5	200	-	-
GA-LAC	15	2.5	200	-	-
GA-LAC	10	3	200	-	-

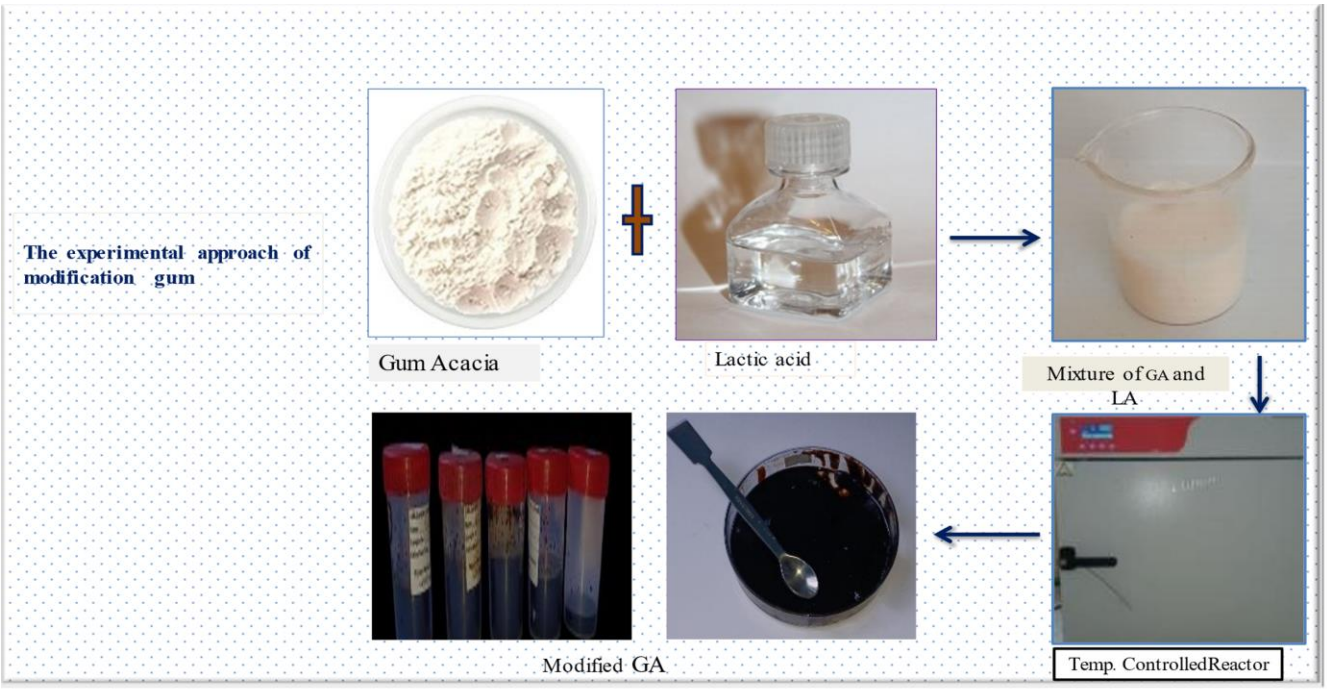

Figure 3.1**:** In situ Modification of LA-based modified GA

Similarly, the synthesis of OLLA-g-ETML was done by poly-condensation reaction as shown in Figure 3.2. In this process, lactic acid and ETML were taken in the proportion of 1:3 (wt/wt) and manually mixed in the round bottom flask (RBF) before synthesis (Yemiserach et al.2021). The RBF reactor maintained at 150^{o}C for 180 min, the reactor was opened up, and cooled to collect the formed bio-conjugate, then taken into beaker washed with distilled to remove homo-polymer (unreacted lactic acid). Finally, the synthesized material *OLLA-g-ETML* was converted into high viscous liquid form upon cooling which was kept on sealed container for further analysis.

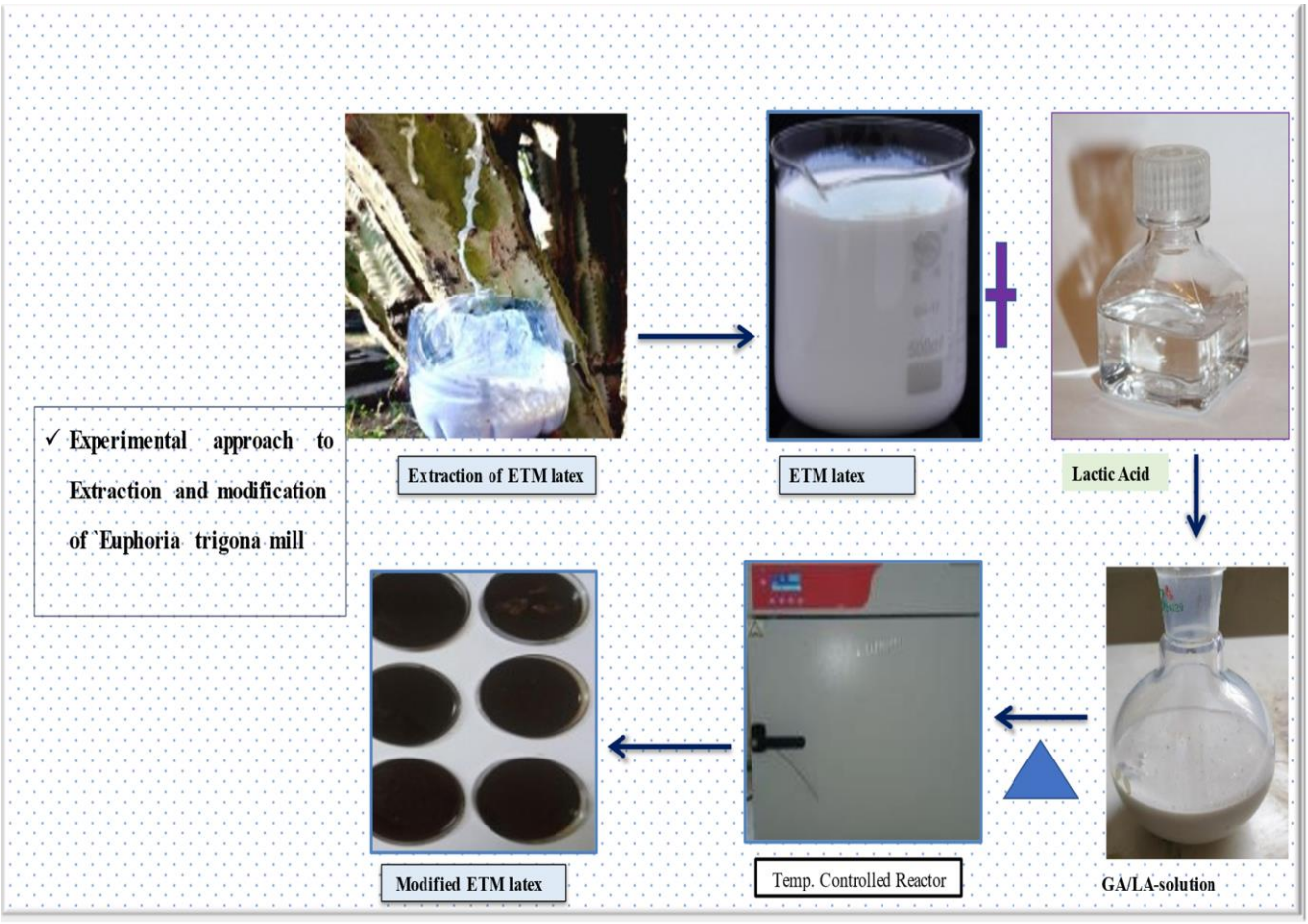

Figure 3.2: In situ Modification of LA-based modified ETML

3.3: Preparation of PLA based films

3.3.1 Bio conjugate (OLLA-g-GA and OLLA-g-ETML) /PLA based bio-composite films

Biopolymer films were prepared through solution casting method, *modified gums (OLLA-g-GA)* mixed with PLA solution. Based on the PLA mass, 1wt%, 2wt% and3wt% based films were prepared by dissolving OLLA-g-GA with pre-dissolved PLA (3g) in chloroform (90ml) with vigorous stirring magnetically at rotational speed of 20 rps at room temperature as shown in Figure 3.3. The PLA/OLLA-g-GA solutions were poured into Petri dishes and films were peeled off from the Petri dishes after 48 hr. Similarly, PLA/OLLA -g-ETML films were prepared by dissolving 3wt%, 5wt% and10wt% of ETML, based on PLA mass pre-dissolved PLA (3g) in chloroform (90ml) with vigorous stirring magnetically at rotational speed of 20 rps for 3 hr at room temperature as shown in Figure 3.4.

The formed films were peeled off from the Petri dishes after 48 hr. Neat PLA films were also prepared by the same procedure. Finally, the prepared films were stored in desiccator for further analysis.

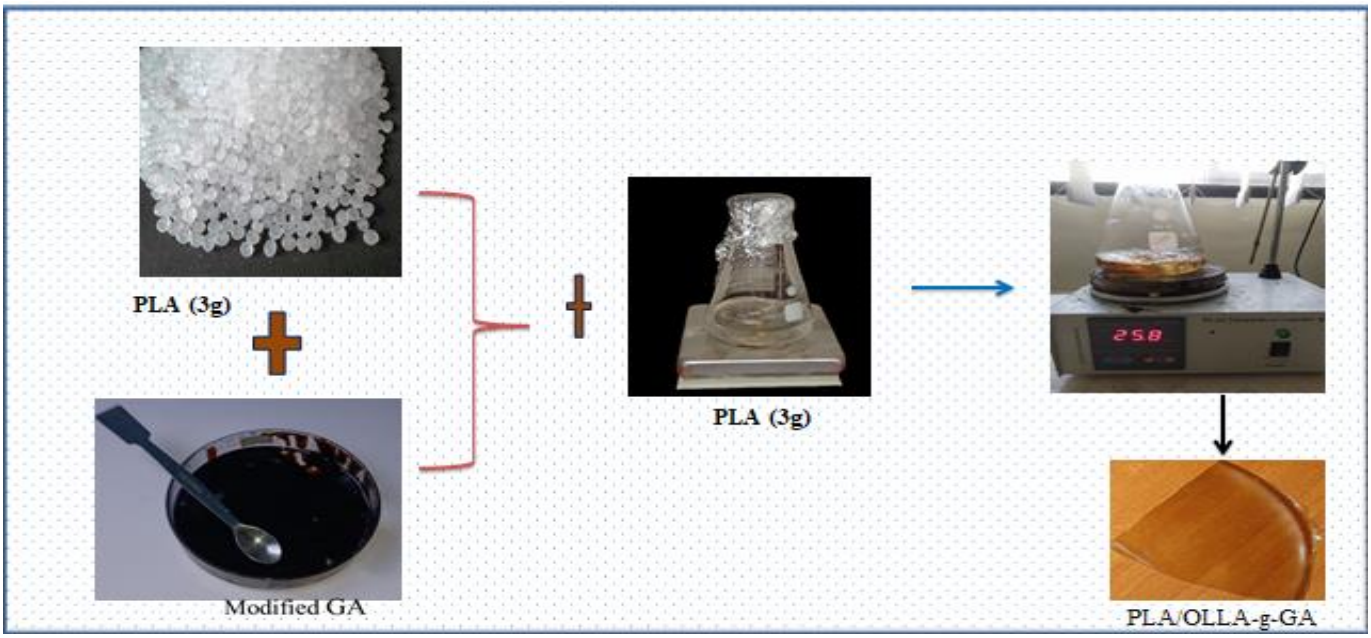

Figure 3.3: Preparation of PLA /OLLA-g-GA bio-composite film

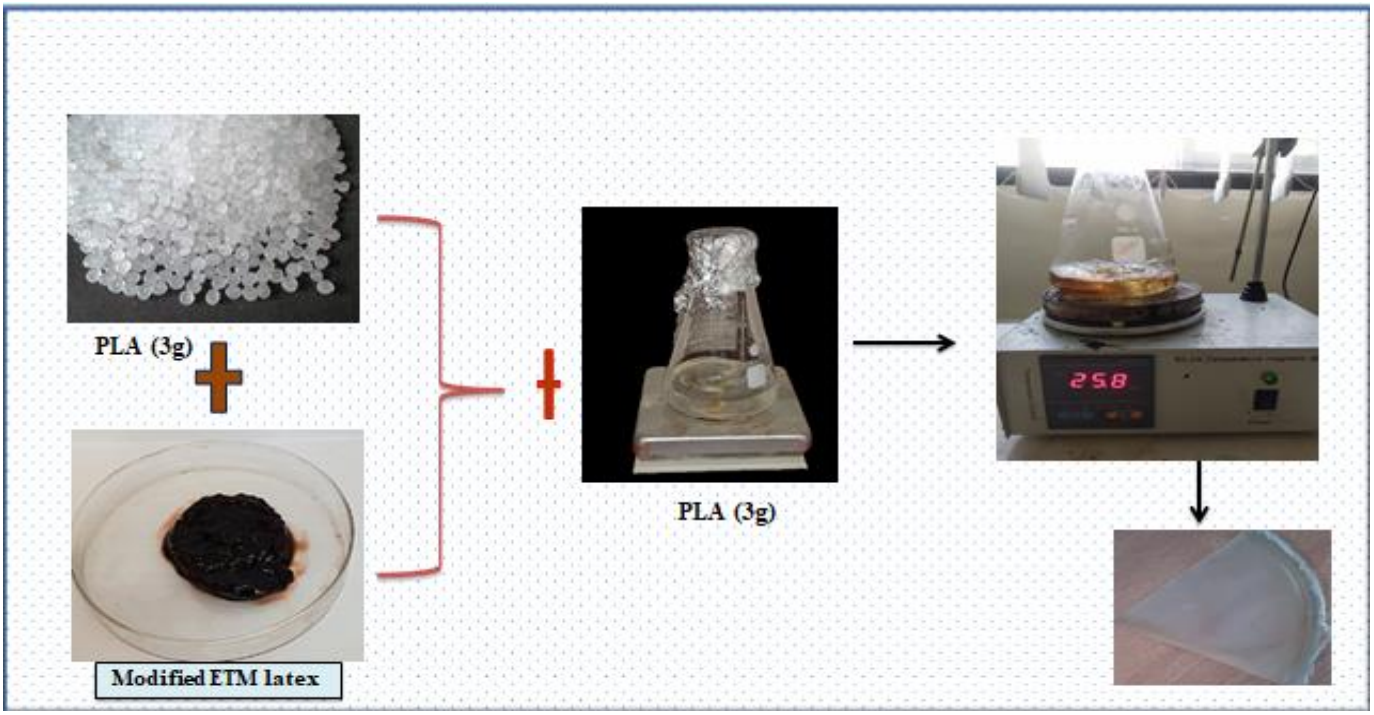

Figure 3.4: Preparation of PLA /OLLA-g-ETML bio-composite film

3.3.2 Master batch (OLLA-g-ETML- OLLA-g-GA)/PLA based bio-composite films

PLA/master batches films were prepared by using solution casting method, dissolving different formulation of OLLA-g-GA and OLLA-g-ETML with pre-dissolved PLA (3g) in chloroform (90ml). The selected modified ETML and GA was loaded into pre-dissolved PLA (3g) in chloroform (90ml) with different weight percent PLA/OLLA-g-GA (1%)-OLLA-g-ETM(3%),PLA/OLLA-g-GA(1%)-OLLA-g-ETM(5%),(PLA/OLLA-g-GA(2%)-OLLA-g-ETM(3%),PLA/OLLA-g-GA(2%)-OLLA-g-ETM(5%),PLA-OLLA-g-GA(3%),-OLLA-g-ETM(3%),PLA-OLLA-g-GA(3%)-OLLA-g-ETM(5%), in order to gets a uniform dispersion, the PLA (3g) is pre-dissolved by chloroform (90ml) and a master batch mixed with vigorous stirring magnetically at rotational speed of 20rps for 3hr at room temperature. The formed films were peeled off from the Petri dishes after 48 h. Neat PLA films were also prepared by the same procedure. Finally, the prepared films were stored in desiccator for further analysis.

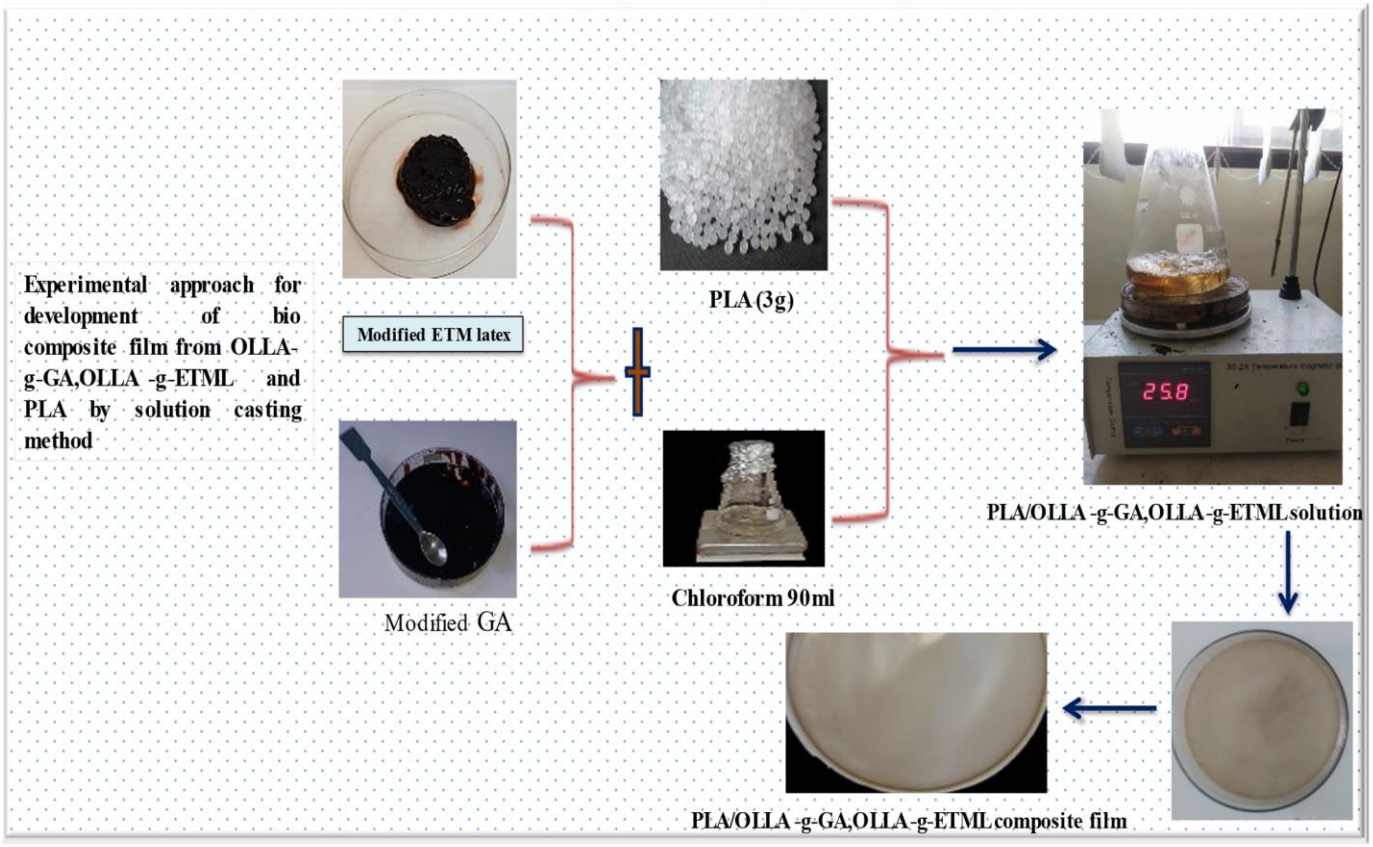

Figure 3.5: Preparation of PLA /master batch bio-composite film

3.4. Experimental Protocol for Characterizations of bio-conjugate

3.4.1. Solubility and grafting calculations

Solubility of all neat gums, OLLA and modified GA was evaluated by dissolving the samples in various solvents such as distilled water, acetone, chloroform and ethyl acetate at a concentration of 20 mg ml^{-1} at room temperature and the solutions were shaken for 10 min by water bath. The solutions were then filtered and the residual weight was measured to determine the percentage solubility (Tripathi and Katiyar 2018).

The grafting efficiency was calculated from equations (1).

$$\text{Grafting efficiency (\%)} = \left(\frac{W1 - Wo}{W2} X100\right) \ldots \ldots \ldots \ldots \ldots \ldots \ldots \ldots \ldots \ldots \ldots \ldots \ldots \ldots \ldots \ldots \ldots \ldots \ldots \ldots \ldots \; eqn. 3.1$$

$$\text{Percent of solubility (\%)} = \left(\frac{W3 - W4}{W5} X100\right) \ldots \ldots \ldots \ldots \ldots \ldots \ldots \ldots \ldots \ldots \ldots \ldots \ldots \ldots \ldots \ldots \ldots \ldots \ldots \; eqn. 3.2$$

Were, W_0: weight of neat GA; W_1: weight of grafted copolymer; W_2: weight of lactic acid, W_3: mass of filter paper with filtrate and filter W_5: mass of initial filter paper and W_6: initial mass of sample.

3.4.2. Nuclear magnetic resonance analysis OLLA, OLLA-g- GA, ETUM and OLLA-g- ETUM

Proton nuclear magnetic resonance (^{1}H NMR) and ^{13}CNMR) analysis was performed for OLLA, *OLLA-g-*GA, ETML and OLLA-g-ETML samples by using Bruker Ascend^{TM} 600 nuclear magnetic resonance spectrometer o analysis lactic acid grafting GA and ETML. The OLLA, OLLA-g- GA of ~10 mg/ml concentration was prepared by dissolving the samples in deuterated chloroform (CDCl3). The prepared solutions were filtered and transferred into NMR tubes for analysis at room temperature. Similarly done for ETML and OLLA-g-ETML. For ^{1}H NMR, chloroform (at 7.26 ppm) was used as the reference line and 77 ppm for ^{13}C NMR.

3.4.3 Fourier transform infrared spectroscopy (FTIR) analysis GA, OLA, OLLA-g- GA, ETUM and OLLA-g- ETUM

IR spectra of synthesized bio-conjugate were measured using an FTIR spectrometer (Nicolet Avatar 360, Madison, WI). Samples were diluted at 1:20 with KBr before acquisition. A background of pure KBr was acquired before the sample was scanned. The FTIR spectra of lactic acid neat GA, OLLA-g-GA raw ETM, OLLA-g-ETML and lactic acid oligomer were recorded raw by using FTIR spectrophotometer (model IS50-ABX) in the range of between 400 and 4000 cm-1; The recorded

spectra were analyzed and compared to study the grafting reaction of GA and ETUM with lactic acid oligomer.

3.4.4 Thermal gravimetric analysis GA, OLLA-g- GA, ETML and OLA-g- ETML

Thermal stability of the GA, OLLA-g- GA (3%), Raw ETML and *OLLA-g- GA* were determined by thermo gravimetric analysis. The analysis was performed in the range from 25^{o}C to 800^{o}C at a rate of 10 ^{o}C/min heating range under a controlled inert atmosphere by measuring their mass as a function of temperature. The behavior of mass loss and decomposition temperature was observed from the TGA thermograph.

3.5. Experimental Protocol for Characterizations of films

3.5.1 Surface morphology

The dispersion quality and degree of self-aggregation of PLA/*OLLA-g-GA* (1,2,3and5%), PLA- *OLLA-g-ETML* (3,5,10) and PLA-master batch samples was investigated using an optical microscope using a LV-100 nikon Eclipse equipped with a Nikon slight camera at 50X magnification.

3.5.2 Optical properties

The transmittance of neat PLA, PLA/OLLA-g-GA (3%), PLA/OLLA-g-ETML (5%), and PLA/master batch films processed by hot-pressing of mixtures obtained by Brabender plastograph was assessed by ultraviolet-visible (UV-VIS) spectroscopy (Orion AquaMate 8000, Thermo Scientific Water Analysis Instrumentation, Chelmsford, MA, USA). The scans were carried out from 300 to 800 nm with a scan speed of 240 nm/min (Rhim et al. 2009). The transparency of the films was calculated according to (Han and Floros 1997), as follows:

Transparency values=$\left(log\frac{\mathrm{T600}}{x}X100\right)$ …… $eqn.$ 3.3

Where T600 is the fractional transmittance at 600 nm; and x: is the film thickness in mm.

3.5.3 Fourier transformed infrared spectroscopy (FTIR)

FTIR spectra of samples are collected by Spectrum FTIR (Make: Frontier, Perkin Elmer). IR spectra are recorded in transmission mode with attenuated total reflectance (ATR) assembly. Extruded film is placed on KBr crystal in the wavenumber range (4000–600 cm^{-1}). A background spectrum is collected prior to analysis to compensate the influence of humidity and carbon dioxide present in air by

subtracting spectra. FTIR analysis is carried out to investigate the possible interaction between the PLA and OLLA-g-GA, OLLA-g-ETML master batch.

3.5.4 Mechanical Characteristics

Before preparing the sample for the test, the bio composite films of PLA/*OLLA-g*-GA, PLA/*OLLA-g*-ETM and PLA/ *OLLA-g*-GA- *OLLA-g*-ETM (master batch) were conditioned overnight, under a conditioning oven at 20°C and 65.78% humidity. After this step sample was prepared in 100 cm length by 13cm width by using ruler, pen (marker) and scissor.

This test was performed By the Ethiopian Conformity Assessment Enterprise, following the ASTM D638 tensile strength measuring procedure using universal tensile strength testing machine. The force at break and tensile strength was done simultaneously.

3.5.5 Thermal gravimetric analysis of bio composite

Thermal stability of the synthesized neat PLA, master batch (PLA/*OLLA-g*-GA (3%)- *OLLA-g*-ETML (5%) and bio-composite (PLA-*OLLA-g*-GA(3%)-*OLLA-g*-ETML(5%)) were determined by thermo gravimetric analysis. The analysis was performed in the range from 25^0C to 700^0C at a rate of 10^oC /min heating range under a controlled inert atmosphere by measuring their mass as a function of temperature. The behavior of Wight mass loss and decomposition temperature was observed from the TGA thermograph through iSolution DT software. For preparing thin films for the optical microscope, the composite were melted on a glass slide at 150 °C for 10 min and another glass slide was put on the melted samples as a cover glass to prepare a flat thin film for each formulate

3.5.6 Thermal degradation study

Thermal degradation kinetics is a handful tool to understand deeply the degradation mechanisms and analyze the thermal degradation process, which can be achieved through thermo gravimetric analysis (TGA). Kinetic analysis can help to calculate accurately the activation energy (E_a) as a function of the degree of conversion, order of reaction (n) and the pre-exponential factor (A).

In most cases, the rate of degradation of polymers is assumed to be governed by a single step kinetic equation, in which the rate of change of mass is dependent on the temperature rate constant k (T) and the reaction model f (α).

$$\frac{dt}{d\alpha} = k(T) = \beta \frac{d\alpha}{dT} = Ae^{(-E/_{RT})} f(\alpha) \dots \dots \dots \dots \dots \dots \dots \dots \dots \dots \dots \dots \dots \dots \dots \dots \dots \dots \dots \dots \dots \dots \quad (3.4)$$

For constant heating rate β= dT/dt, infinitesimal change of conversion (α) with respect to temperature can be expressed as function of heating rate (β), activation energy (E), R is the gas constant (8.3145 J mol^{-1} K^{-1}) and temperature (T). This fundamental expression coupled with the kinetic model function f(α) can be considered as foundation for kinetic triplet calculation. The conversion values (α) and the reaction rate constant (k) were obtained from thermogravimetric analysis (TGA) by weight loss at different heating rate (β) and from the Arrhenius equation as mentioned in Eqs. (3.1)

$$\alpha = \frac{wi-w}{wi-wf} \quad (3.5)$$

The temperature dependence of the rate constant k (T), for the process is assumed to follow the Arrhenius equation:

$$k = Ae^{-E/RT} \quad (3.6)$$

Where, α is the decomposed fraction at any given temperature, wi = the weight at given temperature, wi = the weight at chosen temperature, wf = the weight at final temperature, Ea = activation energy, β = heating rate, T = absolute temperature (K).

From the generalized rate equation (Eq. (3.3)), it can be clearly observed that the rate of degradation is influenced by the Arrhenius equation parameters (E and A) and kinetic model f (α). Therefore, in order to understand the reaction phenomenon, the kinetics triplet (E, A and f (α)) need to be determined carefully (Pal and Katiyar 2017a; Patwa, Singh, et al. 2019).

In order to determine the kinetic triplet (A, E and f(α)), various methods have been developed. They are classified as isoconversional and model fitting methods. In this study five isoconversional models (i.e., Augis and Bennett, Kissinger, Friedman,,Ozawa Flynn Wall and Kissinger Akahira Sunose model) and one model fitting methods (Coats-Red fern) are considered for determining the kinetics of thermal degradation and thermal stability of pristine PLA and PLA/master batch bio-composites.

Isoconversional analysis

Augis and Bennett method

According to Augis & Bennett method, the activation energy can be determined by the

$$\ln\left(\frac{\beta}{Tm-To}\right) = \ln A - \left(\frac{Ea}{R}\right)\frac{1}{Tm} \quad (3.7)$$

Where, Tm and To are peak or maximum temperature and onset temperature of the DTG peak respectively. The activation energy E_a can be obtained from the slope of the straight line in $\ln\left(\frac{\beta}{Tm-To}\right)$ versus $\frac{1}{Tm}$ (Saraswat et al .2016)

Kissinger model

Kissinger method is one of the widely used isoconversional methods to determine activation energy of solid-state decomposition reaction based on the study of rate equation at maximum decomposition temperature. It considers the changes in temperature at which maximum weight loss occurs with respect to the change in heating rate and it depends on the reaction activation energy. As described in Eq. (3.5) activation energy can easily be determined from the slope of the graph ln (β /Tm^2) vs 1/Tm, where Tm is the temperature at maximum weight loss (Tesfaye et al. 2016; Sergey Vyazovkin et al. 2011).

$$\ln\left(\frac{\beta}{Tm2}\right) = \ln\left(\frac{AR}{E}\right) - \frac{E}{RTm} \quad (3.8)$$

Friedman (FD) method

The differential isoconversional method suggested by Friedman is based on Eq. (3) that leads to:

$$\ln\left(\beta\frac{d\alpha}{dT}\right) = \ln A + lnf(\alpha) - \frac{E}{RT} \quad (3.9)$$

For a constantα, the plot of $\ln\left(\frac{d\alpha}{dT}\right)$ vs. 1/T obtained from curves recorded at several heating rates should be a straight line whose slope gives us the value of E. It is obvious from Eq. (6) that if the function f(α) is constant for a particular value of α , then the sum lnf(α)+lnA/β is also constant (Chrissafis 2009).

Ozawa Flynn Wall (O-F-W) Model

OFW model is an integral isoconversional method derived by using Doyle's approximation using multiple heating rates TGA data. The important assumption in this model is that the conversion function of $f(\alpha)$is independent with the alteration in heating rate for all values of the degree of conversion α. It follows Arrhenius type temperature dependence without any assumptions related to the form of the kinetic equation. The main advantage of this method is that the calculation of activation energy (E) had no relationship with real degradation process, and also the reaction order was not necessary.

The model expression is given by

$$Log\ \beta = \frac{logAE}{f(\alpha)R} - 2.315 - \frac{0.4567E}{R} \dots\dots\dots\dots\dots\dots\dots\dots\dots\dots\dots\dots\dots\dots\dots\dots\dots\dots\dots\dots\dots\dots\dots\dots\dots\dots\dots. (3.10)$$

The plot of log β vs. 1/T gives a straight line whose slope is equal to –0.4567E/RT from which activation energy can be calculated. Pre-exponential factor is calculated from the intercept of the resulting straight line by assuming a reaction model (Thomas et al. 2020).

Kissinger akahira sunose (K-A-S) model

Kissinger method calculates the activation energy (E) uses the maximum decomposition temperature (Tp) at which the rate of mass loss is the highest Kissinger method calculates the activation energy (E) uses the maximum decomposition temperature (Tp) at which the rate of mass loss is the highest. This method is most widely used for analysis of single heating rate TGA data (Habibu et al. 2019). The equation for this method is

$$Log\ \left(\frac{\beta}{T^2}\right) = ln\left(\frac{AR}{E\ f(\alpha)}\right) - \frac{E}{RT} \dots\dots\dots\dots\dots\dots\dots\dots\dots\dots\dots\dots\dots\dots\dots\dots\dots\dots\dots\dots\dots\dots\dots\dots\dots\dots\dots. (3.11)$$

Model fitting methods

Coats-Redfern model

This is an integral method that involves the mechanism for thermal degradation. The activation energy is calculated based on the f(α) functions according to equation (2.12) derived by applying an asymptotic approximation (Snegirev et al. 2017)

$$ln\frac{g(\alpha)}{T2} = ln\left[\frac{AR}{\beta E}\left(1 - \frac{2RT}{E}\right)\right] - \frac{E}{RT} \dots\dots\dots\dots\dots\dots\dots\dots\dots\dots\dots\dots\dots\dots\dots\dots\dots\dots\dots\dots\dots\dots\dots\dots\dots\dots. (3.12)$$

This method is most widely used for analysis of single heating rate TGA data. The equation for this method. The Coats–Redfern method assumes that the activation energy does not depend on the degree of conversion. The activation energy for each model is acquired using the slope obtained from the plot of $ln\frac{g(\alpha)}{T2}$ against 1/T. Achievement of high correlation coefficient (R^2), as well as agreement between the activation energy obtained by this method compared with those obtained by previous methods, allows for the selection of the kinetic model. The f(α) expressions for various mechanisms are listed in table 3.4 and the same values of α were used as in the isoconversional methods.

Table 3.3: Kinetic model models and their mathematical explanation

Kinetic Model	Symbo	f(a)	g(α)
n-order reactions			
First order	F_1	$1 – \alpha$	$-\ln (1 - \alpha)$
Second order	F_2	$(1 - \alpha)^2$	$(1 -\alpha)-1-1$
n th order	F_n	$(1 - a)^n$	(1- α)-n-1
Diffusion			
1-D diffusion	D_1	1/2a	α^2
2-D diffusion	D_2	$[- \ln(1 - a)]-1$	$[1 - (1 - \alpha)^{1/3}]^2$
3-D diffusion	D	3/2(1 − a) 2/3h 1 − (1 − a) 1/3i	- -
-Jander			
Phase-boundary reactions			
Contracting area	R_2	$2(1 - \alpha)^{1/2}$	$1 - (1 - \alpha)^{1/2}$
Contracting volume	R_3	$3(1 - \alpha)^{1/3}$	$1 - (1 - \alpha)^{1/3}$
Nucleation and growth			
Avrami-Erofeev	A_2	$2(1 - \alpha)[-\ln(1 - \alpha)]^{1/2}$	$[-\ln(1 - \alpha)]^{1/2}$
Avrami-Erofeev	A_3	$3(1 - \alpha)[-\ln(1 - \alpha)]^{2/3}$	$[-\ln(1 - \alpha)]^{1/3}$
Avrami-Erofeev	A_4	$4(1 - \alpha)[-\ln(1 - \alpha)]^{3/4}$	$[-\ln(1- \alpha)]^{1/4}$
Avrami-Erofeev	$A_{3/2}$	$3/2(1 - \alpha)[-\ln(1 - \alpha)]^{1/3}$	$[-\ln(1 - \alpha)]^{2/3}$

Table 3.4: Mathematical models used for thermal degradation kinetics of neat PLA and PLA/master batch kinetics

Methods	Expressions	Plots
Augis and Bennett method	$\ln\left(\frac{\beta}{Tm - To}\right) = \ln A - \left(\frac{Ea}{R}\right)\frac{1}{Tm}$	$\ln\left(\frac{\beta}{Tm-To}\right)$ vs $\frac{1}{Tm}$
Kissinger mode	$\ln\left(\frac{\beta}{Tm2}\right) = \ln\left(\frac{AR}{E}\right) - \frac{E}{RTm}$	$\ln\left(\frac{d\alpha}{dT}\right)$ vs.1/Tm
Friedman method	$\ln\left(\beta\frac{d\alpha}{dT}\right) = \ln A + lnf(\alpha) - \frac{E}{RT}$	$\ln\left(\frac{d\alpha}{dT}\right)$ vs. 1/T
Flynn–Wall–Ozawa (F–W–O)	$log(\beta) = \left\{log\frac{EA}{g(\alpha)R} - 2.315\right\} - \frac{0.457E}{R}$	*log(β) vs. (1/ Tα)*
Kissinger–Akahira–Sunose (K–A–S)	$Log\ (\frac{\beta}{T\hat{}2}) = ln(AR/(E\ f(\alpha))) - E/RT$	$ln(\beta/T^{\alpha 2}) vs 1/T\alpha$
Coats–Redfern (C–R)	$ln\frac{g(\alpha)}{T2} = ln\left[\frac{AR}{\beta E}\left(1 - \frac{2RT}{E}\right)\right] - \frac{E}{RT}$	Y vs. (1/T)

3.5.7 Differential Scanning Calorimeter (DSC):

Crystallization and melting behavior studies of neat PLA and PLA based bio composites were investigated on a differential scanning calorimeter (DSC). DSC measurements of the neat PLA, PLA-*OLLA*-*g*-GA (3%) *PLA*-*OLLA*-*g*-ETUM (5%) master batch((PLA-*OLLA*-*g*-GA(3%) -*OLLA*-*g*-ETUM(5%) after annealing time of 30min 1:30hr and 2.5hr were performed on DSC Q200 (TA Instruments, New Castle, DE, USA) over a temperature range from 25 to 200 °C at a heating rate of 10 °C/min and then held for 5 min, and then samples were cooled down to 25 °C at a cooling rate of 5 °C/min. The second heating was performed at the same range and heating rate to determine glass transition temperature (Tg), crystallization temperature (Tc), melting temperature (Tm). The Degree of crystallinity of samples were calculated using.

$$Xc = \left(\frac{\Delta Hm}{Wf\ x\ \Delta Hm\ o}\right) x100 \ldots\ldots\ldots\ldots\ldots\ldots\ldots\ldots\ldots\ldots\ldots eqn\ (3.13)$$

Where ΔHm is the melting enthalpy, ΔHm^{o} is the 100% crystalline melting enthalpy for PLA and 100% crystalline PLA and Wf is the polymer weight fraction in the blend.

3.5.8 Antimicrobial Activity

Four typical food pathogens including two Gram-positive bacteria, *P.aeruginosa* ATCC27853, *S.pyogen* ATCC19615, and two Gram-negative bacteria, *S.aureus* ATCC2592 and Escherichia coli ATCC25922 were used to test the antimicrobial activity of neat PLA film, 3%GA/PLA, 5%ETM/PLA and 3%GA-5%ETM/PLA, 5%ETM/PLA films. The agar medium was prepared within dissolving 38 g of Mueller Hinton agar medium (MHA) in 1000 mL of distilled water autoclaved at 121 °C for 15 min. The autoclaved medium was poured into sterile plates (20-25 mL/plate) and the plates were allowed to solidify under sterile condition at room temperature (Rhim et al. 2006). After solidification, the plates were seeded with overnight grown culture approximately 1.5 X 10^8 CFU/mL by swabbing evenly on to the surface of the medium with a sterile cotton swab. According to the methods described by Clinical and Laboratory Standards Institute (CLSI) with slight modification of PLA/OLLA-g-GA (3%), PLA/OLLA-g-ETML (5%) and PLA/OLLA-g-GA (3%)- OLLA-g-ETML (5%) bio-composite films were cut in the diameter of approximately 6 mm (as discs) using puncher. The 6mm PLA and PLA composite biofilm were placed and position on the surface of the medium with sterile forceps and gently pressed down to ensure contact with the minimum inhibitory concentration (MIC). Ampicillin was used as standard antibiotics and then plates were inverted and then incubated at 37 °C for 24 hrs. After incubation the inhibition the zones of growth inhibition around each of the antibiotic disks against *E. coli*, *S.aureus*, *P. aeruginosa and S.pyogen* were measured to the nearest millimeter. Zone halo of growth produced by the synthesized biofilms were evaluated by measuring the diameter (mm) of the clear zone around the disc against the test organisms using a ruler.

CHAPTER FOUR

4. RESULT AND DISCUSSION

4.1 Synthesis and Characterization lactic acid oligomer grafted Gum Arabic and *Euphorbia trigona mill* latex

During grafting of GA, the bubbling in the reaction mixture was observed that signifies the formation of water molecules which was condensed out in the condenser (Tripathi and Katiyar 2018). After reaction, formation of dark brown color in all the composition (at different temperature and reaction time) was observed. During this reaction, the free radicals were generated on polar groups of the polysaccharide gum backbone and LA monomer (Alang et al. 2012). The free hydroxyl groups and amine group in GA molecules which were grafted with the reducing end groups (carboxylic) of the LA molecules. In similar manner the grafting reaction took place between hydroxyl group of *euphorbias trigon mill* latex and the carboxylic group of lactic acid via a condensation reaction. During the synthesis of OLLA-g-ETM bio-conjugate it's believed that the reaction mechanism consists both oligomerization of lactic acid and attachment of the OLLA to the back bone of ETM latex.

4.1.1 Solubility study

The simplest method for verifying the transformation of a hydrophilic GA, ETML into a hydrophobic nature. Solubility test of all GA, ETML, OLLA modified ETML and modified gums was performed in a series of solvents such as water, acetone, chloroform and ethyl acetate as shown in Table 4.1. It clearly showed that the solubility of GA and ETML was different from that of the modified ones. Due to replacement of polar groups present on GA and ETML backbone by long hydrophobic alkyl groups the modified GA and ETML (*OLLA-g-*GA and *OLLA-g-* ETML) converted into hydrophobic property. The strong intra-molecular hydrogen bonding was also one of the important factors for insolubility of modified GA and ETML in water. The difference in solubility confirms that the chemical modification occurred on GA, ETML (Bucheery 2001; Indah Sari et al. 2017)

Table 4.1: Solubility of neat GA, ETML, OLLA, OLLA-g-GA, and OLLA-g-ETML

Samples	Water	chloroform	Ethyl acetate	Acetone
GA	++	--	-	-
OLLA-g-GA	--	++	+	+
ETML	++	-	-	+
OLLA-g-ETML	--	++	+	+
OLLA	-	++	+	+

+' denotes slightly soluble, '++' denotes strongly soluble, '−' denotes insoluble and '−−' denotes strongly insoluble.

4.1.2 ANOVA for Quadratic model

The experimental results of the effect of three variables which were time, temperature and mixing ratio were designed using the box Behnken of ANOVA and the results of the analysis of variance were presented in the following table and discussed.

4.1.2.1 Optimization of temperature, time and mixing ratio process variables

In this design of experiment, finding the right combination of process variables that would result in high grafting products was sought. In this context, with fewer experimental sequences and less time, experimental designs may potentially support in studying the effects of individual process variables and their interactions. In this study, BBD was developed using Design Expert (DX, 11.1.0.1; Stat Ease Inc., Minneapolis, USA) for optimizing three different independent process variables i.e., Temperature, Time and Mixing Ratio on grafting efficiency and percentage solubility, the dependent factors. Sequential experiments were carried out to develop the process. Appropriate statistical trials were run, the best fit model was chosen, and independent variables that could generate optimal responses were further determined. Design Expert Version 11.1.0.1 provided 17 test formulations for BBD; the result of grafting efficiency and percent solubility for all the 17 formulations is summarized in Table 4.2.

Table 4.2: Grafting efficiency and percentage of solubility of modified gum at different condition

Sample	Mixing ratio (wt/wt %)	Time (hr)	Temperature (^{o}C)	(%) Solubility	Grafting efficiency (%)
GA-LAC	5	2.5	150	55.06	67.1
GA-LAC	10	2	150	59.6	68.73
GA-LAC	15	2.5	150	61.66	68.67
GA-LAC	10	3	150	62.5	64.12
GA-LAC	10	2.5	175	75.6	68.79
GA-LAC	15	2.5	175	59.1	56.83
GA-LAC	5	2	175	64.5	51.489
GA-LAC	5	3	175	74.29	52.18
GA-LAC	15	2.5	175	76.1	48.6
GA-LAC	10	2	200	49.1	53.555
GA-LAC	5	2.5	200	52.2	54.1
GA-LAC	15	2.5	200	68.23	49.67
GA-LAC	10	3	200	64.2	51.27

4.1.2.2 Effect of formulation variables on the grafting efficiency and solubility

Analysis of variance (ANOVA) results for both models are given in Tables 4.3 and Table 4.4. The developed model "F-value" was found to be 28.61 (grafting efficiency) and 8.03 (percentage solubility), depicting that both these models are statistically significant. Large P values may occur due to noise and there is only 0.01% to 0.017% chance. Values of "Prob> F" were observed to be less than 0.0500, indicating that both the model terms are significant.

The F-value of the model is high 28.61, and 8.03 indicating that it is significant. Just 0.01% of the time does noise causes such a strong F-value. The model expressions are important if the Prob > F value below 0.05 observed to be less than 0.0500, indicating that both the model terms are significant.

Table 4.3: ANOVA of quadratic response surface model for grafting efficiency

Source	Sum of Squares	df	Mean Square	F-value	p-value	
Model	1051.09	9	116.79	28.61	0.0001	Significant
A-Temperature	450.90	1	450.90	110.46	< 0.0001	
B-Time	5.44	1	5.44	1.33	0.002860	
C-Mixing Ratio	9.90	1	9.90	2.43	0.001633	
AB	1.36	1	1.36	0.3325	0.04823	
AC	9.09	1	9.09	2.23	0.01793	
BC	0.2970	1	0.2970	0.0728	0.03951	
A^2	7.22	1	7.22	1.77	0.00253	
B^2	287.67	1	287.67	70.47	< 0.0001	
C^2	255.56	1	255.56	62.61	< 0.0001	
Residual	28.57	7	4.08			
Lack of Fit	9.76	3	3.25	0.6913	0.6034	not significant
Pure Error	18.82	4	4.70			
Cor Total	1079.67	16				

T*able* 4.4: ANOVA of quadratic response surface model for percentage solubility

Source	Sum of Squares	df	Mean Square	F-value	p-value	
Model	998.29	9	110.92	8.03	0.0059	Significant
A-Temperature	3.24	1	3.24	0.2345	0.04430	
B-Time	179.46	1	179.46	13.00	0.0087	
C-Mixing Ratio	84.11	1	84.11	6.09	0.0430	
AB	37.21	1	37.21	2.69	0.01447	
AC	22.23	1	22.23	1.61	0.02451	
BC	0.0240	1	0.0240	0.0017	0.050067	
A^2	641.42	1	641.42	46.45	0.0002	
B^2	8.34	1	8.34	0.6040	0.04625	
C^2	3.96	1	3.96	0.2869	0.00588	
Residual	96.67	7	13.81			
Lack of Fit	66.67	3	22.22	2.96	0.1607	not significant
Pure Error	30.00	4	7.50			
Cor Total	1094.96	16				

Model terms A, B, C, AB, AC, BC, A2 B^2 and C^2 are found to be significant for both models. P values for both models were observed to be is values for both models were observed to be is < demonstrating the level of significance for developed models. If the p-values are greater than 0.10, the model terms are insignificant. Besides p value, other statistical parameters such as coefficient of determination or R^2, adjusted R^2 (R^2 adj), predicted R^2 (R^2 pred), coefficient of variation (CV %) were also used to evaluate the competence of developed models. R^2 values and R^2 adj for grafting efficiency was found to be 0.974 and 0.945. Similar values were obtained for percentage solubility (R^2=0.911 and R^2 adj 0.800) as well. The standard deviation for both the models were also found to be small i.e., 0.94 and 8.19 respectively. R^2 values close to unity and smaller standard deviation values indicate better predicting response of the model developed. Similar values were obtained for percentage solubility (R^2=0.989 and R^2 adj =0.963) as well. R^2 values close to unity and a smaller standard deviation value indicates better predicting response of the model developed. The predicted R^2 value was found to be in close agreement with the adjusted R^2. “Adeq Precision” determines the signal to noise ratio, of which a ratio more than 4 is desirable. In this study, the observed ratio for both models was found to be 99.42

and 5.92, respectively signifying the presence of adequate signal for navigating the design space (Kumari and Gupta 2019).

4.1.2.3 Model analysis via 2D contour graphs and 3-D surface plots.

To analyze the combined effect of the factors on grafting efficiency, graphical representation of the regression equation i.e., 2D contour graphs and 3-D surface plots were employed (Fig. 4.1A) and Fig.4.1B). The 2D contour plot represents that high grafting efficiency of GA was obtained in reaction time of 150min and at temperature of 168^{o}C, whereas maximum percentage solubility was found at slightly higher reaction time and temperature of 174^{o}C, 170min 10wt/wt%. But, when temperature was increased to 200^{o}C, marked decrease in the grafting efficiency and percentage solubility was witnessed as depicted from 2D contour plots (Figure 4A and 4B). RSM (BBD) analysis revealed that the grafting efficiencies decreased with increase in temperature and mixing ratio. Maximum grafting efficiency of GA was observed at 168^{o}C and 150hr whereas maximum grafting efficiency at 174^{o}C and 170min. The decrease in grafting efficiency at high temperature due degradation of the GA might be happen, while the decreasing of grafting efficiency at higher mixing ratio due to the unavailability of LA monomers for chain propagation. So, all the available active sites of GA molecules were not consumed by LA. Whereas, another possible reason for reduction was due to the formation of more homo-polymer through competing reaction process at high temperature (Alang et al. 2012). This simultaneous decrease in grafting efficiency and percentage solubility at high temperature indicated that optimum grafting of reached and was found to be constant temperature (Alang et al. 2012).

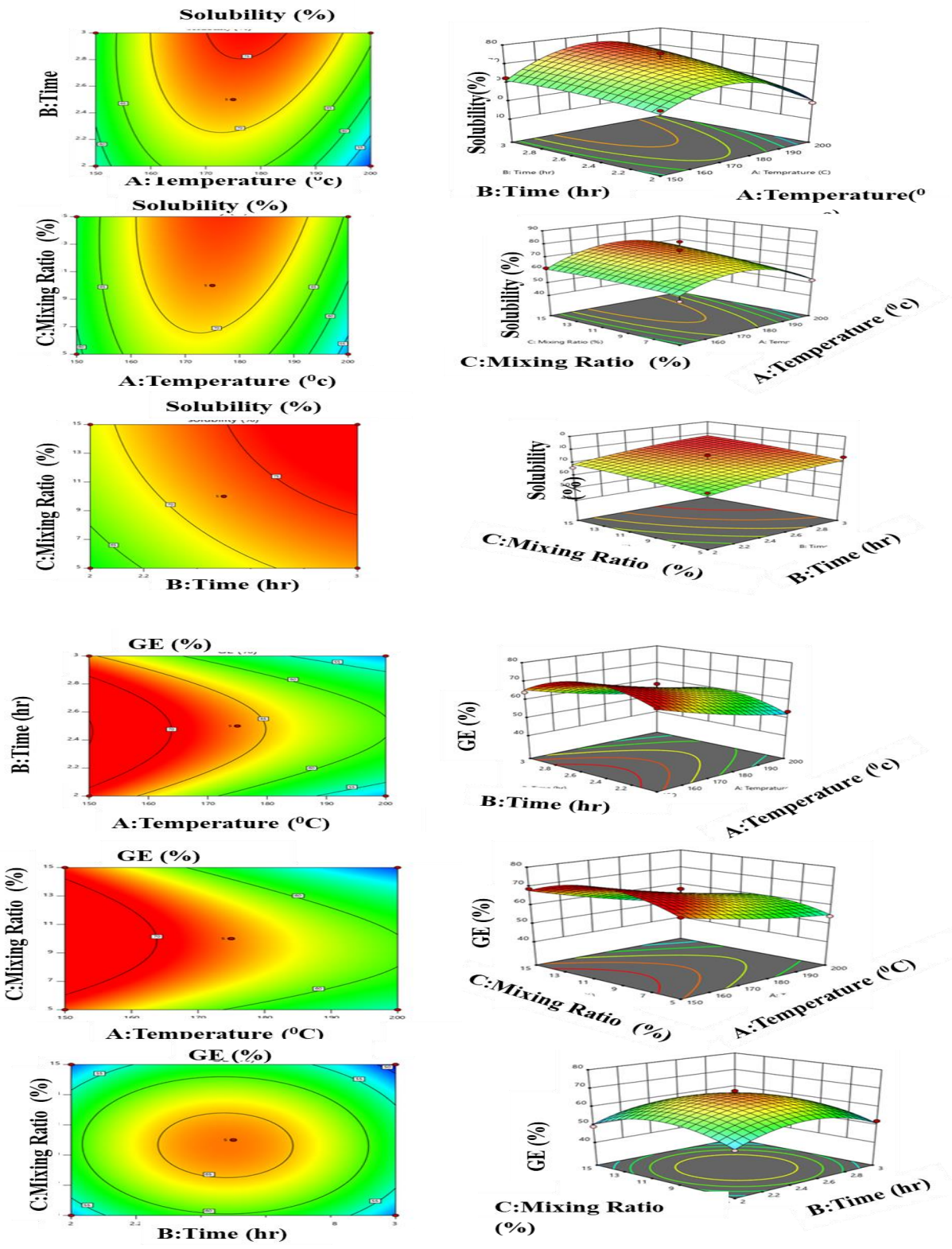

Figure 4.1: 2D Contour and 3D surface plots (a) Grafting efficiency (b) Percentage solubility

Model validation. Experiments were performed under the predicted optimal conditions to verify optimization results. Design expert software predicted significant grafting efficiency (68.75) and percent solubility (71.6%) under optimized conditions. The experimental results closely agreed with those obtained using RSM (box-benken) and therefore validated the findings of response surface optimization.

Table 4.5*:* Grafting Response Variables, Obtained Linear Regression Models

Response variable	Regression model	R^2 (%)
Grafting Efficiency	$66 - 7.51A - 0.825B - 1.11C + 0.5825AB - 1.51AC - 0.2725BC + 1.31A^2 - 8.27B^2 - 7.79B^2$	97.4
Percentage Solubility	$72.6 - 0.6363A + 4.74B + 3.24C + 3.056AB + 2.36AC + 0.0775BC - 12.34A^2 - 1.41B^2 - 0.970C^2$	91.1

Where A Represents Temperature B Time and C Represents GA Percent in the lactic acid

Similar optimization was done for *euphorbia trigona mill* by yemisrach et.al (2021) and the maximum grafting efficiency and percentage solubility was obtained at 150 ^{o}C, 180min and 1:3mixing ratio.

4.1.3 Chemical Structure Analysis/NMR

4.1.3.1 Structural analysis of OLLA bio conjugates and modified Gum Arabic

Both the proton NMR (^{1}H NMR) spectra and carbon NMR (^{13}C NMR) were particularly useful to confirm the lactic acid oligomer grafting of GA. In order to investigate and confirm the possible modification appeared during the synthesis of lactic acid oligomer grafted GA defining the chemical structure of the starting material is a crucial step. The intensity of the signal and peak shifting can help to validate the poly-condensation reaction between OLLA and GA. Thus, by comparing NMR spectra of lactic acid oligomers and lactic acid oligomers grafted gum Arabic, poly-condensation between two molecules were confirmed. Here the NMR spectra of lactic acid were used for comparison over neat GA due to the insolubility of neat GA in deuterated chloroform ($CDCl_3$) to perform NMR analysis (Emam et al. 2019).

OLLA:

Nuclear magnetic resonance spectra of lactic acid oligomers were used confirm chemical structure of molecules. It is known that 88% lactic acid aqueous solutions contain a series of oligomers at equilibrium with lactic acid, the latter being the predominant species (Espartero et al. 1996). Such a solution was taken as a typical mixture of the smallest oligomers up to tetramer and the corresponding 1HNMR spectra were given in the Scheme 4. 1.

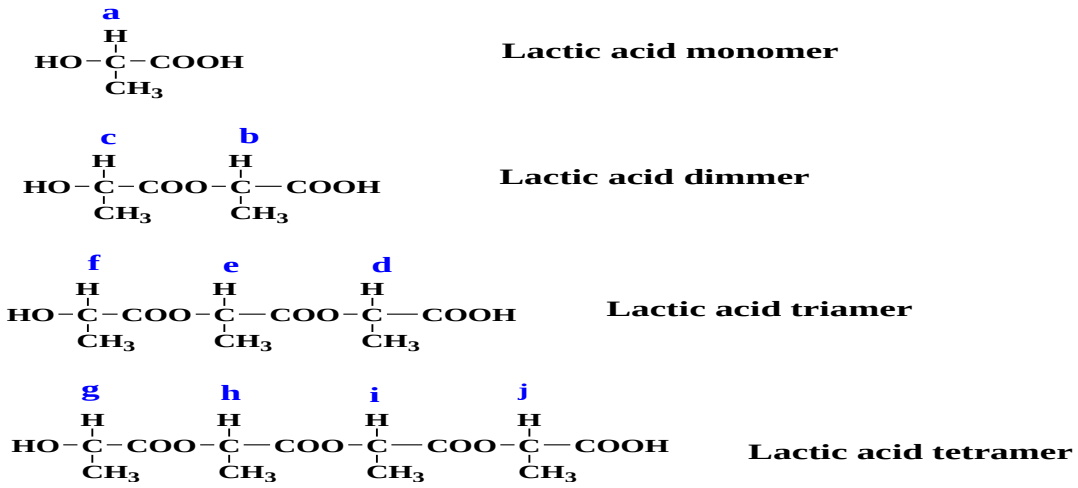

Scheme.4.1 Reaction Scheme for the synthesis of Lactic Acid Oligomer (OLL

The methine group in the free lactic acid monomer has a singlet peak at chemical shift of 4.03 ppm, methane group in the terminal position, beside the carboxylic and hydroxyl groups can be found at around 4.92 ppm and 4.28 ppm respectively. The other position for this group is between the two terminals, which also called in the middle chain, having a singlet peak at ~ 5.1 ppm. On the other hand the methyl group of lactic acid can be found in the unreacted monomer and also in the terminal position (close to carboxylic or hydroxyl group) of lactic acid oligomer, and in between the chain with a chemical shifting of 1.23 ppm,1.38 ppm, 1.27 ppm and 1.4 ppm respectively. The two terminals of methyl and methine group positions of lactic acid oligomer were formed due to the esterification of OH and COOH groups of lactic acid. As the chain length of the OLLA increases the chemical shifting of the chemicals became greater or moved to the left for all hydrogen types as given in Table 4.6,for OLLA the shifting for the COOH free H in CH of dimmer, trimmer, and tetramer would increase to 4.36, 4.98, and 4.99, respectively and for the OH free Hydrogen in CH group the shifting will changes to 4.19, 4.20 and 4.20 for dimmer, trimmer and tetramer respectively (Espartero et al. 1996).

Table 4.6: ^{1}H NMR Chemical Shifts (in ppm) of CH and CH3 Protons in a-j units of L-Lactic Acid Oligomers (CDCl3, 303 K, 360 MHz)

	Monomer	Dimer		Trimer		Tetramer				Polymer
	A	B	C	D	E	F	G	H	I	
CH	4.03	4.92	4.28	4.36	5.10	4.30	4.93	5.16	5.12	
CH3	1.23	1.38	11.43	1.40	1.55	1.44	1.40	1.45		

The 1H-NMR spectra of OLLA has been presented in Fig.4.2. The four different doublets peaks occurred at ~ 1.48 ppm, 1.51 ppm, 1.53 ppm, and 1.55 ppm attributed to methyl group protons (a,CH_3) of the methyl protons of the OLLA side chain, terminal group and hydrogen of lactyl moiety respectively. In addition, the other a doublet and quartet peak at ~4.30-4.31 and 4.33-4.34ppm, respectively was corresponds to the methine group of OLLA in the middle chain. The multiplet peaks at resonance range of 5.1-5.16 ppm was a methine hydrogen having OH free or COOH esterified end. Therefore, this lactic acid oligomer is an oligomer, which has contained a developed structure to tetramer and polymer macromolecule. The ^{1}HNMR depicts that the absence of resonance spectral peak at ~ 11ppm indicate the absence of unreacted lactic acid monomer (Perry and Shaver 2011)

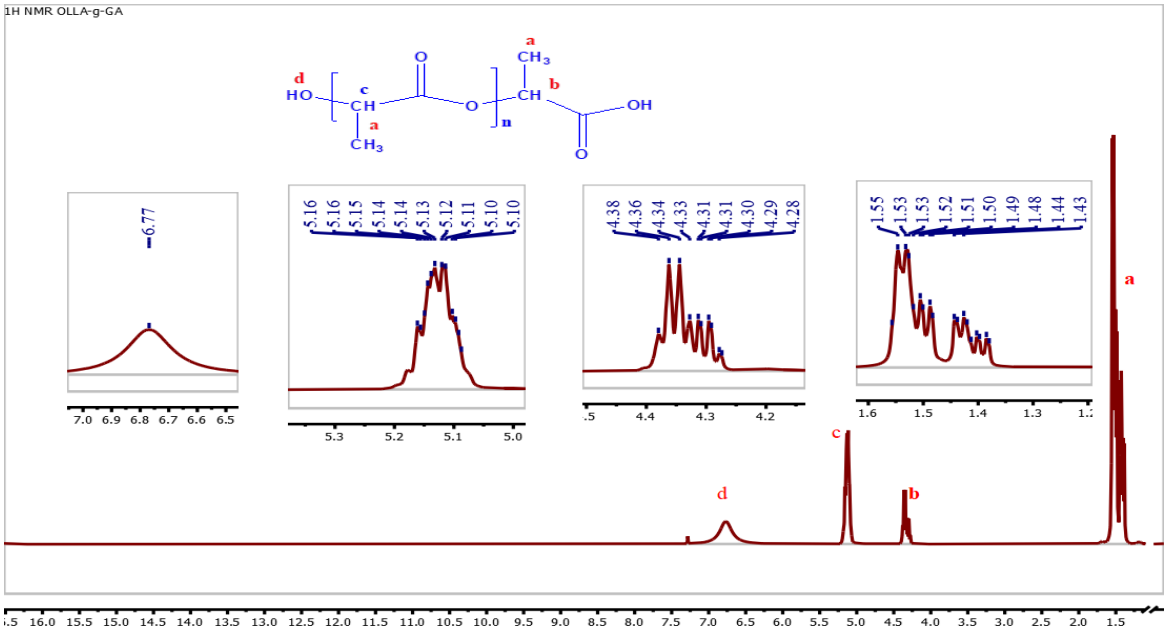

Figure 4 2: ^{1}H-NMR Spectra for OLLA

OLLA-g-GA Bio-conjugate:

There were small, and less intense doublet peaks at 1.38-1.58 ppm which reduction in number of doublet peak and shifted up-field compared to OLLA resonance peak as shown in Figure 4.3, this was due the reduction of hydroxyl group as a result of ester formation. Additionally, the multiplet resonance peak of methine hydrogen of OLLA-g-GA was changed a doublet which shows a decrement in CH groups in a conjugate. The reduction of OLLA CH which was carboxylated within the internal main chain (methine group in the lactic acid polymer), that occurred at the resonance of 5.07-5.16 ppm range was confirmed by the decrement of those multiplet peaks on the OLLA-g- GA bio-conjugate, this confirmed modification of GA.

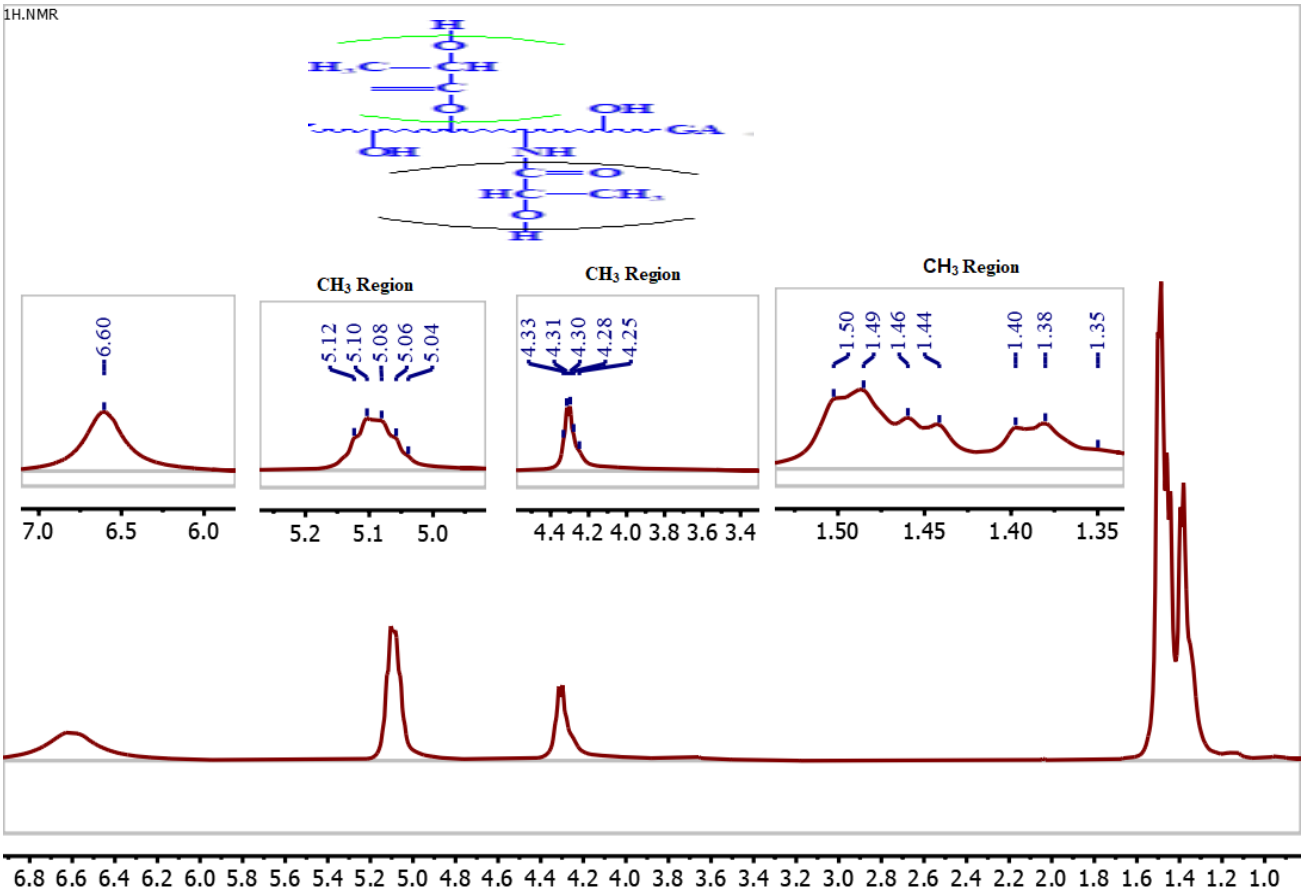

Figure 4.3: ^{1}H NMR spectra for OLLA-g-GA

4.1.3.2 Chain Length Analysis of OLLA and OLLA-g-GA

Lactic acid oligomer:

The ^{13}C NMR spectra of lactic acid oligomer was shown in Figure 4.4, different types of carbonyl bonds were expected for the conjugates, including main-chain carbonyls, LA carbonyl groups adjacent to the core molecule (-OCH_2) branches, and end-group carbonyls for unreacted lactic acid. In ^{13}C NMR spectrum analysis the intense peaks at characteristic chemical shifts of 16.150–20.13ppm was associated with the methyl groups (CH_3) of lactic acid oligomer. The other carbons shifted to the higher chemical shift values due to the attachments to the hydroxyl group at the end of the lactic acid oligomer chain located at 66.50 – 69.07 ppm attributed to α methine group (-CH-OH), the carbon at the peak of 66.50 ppm (circled) resembled for the methine group (CH) of free lactic acid whereas the other carbons belong to the conjugate chain as well as lactic acid within the internal chain and the methine group that de-shielded to the downfield of the chemical shift values due to the presence of ester bond (-C(O)-O-CH(CH_3)-) attachment at 69.07 ppm carbons of the α-methine group at the ester group

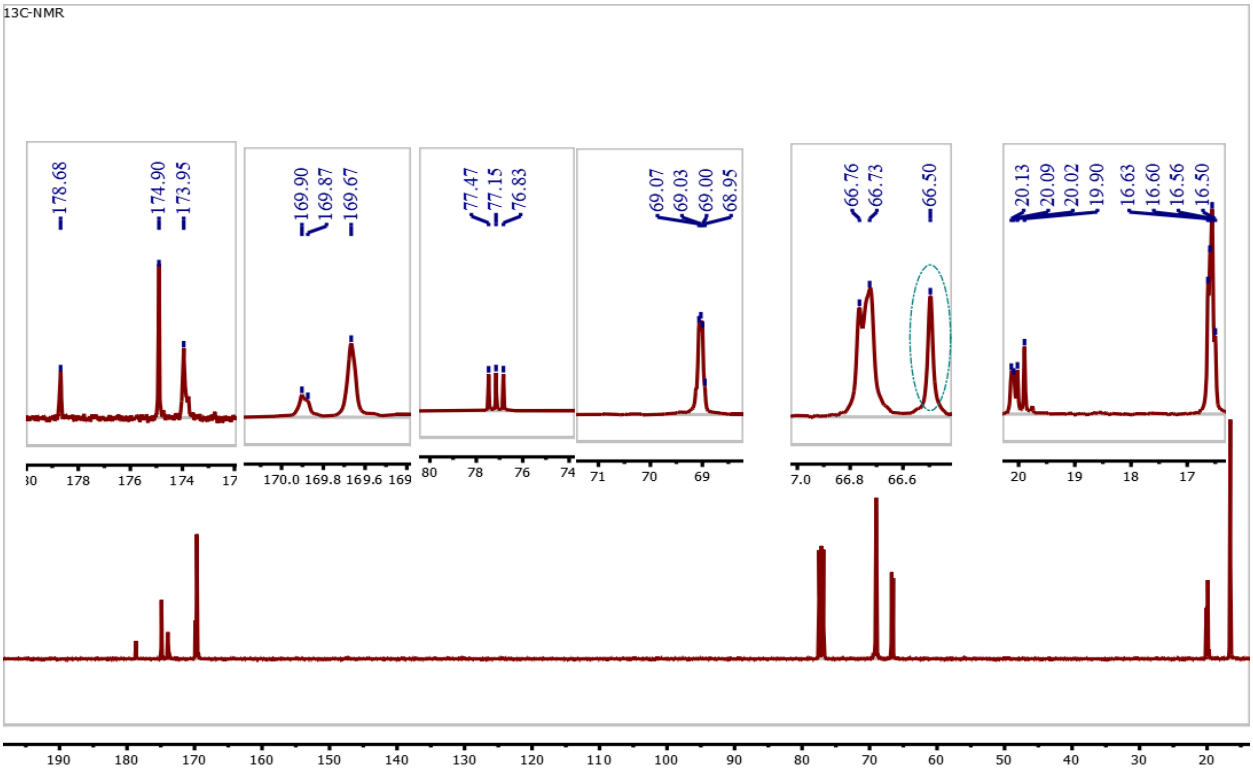

Figure 4-4: ^{13}C-NMR Spectra of OLLA

OLLA-g-GA Bio-conjugate:

The ^{13}C NMR spectra of OLLA-g-GA was shown in Figure 4.5, a less intense and up- shielded peaks as compared to OLLA at characteristic chemical shifts of 16.49– 20.11 ppm are associated methyl group of modified gum was observed. The intensity of methine carbonyl group for the conjugates, including main-chain carbonyls, OLLA carbonyl groups adjacent to the core molecule (-OCH_2) branches was decreased as compared to lactic acid oligomer peak, additionally the methine carbon of free lactic acid in the lactic acid oligomer in Figure 4.4 was disappeared, this might be due to grafting on the GA backbone. The carbonyl group area of the OLLA-g-GA bio-conjugate in the ^{13}C-NMR spectra was less intense and up shielded as compared to OLLA spectra, which confirmed the modification of GA.

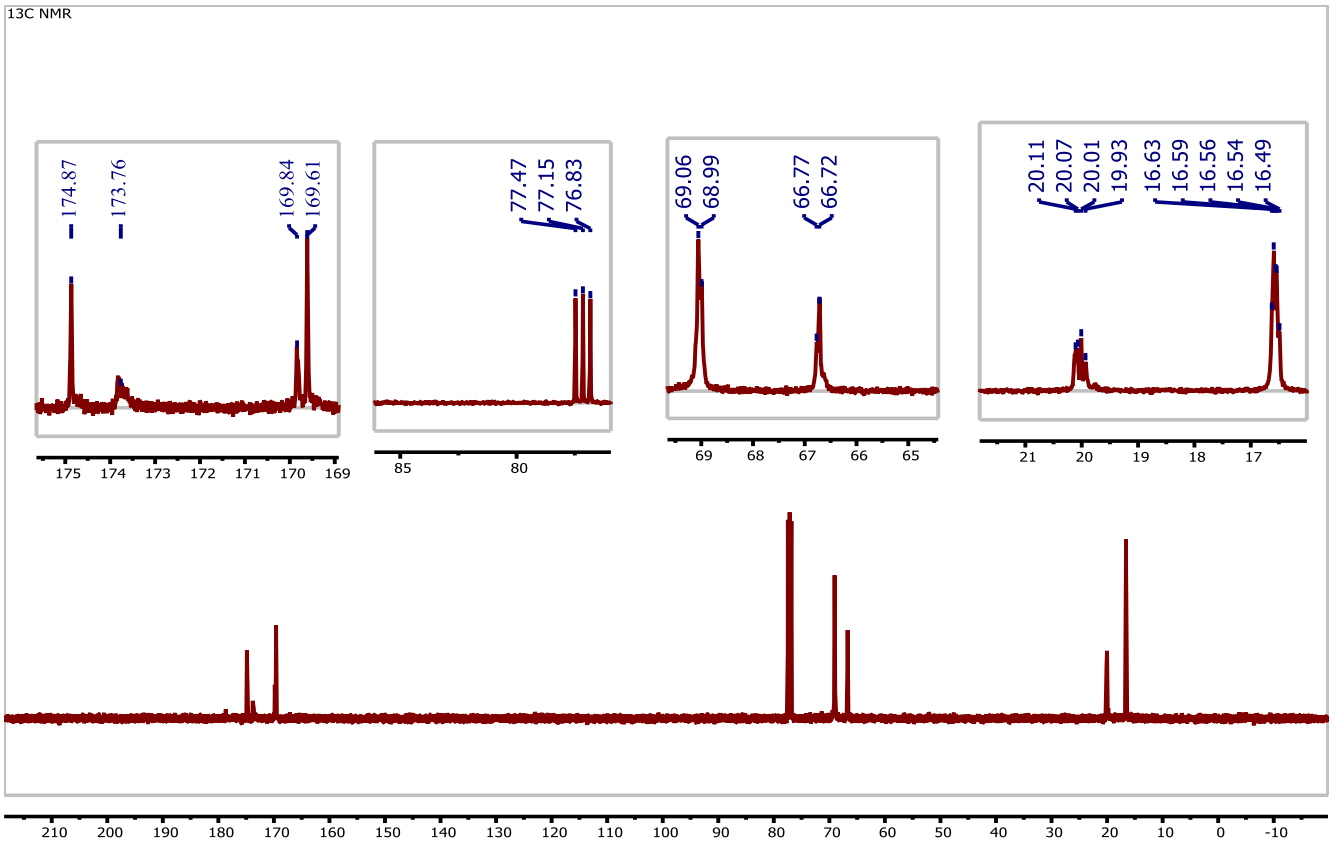

Figure 4-5: ^{13}C-NMR Spectra of OLLA-g-GA bio-conjugate

4.1.3.3 Structural Analysis of ETML and Modified ETML

ETML:

The ^{1}H-NMR spectra of ETML has been presented in Figure 4.6. The, a multiplet peak were observed at a chemical shift of δH 0.73ppm -1.23ppm, a doublet peak1.47-1.65ppm multiplet peak was observed our different doublets peaks occurred at ~ 1.48 ppm, 1.51 ppm, 1.53 ppm, and 1.55ppm and singlet peak at 2.07 which were attributed to methyl protons of polyisoprene of *Euphorbia trigona latex*. All those ^{1}H NMR spectra chemical shifts suggest that the *Euphorbia trigona* latex contains polyisoprene units (Zahir et al. 2021). The hydroxyl proton was observed at chemical shift of δH 3.33 (H-3), olefinic protons were observed at a chemical shift of δH 5.08ppm-5.01ppm.

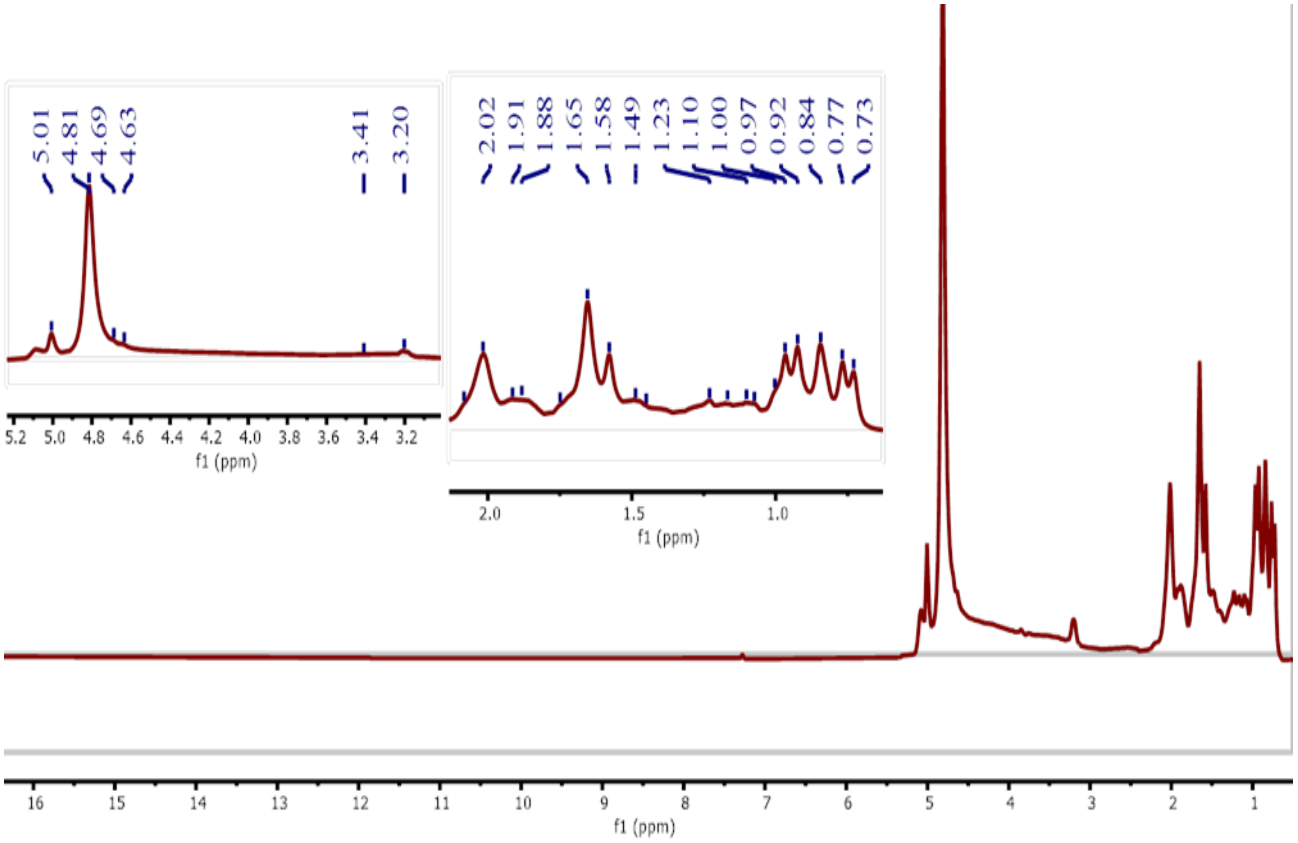

Figure 4. 6: ^{1}H NMR of ETML

OLLA-g-ETML BIO-conjugate:

As shown on the Figure 4.7 the increment intensity, additional formation of doublet and singlet peak of methyl group of modified ETML was observed as compared CH_3 region of ETML due grafting with lactic acid oligomer. The highly decrement intensity of ETML CH which was carboxylated within the internal main chain (methine group in the polyisoprene), that occurred at the resonance of 5.08-5.21 ppm range was observed. The two additional 4.36 and 4.37ppm peaks were for the lactic acid oligomer methine group. The new peak at on chemical shift environments of 2.28 – 3.28 ppm which depict ester formation during grafting reaction, confirmed the modification of ETML by lactic acid oligomer. The possible schematic diagram for reaction mechanism of OLLA-g-ETML bio-conjugate was indicated in Scheme 4.2

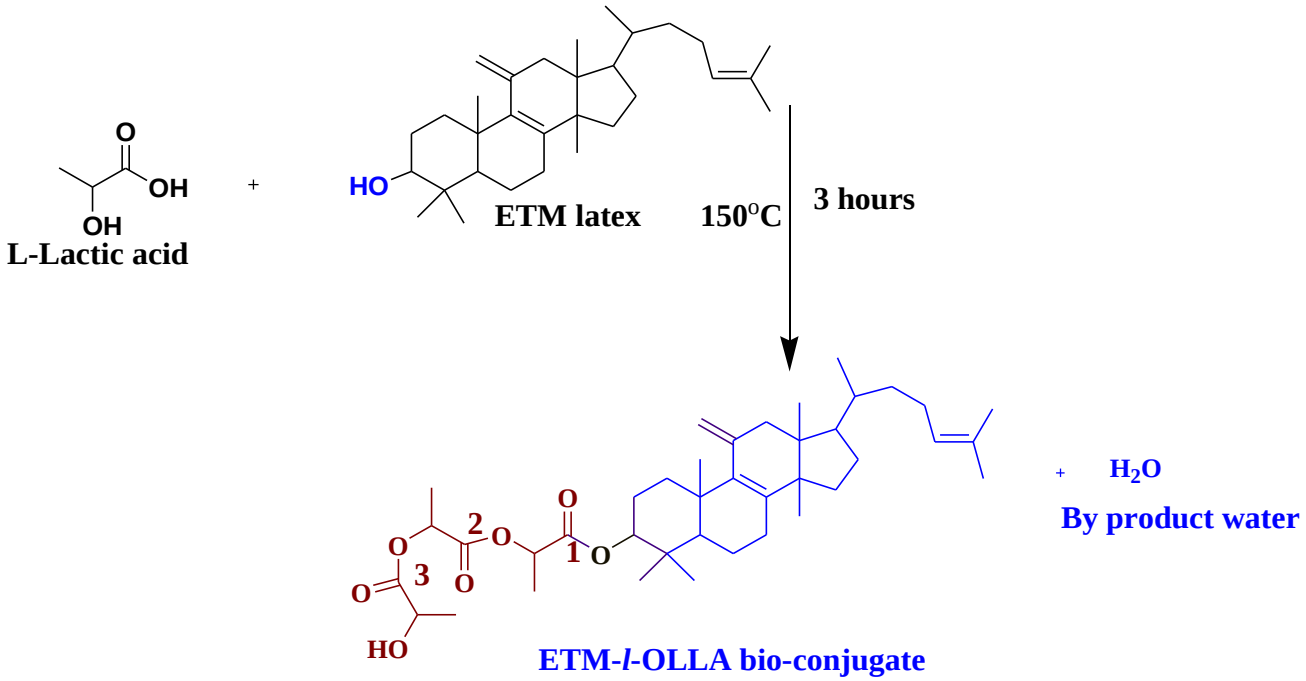

Scheme 4.2: Schematic representation of reaction mechanism for the synthesis of bio-conjugate

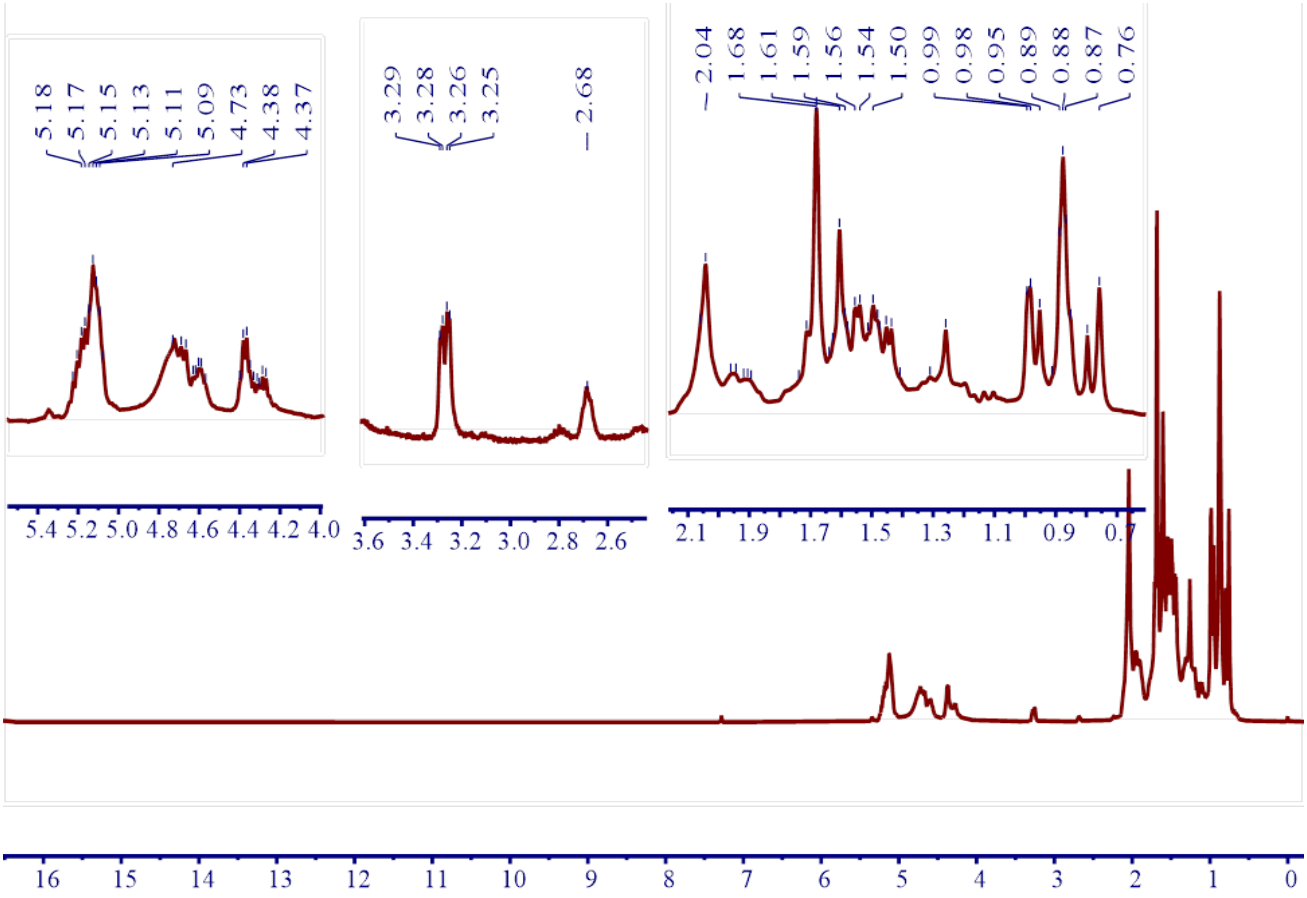

Figure 4.7: ^{1}H NMR spectra of OLLA-g-ETM bio-conjugate

4.1.3.4 Chain Length Analysis of ETML and OLLA-g-ETML:

ETML:

The ^{13}C NMR spectra ETML shows a characteristic chemical shift of cis-1, 4-polyisoprene unit methyl carbon of at 15.5 to 50 ppm as shown in figure 4.8. The methylene carbon is observed at 32.15 ppm. The olefinic carbon peak that is generally expected in the region of 120-135.16 ppm was observed at 124.48, 125.17 ppm corresponding to olefinic ethylene carbon that was =C-CH_3. Also ^{13}C NMR spectra ETML showed the presence of symmetry oxygenated methine resonating at 76ppm-78.92ppm.

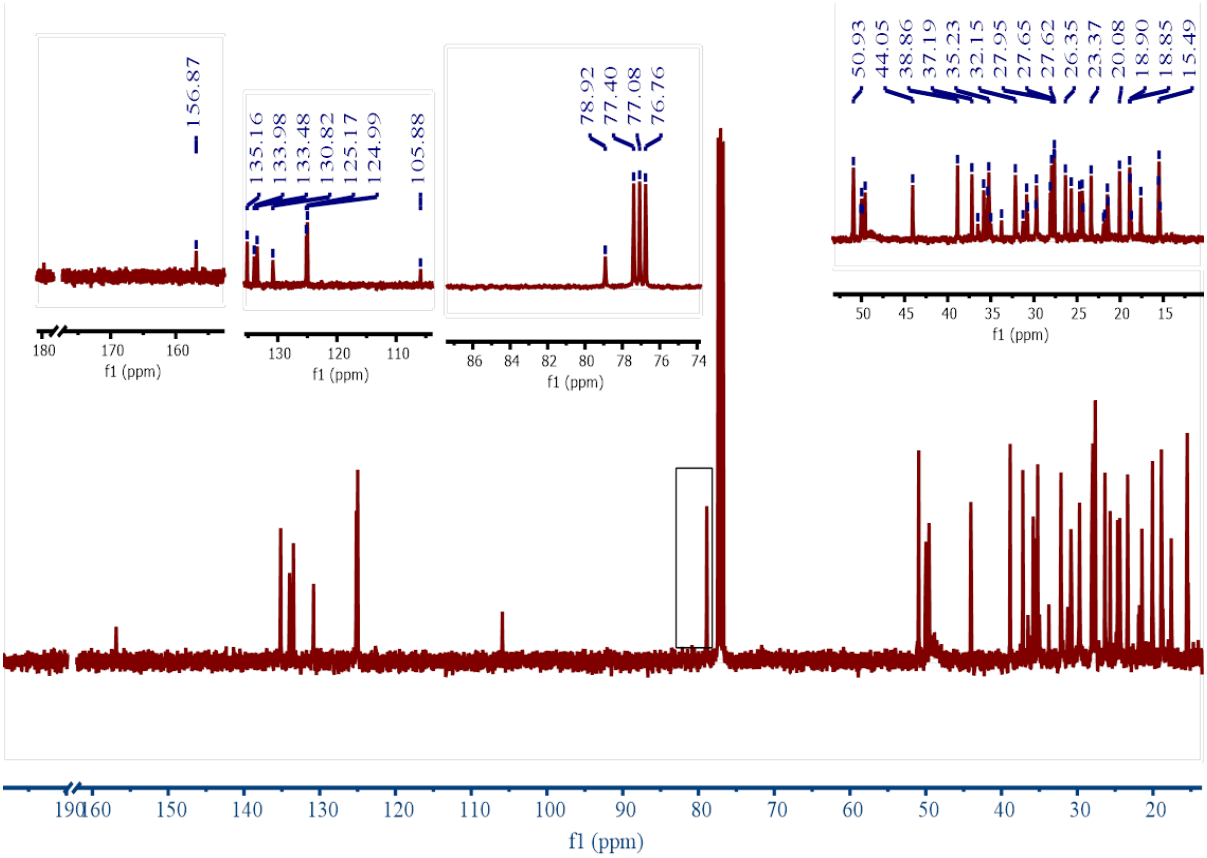

Figure 4.8: ^{13}C NMR spectra of ETML

OLLA-g-ETML BIO-conjugate:

From the ^{13}C-NMR of the conjugate the carbon (C-3) atom attached to the OH group has shown change in chemical shift from 78.91 ppm to 82.69 ppm. While in modified ETML new peak of two oxygenated carbon which implies the additional oxygenated methiene, which originated from lactic acid at 78 and 81 ppm and additional two ester resonated at 175 and 178ppm (Zahir et al. 2021).

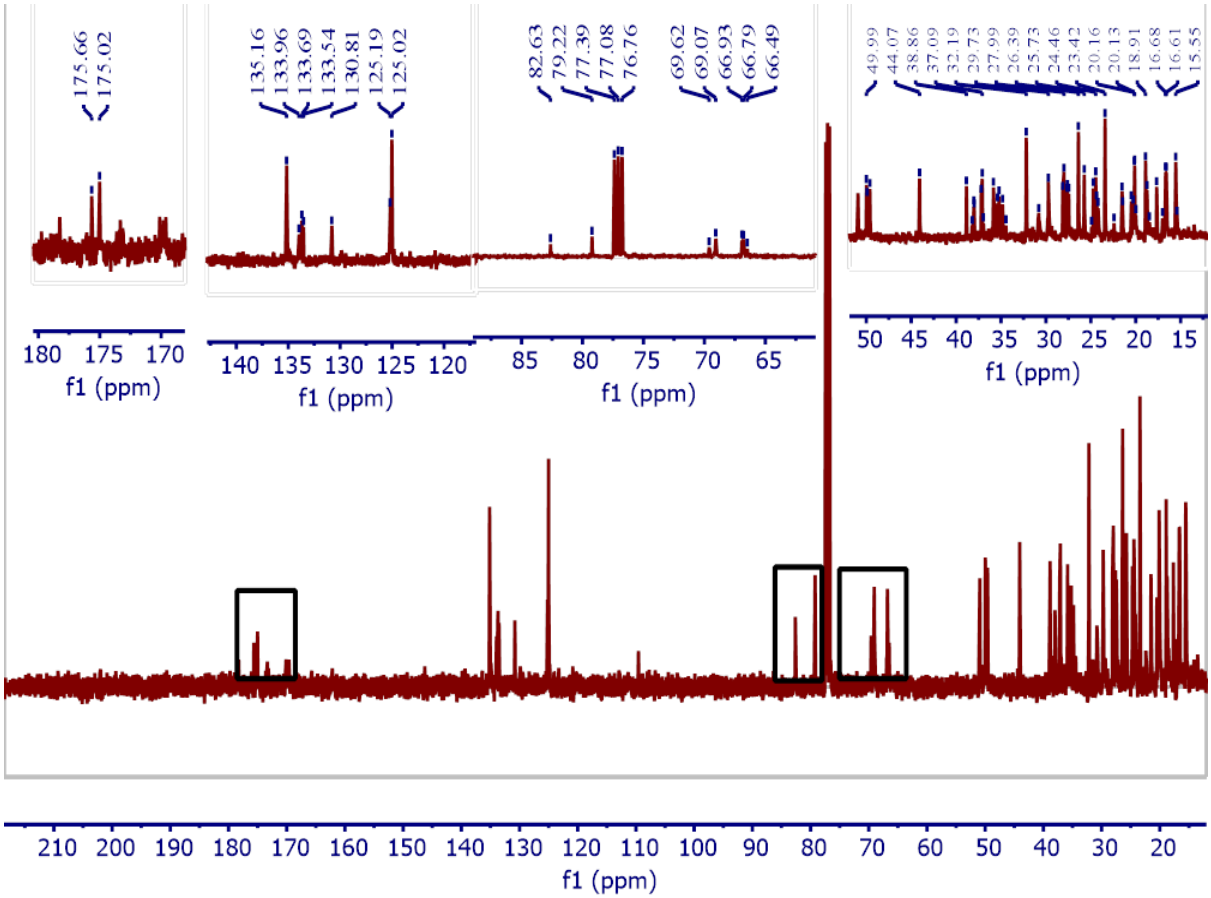

Figure 4.9: ^{13}C NMR of OLLA-g-ETM bio conjugate

4.1.4 Grafting by FTIR analysis

FTIR spectroscopy was used to validate the change in the chemical structure of the GA, raw ETM, OLL-g- GA and *OLLA-g*-ETM.

4.1.4 .1. FTIR Analysis of GA and OLLA-g- GA

Intermolecular interaction and grafting were proved by comparing FTIR spectra of neat gums and their respective modified gums as shown in Figure 4.10. The technique involves subjection of GA,OLLA and OLLA-g-GA sample to infrared radiation resulting in atomic vibrations of a molecule in the sample, resulting the giving specific absorption and/or transmission of energy (Nandiyanto et al 2019). The clear changes in molecular structure of modified gums were noticed from the FTIR spectra.

The IR spectra of GA showed the broad absorption band from 3614-3181 cm^{-1} due to the overlapped stretching and vibration of OH group and N-H (amine) group (Alang et al. 2012). The same broad

vibration was found narrow in the case of OLLA due to OH stretching and narrower in the case of OLLA-g-GA (10%) samples. It suggested that the grafting was happened at both OH and N-H groups. The peak at 2926, 2985,2994 cm^{-1} suggested that the stretching and vibrations of C-H group in neat GA, OLLA, *OLLA-g*-GA respectively (Appolonia Ibekwe et al. 2017).

The sharp and intense Peak at 1742 cm^{-1} attributed to -C=O (carbonyl) stretching which present in the spectra of OLLA and *OLLA-g-GA* (10%) but not found in the spectra of GA. A peak at 1615 cm^{-1} in GA attributed to the N-H bending which falls in the range of NH-(Kaur and Gupta 2020) bending which was not present in modified GA which confirmed the grafting . The regular peaks at 1139 cm^{-1}, 1085 cm^{-1}, 1048 cm^{-1} and 885cm^{-1} confirmed the -C-O- stretching in OLLA and *OLLA-g*-GA samples. The Peak 1452 cm^{-1} attributed to -CH_3 bending in OLLA and *OLLA-g*-GA grafted. A broad vibration was observed at 1035cm^{-1} in pure GA which is the finger print spectra of carbohydrates present in the sample. The same peak was also observed at 1207 cm^{-1} in OLLA-g-GA which was merged with -C-O- stretching. Hence, the OLLA chains were grafted on GA backbone at OH and N-H functional groups as shown in scheme 4.1 (Almuslet et al. 2012; Tripathi and Katiyar 2016).

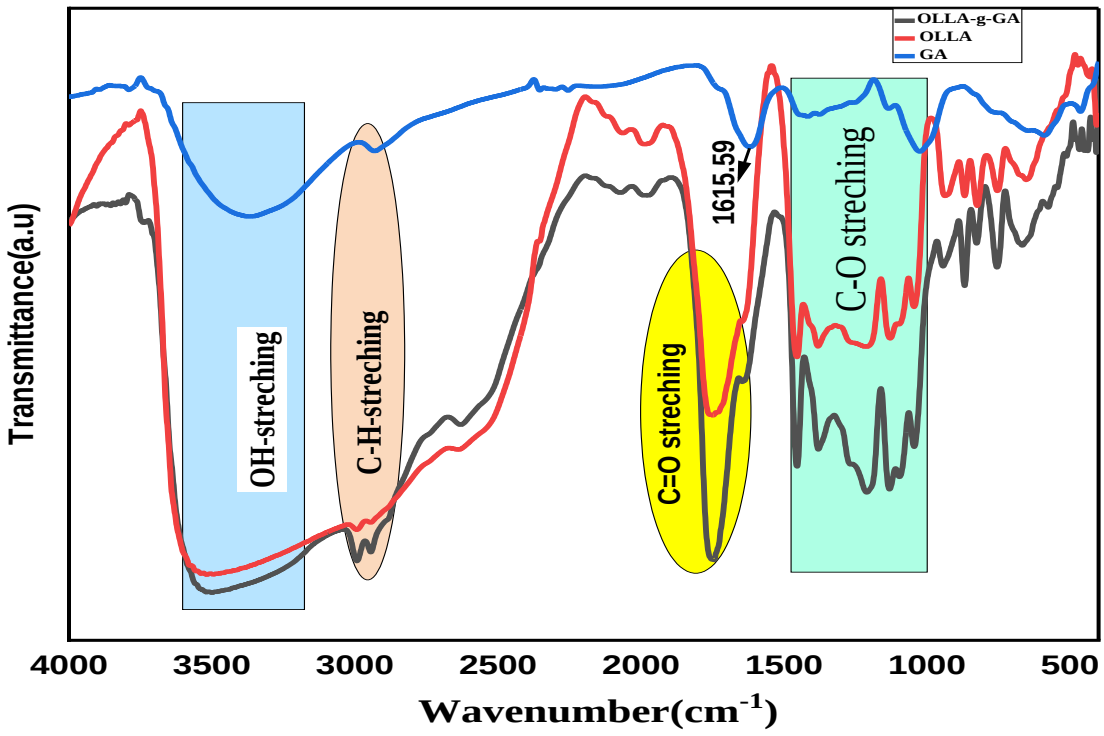

Figure 4.10: FTIR Spectral Features of the Raw, OLLA and OLLA-g-GA

FTIR Analysis of ETML and m ETML

The FTIR spectra of ETML and *OLLA-g*-ETML were obtained. The changes observed from both (ETM and *OLLA-g*-ETML) materials were used as in indication of the modification process. Due to "free" hydroxyl groups (-OH) the O–H band for the ETML samples became more pronounced, broader and shifted to slightly lower wave numbers 3670-2935cm^{-1} as shown in a Figure 4.11. Similar work was reported (Bautista-Hernández et al. 2021; Wang et al. 2015). The absorption peak which was observed at 3565-3039 cm^{-1} was attributed to the hydroxyl group of unreacted lactic acid oligomer. In case of *OLLA-g*-ETM, a broader band of OH spectra was observed at 3407-3200 cm^{-1} as due to additional OH from lactic acid oligomer. The intensity of peak at 1753 which attributed to C=O become increased due the formation of ester bond between the OH of ETML and carboxylic of lactic. Both confirm the formation of a new peak during modification. The characteristic peak observed for OLLA and *OLLA-g*-ETML at 2931 cm^{-1} attributed to CH_3 asymmetric stretching results from shifts from both lactic acid and latex characteristic peak this confirms the possible interaction between unsaturated polyisoprene units in ETML. A similar work for modification of natural rubber latex with hydrophilic grafting monomer (Kangwansupamonkon, et.al 2005).

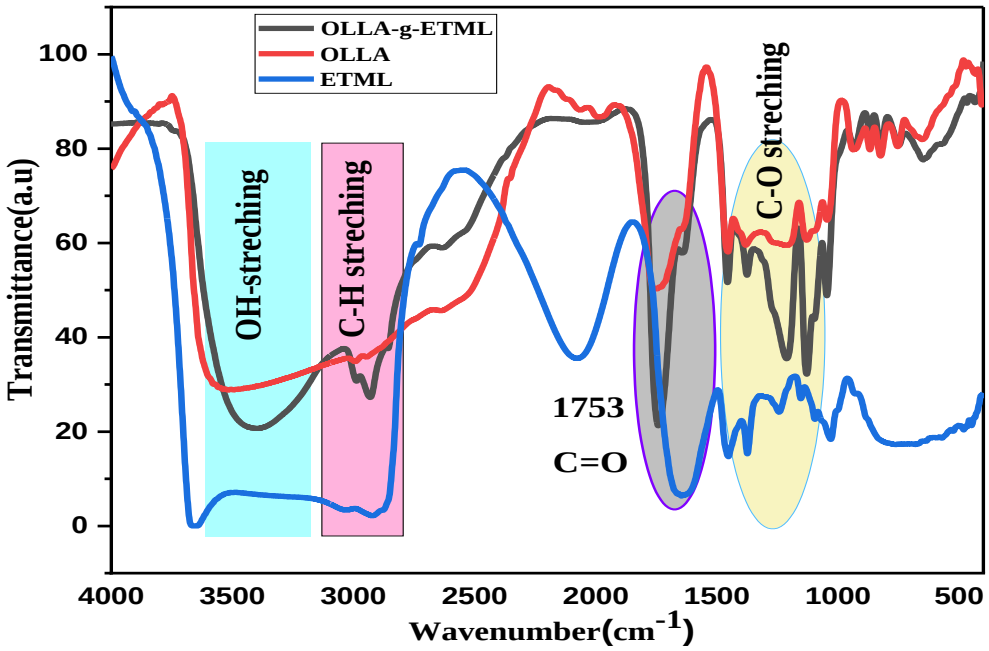

Figure 4.11: FTIR Spectral Features of the neat ETML, OLLA and OLLA-g- ETML

4.1.5. Thermal Stability Analysis of the GA, raw ETML, OLLA-g-ETML and OLLA-g-ETML Thermo gravimetric Analysis of GA and m GA.

Thermo gravimetric analyses (TGA) curves were used to see the change of thermal stability caused by grafting of gum arabic. The TGA and DTG curves for the Gum Arabic and modified Gum Arabic were shown in Figure 4.12. Two significant curves were observed at different temperature ranges for GA powder which denote the different weight losses during heating. The first broad peak in the temperature range of 51-123°C denotes the removal of unbound and bound moisture accounts about 11.81% weight loss. Whereas, no such peaks were observed for OLLA-*g*- GA samples in this temperature range, shows unavailability of free OH (hydrophobic nature). While the second stage starts from the onset temperature of 132°C and continued till 201 °C the mass loss is due to thermal degradation of the GA molecules which accounts 58.71% (Ganie, et al.2015). The third stage starts from 295^{0}C continued till 660^{0}C represents thermal degradation of high molecular GA molecules. The single degradation peak or peak temperature (Tp), was observes in the grafted molecule which indicated that the grafted occurred between OOLA and GA (Tripathi and Katiyar 2016). The onset temperature for GA powder and OLLA-*g*- GA were observed at 237,144 °C and offset temperature at 355,387°C respectively. The maximum degradation temperature for grafted GA (OLLA-g-GA) was (T_{max} =306°C) which is less than the maximum degradation temperature of gum Arabic powder (GA) (T_{max} =333°C). This may be due to the occurrence of low molecular weight OLLA molecules on grafted GA which lower thermal stability.

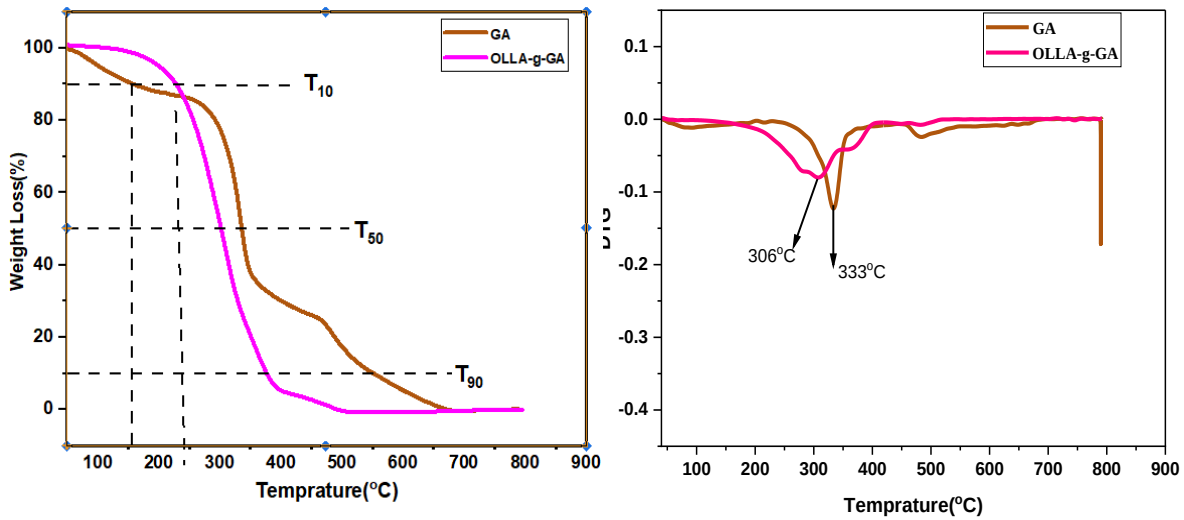

Figure 4.12: TGA and DTG analysis of GA and OLLA-g-GA

Table 4.8: TGA analysis of GA and modified GA

Samples	Temperatures at Different Weight loss (°C)			
	T_{10}	T_{50}	T_{90}	T_{max}
GA	199	338	544	333
OLLA-g-GA	297	230	377	306

Thermo-gravimetric Analysis of ETM and OLLA-*g*- ETML latex

In similar manner as above thermal analysis was done for raw ETML and OLLA-*g*-ETUML. The TGA curve for the ETM latex show three stage degradation curves. The first degradation curve is the dehydration curve in which the physically adsorbed released, volatile components and hydrogen-bonded water evaporate accounts about 65.32% weight loss. This degradation phase appears in a temperature range of 90 °C to 217 °C with the maximum degradation temperature of (T_{max} = 100°C) as shown in Figure 4.13. At its liquid state ETML latex contains large amount of water and other low molecular weight volatile compound. The second weight loss (30.05%) starts in the temperature range of 220°C to 428°C having a maximum degradation temperature of 340°C. This weight loss is due to the degradation of the polymeric material contained in the latex to its monomer units (Olalere and Gan 2021). The final weight that from the TGA curve is around 4.06% with maximum degradation of 552°C.

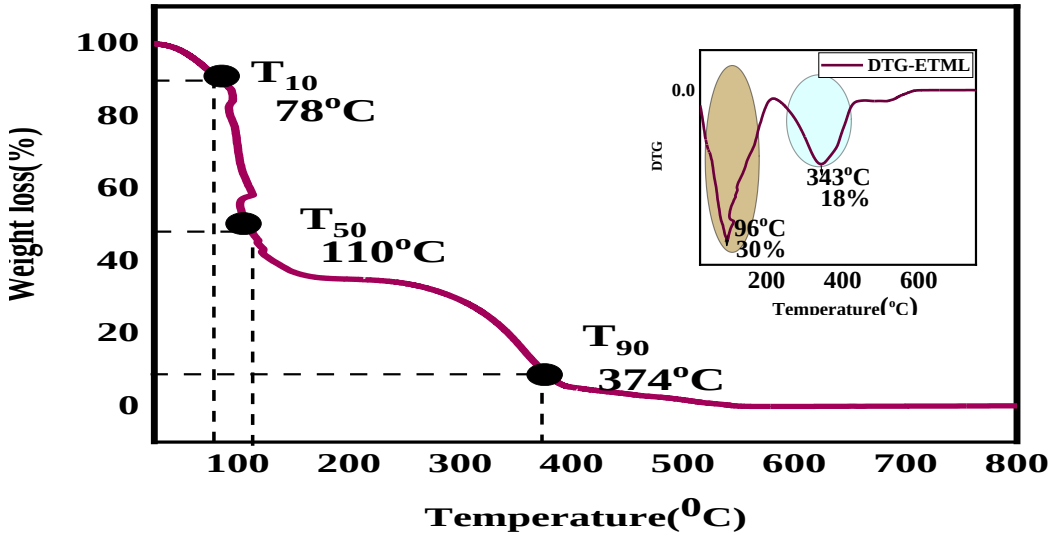

Figure 4.13: TGA and DG curve for the Euphorbia Trigona Mill Latex

The TGA analysis of the OLLA-*g*- ETML shows degradation in two mass loss steps with one major degradation curve, as shown in Figure 4.14, the first and major decomposition steps show 69% weight loss in the temperature of 380℃. This may be attributed to the decomposition of modified cis-1, 4-polyisoprene group. The second weight loss is 3% which is at a temperature of 597℃. This is attributed to the decomposition macromolecules formed during the modification reaction (Phomrak and Phisalaphong 2020). Moreover, the decomposition temperature when weight loss is at T_{10}, T_{50}, T_{max} and $T_{90,}$ are 189℃, 352℃, 380 ℃ and 435℃ respectively.

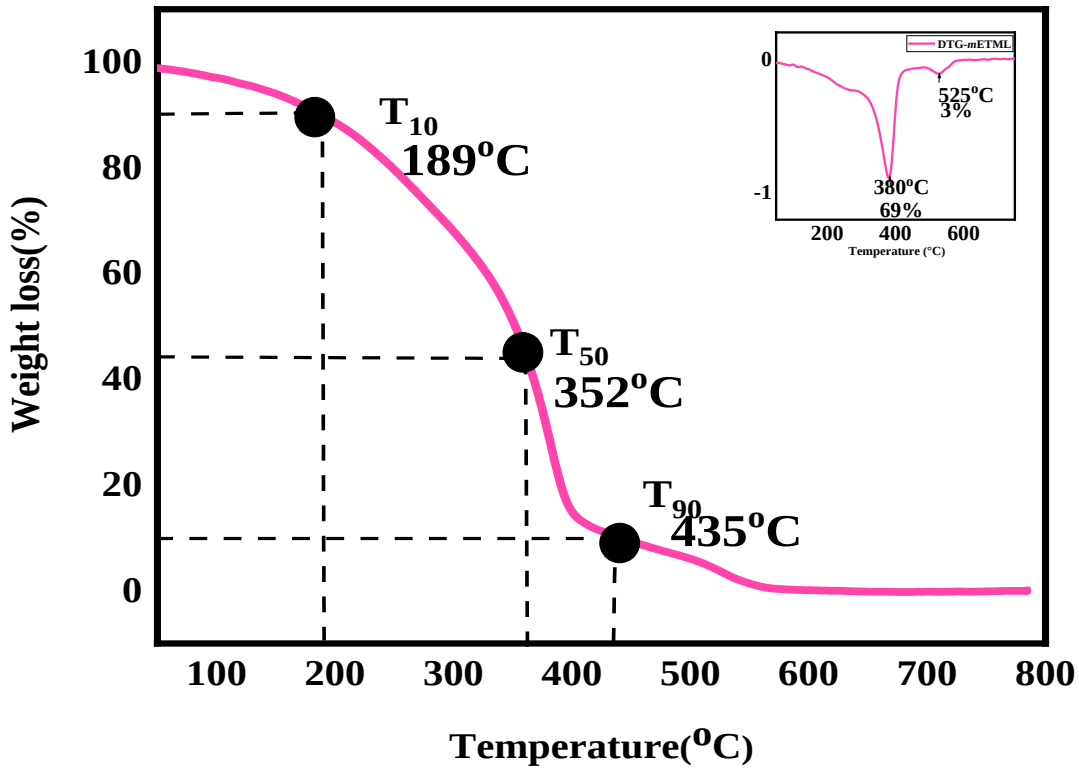

Figure 4.14: TGA and DTG curve of Modified ETM-latex

From TGA results, it can be observed that the maximum and *OLLA-g*-ETML decomposition or weight loss, which occurs in the temperature range from 297 ℃ to 427℃ which is more stable than raw ETML. Therefore, for both raw ETML and *OLLA-g*-ETML chemical reaction to take place, it should be below the maximum degradation.

4.2 Bio-composite Film Properties

4.2.1 Fourier transforms infrared spectroscopy analysis

The infrared spectrum of PLA, PLA/OLLA-g-GA, PLA/OLLA-g-ETML and PLA/master batch film bio-composites were obtained and shown in Figure 4.15 to examine the existence and type of interfacial interaction in the composites compared to neat PLA (M. Hao, Wu, and Zhu 2017).

The spectrum peak at 2960 cm^{-1} attributed -C-H stretching of methyl group, the peak at 1752 cm^{-1} attributed to C=O stretching,1434cm^{-1},1382cm^{-1},1182cm^{-1}and1083cm^{-}attributedto-CH3 bend, -CH- deformation (including symmetric and asymmetric bend), -C-O- bond stretching of the -CH-O group of PLA respectively. In the spectra of PLA/ OLLA-g-GA films, a new spike peak originated at 3502 cm^{-1} which corresponds to –NH of GA. As seen in Figure. 4.15 it was noted that all the peak positions are same for both PLA and PLA/ OLLA-g-GA bio composites films but the intensity of CH stretching (2990 cm^{-1}) and ester linkage (1759 cm^{-1}) of PLA increased in the case of PLA/ OLLA-g-GA films due to oligomer molecules. This indicates the presence of OLLA-g-GA in PLA and the molecular interaction between modified GA and PLA was weak because PLA does not have enough −OH groups to form hydrogen bonds with C=O group. OLLA-g-GA and $-NH_2$ groups in OLLA-g-GA. The broaden peak at 3500 cm^{-1} which attributed to OH stretching of OLLA-g-ETML, the intensified spectrum of a peak at 2980 which corresponding CH stretching of CH_3 both PLA and OLLA-g-ETML. The new peak at 2392 and 2082 cm^{-1} which attributed C ≡ C and C ≡O respectively, the peak at 1760 cm^{-1} assigned to C=O stretching ,similar intensified peak was observed for PLA/master batch.

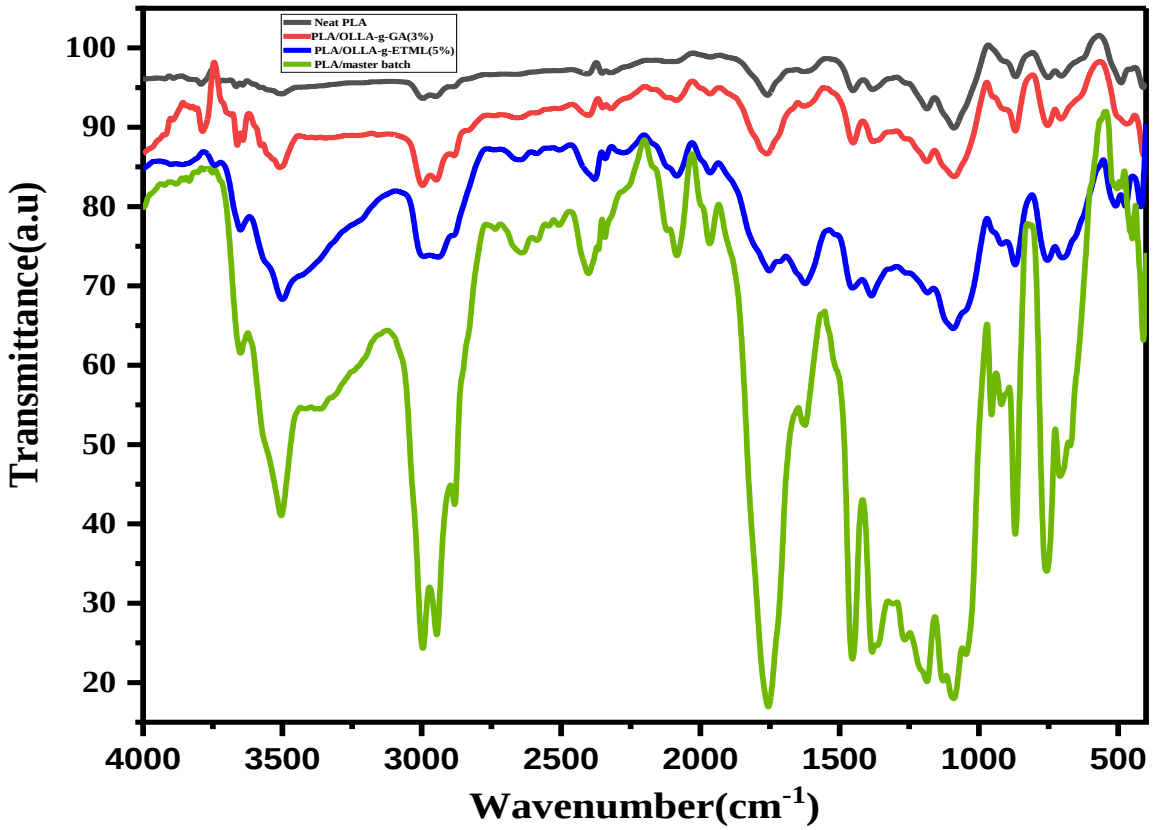

Figure 4.15: FTIR of neat PLA and PLA/master batch bio-composite before and after annealing

4.2.2 Dispersion of filler in PLA matrix

Optical microscopy analysis of all PLA/*OLLA*-*g*-GA, PLA/*OLLA*-*g*-ETML and PLA-master batch composite films were performed to determine the maximum loading of the filler materials for PLA fabrication, based on homogeneous dispersion. The resulting dispersion of fillers in PLA films is shown in Figure 4.16. OLLA-g-GA (Figure.4.16b & c) showed more stable and homogeneous dispersion but, formation of agglomeration was observed as the loading increase Figure (4.16d), due to weak interaction between polymer matrix and filler particle, resulted introduced defects to bio-composites this might resulted reduction of mechanical properties (Shaik et al. 2022). OLLA-g-ETML (Figure. 4.11e–f) showed evenly dispersed in PLA matrix and distinct agglomerates for OLLA-g-ETML (12%) (Figure 4.16h). These phenomena might lead us to conclude that homogeneous dispersion of fillers of fillers depend on the interaction between polymer matrix and filler concentration (loading). From the findings, among all the modified *gum arabic* and modified

euphorbia trigona mill films loading 2 and 3% OLLA-g-GA and 2-10% OLLA-g-ETM loading proved to be the best for selection to obtain suitable loading

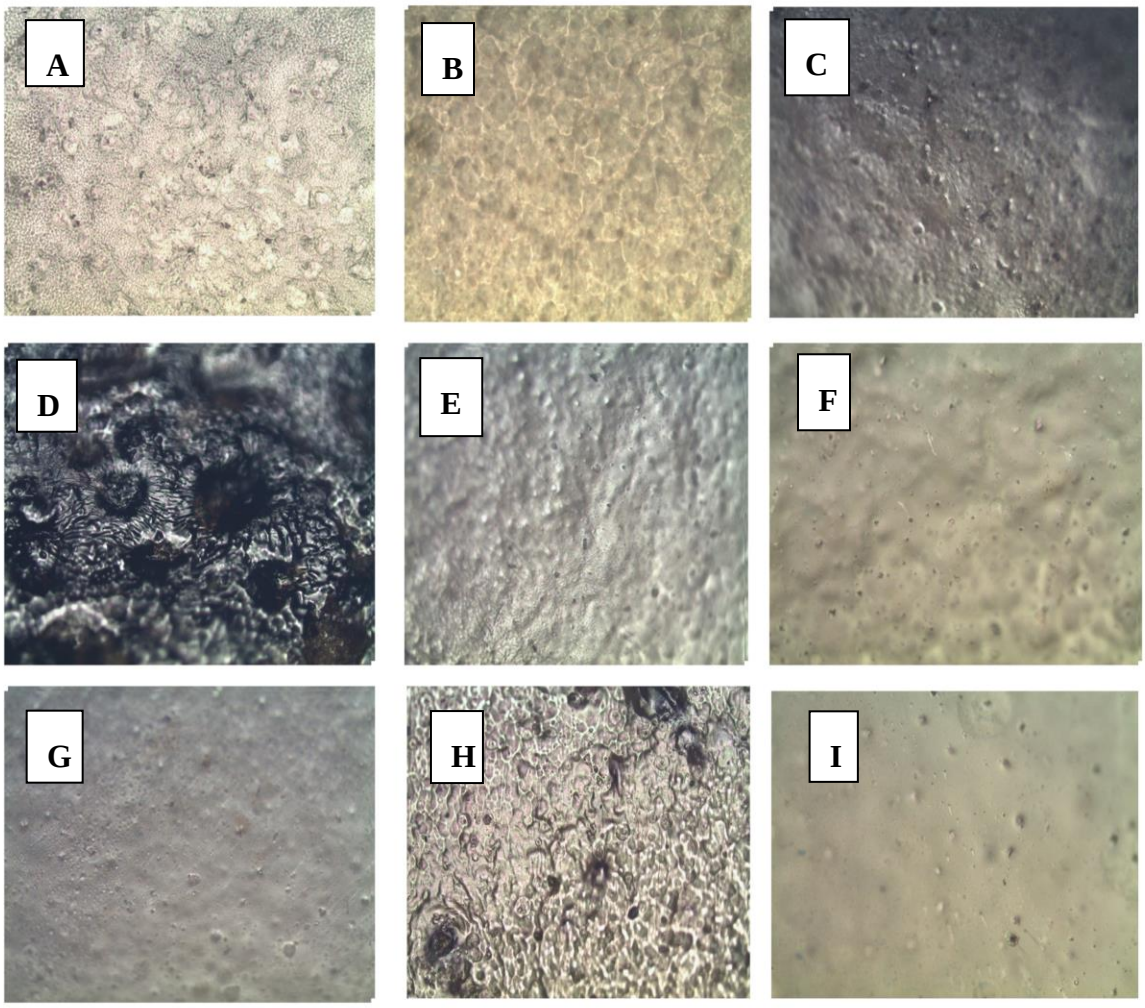

Figure 4.16: Optical micrographs of PLA /OLLA-g-GA, PLA/OLLA-g-ETM and PLA- master batch composites: (A).NeatPLA, (B).PLA/OLLA-g-GA (2%),(C).PLA/OLLA-g-GA(3%),(D).PLA/OLLA-g-GA(5%), (E).PLA/OLLA-g- ETM (3%) (F).PLA/OLLA-g- ETM (5%), (G).PLA/OLLA-g- ETM (10%), (H) PLA/OLLA-g- ETM (12%), (I) PLA/master batch.

4.2.3 Optical transparency

Barrier to UV light is an important property to be considered in the case of polymeric films that have to be used as packaging materials, especially when protection of light-sensitive products during storage is required (W. Yang et al. 2016). Results from UV–Vis characterization and related visual aspect of the neat PLA, PLA/OLLA-g-GA, PLA/OLLA-g-ETML and PLA/master batch bio-composite films were illustrated in Figure 4. 17 and the corresponding values along with transparency value (TV) were reported in Table 4.9. Transparency value of the films were computed with the help of following equation 3.4 above.

Where T600 is the fractional equivalent of percentage transmission of 600 nm wavelength radiation and x is the film thickness in mm. A lower value of TV indicates higher transparency. The lowest value of TV corresponding to neat PLA film indicates highest transparency among the four films. Neat PLA showed the highest transmission in the visible region of the spectra (400– 700 nm) and UV light region (250–400 nm). The incorporation of master batch was not caused significant change on the transparency of PLA, the films resulted highly transparent. The good transparency of PLA/master batch films has been related with the good dispersion of master batch into PLA matrix (Arrieta et al. 2014). In contrast, OLLA-g-GA and OLLA-g-ETML showed a good blocking effect in the UV light region for PLA/OLLA-g-GA and PLA/OLLA-g-ETML. The decrease in the transmittance could also be due to the presence of fillers, ascribe to scattering of light by OLLA-g-GA and OLLA-g-ETML phase dispersed in PLA network (Swaroop and Shukla 2018). Transmission spectra of the films showed that incident energy in the UV range screened more heavily than radiation in the visible range as shown. Despite the fact that our findings indicated a significant reduction in the transparency of the PLA/ OLLA-g-GA and PLA/ OLLA-g-ETML, no variations in appearance from the control film could be seen. Consequently, no effect on their acceptability for the consumer is expected. Comparable results were also reported in (Kanmani and Rhim 2014; Swaroop and Shukla 2018).

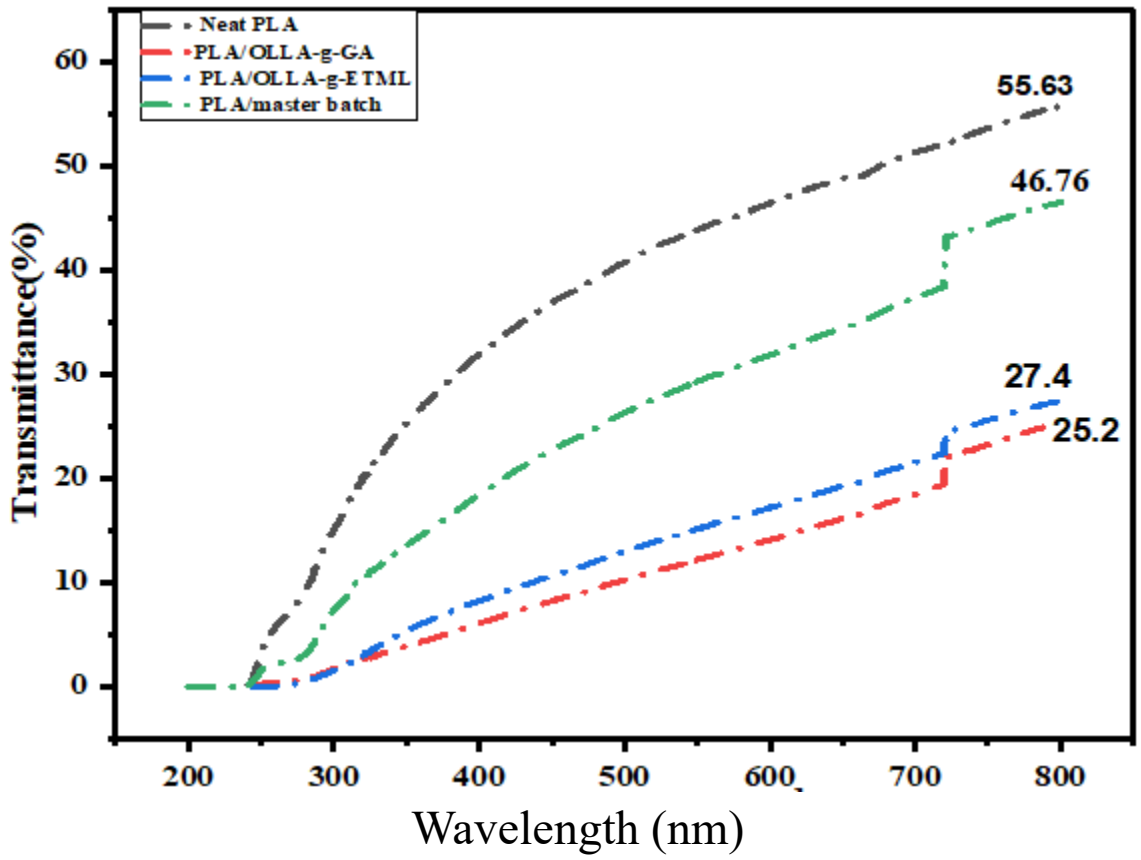

Figure 4.17: Transmittance by UV/VIS for some PLA-based film compared with neat PLA

Table 4.9: UV-visible transmission and transparency values of prepared films

Film sample	Wavelength (nm)	Transparency values
	600	
PLA		1.77
PLA/OLLA-g-GA		4.26
PLA/OLLA-g- ETML		3.85
PLA/master batch		2.54

4.2.4 Antimicrobial Activity

The development and application of active films or coatings containing antibacterial compounds have taken priority over other types packaging materials, in order to inhibit the growth of foodborne bacterial pathogens and also spoilage bacteria. Therefore, the development and application of active films or coatings containing antibacterial compounds have taken priority over other types of active food and other types of packaging materials. The minimum diameter (6mm film) of the PLA, PLA/ *OLLA-g*-GA (3%), PLA/ *OLLA-g*-ETML (5%) and PLA/ *OLLA-g*-GA (3%) - *OLLA-g*-ETML (5%) film particles that could entirely inhibit the growth of the tested pathogens are shown in Figure 4.18. The antibacterial activity of the fabricated PLA films against the tested foodborne pathogens evaluated by disc diffusion agar is shown in Table 4.10. The active film inhibits the growth of four pathogen (*E. coli, S.aureus, P. aeruginosa and S.pyogenes*). The clear zone of inhibition was observed for all. *E. coli, S.aureus, P.aeruginosa and S.pyogenes* have showed on the Figure 4.18. The diameter of halo formed by the PLAfilm,PLA/*OLLA-g*-GA(3%),PLA/*OLLA-g*-ETML(5%) and PLA/*OLLA-g*-GA (3%)-*OLLA-g*-ETML(5%) film was 8,9 and 10.5 mm respectively for bacteria *E. coli* 8.5,9.5 and 11 mm respectively for bacteria *S. aureus 8.5,9 and 10.5 r*espectively for P.aeruginosa bacteria and 9,9 and 11 mm respectively for S. *pyrogen.*

Both euphorbia trigona mill and gum Arabic exhibited effective anti-bacterial activity for both gram positive and negative bacteria. The latex obtained from euphorbia species is known to be the most valuable product because it contains several biologically active natural compounds, such as triterpenoids. In this case, the main structure of the latex of *euphorbia trigona mill latex* was triterpenes, and this phytochemical compound is known to be a potential source of medicine (Salehi et al. 2019).

The activity of this bioactive compound has different action mechanisms towards different types of bacteria. The anti-bacteria activity of this compound results from the hydroxyl, and carbon to carbon double bond (Chung 2020). Similarly, majority of the described antimicrobial effect of *gum arabic* have been attributed to their secondary metabolites or due to presence of saponin, saponin glycosides, volatile oil, hydrolysable tannin, triterpenoid, flavonoids, phenol and alkaloids(Baien et al. 2020; Solomon et al. 2010). Thus, these studies indicated PLA/*OLLA-g*-GA (3%), PLA/ *OLLA-g ETML* (5%) and PLA/master batch have anti-microbial characteristics.

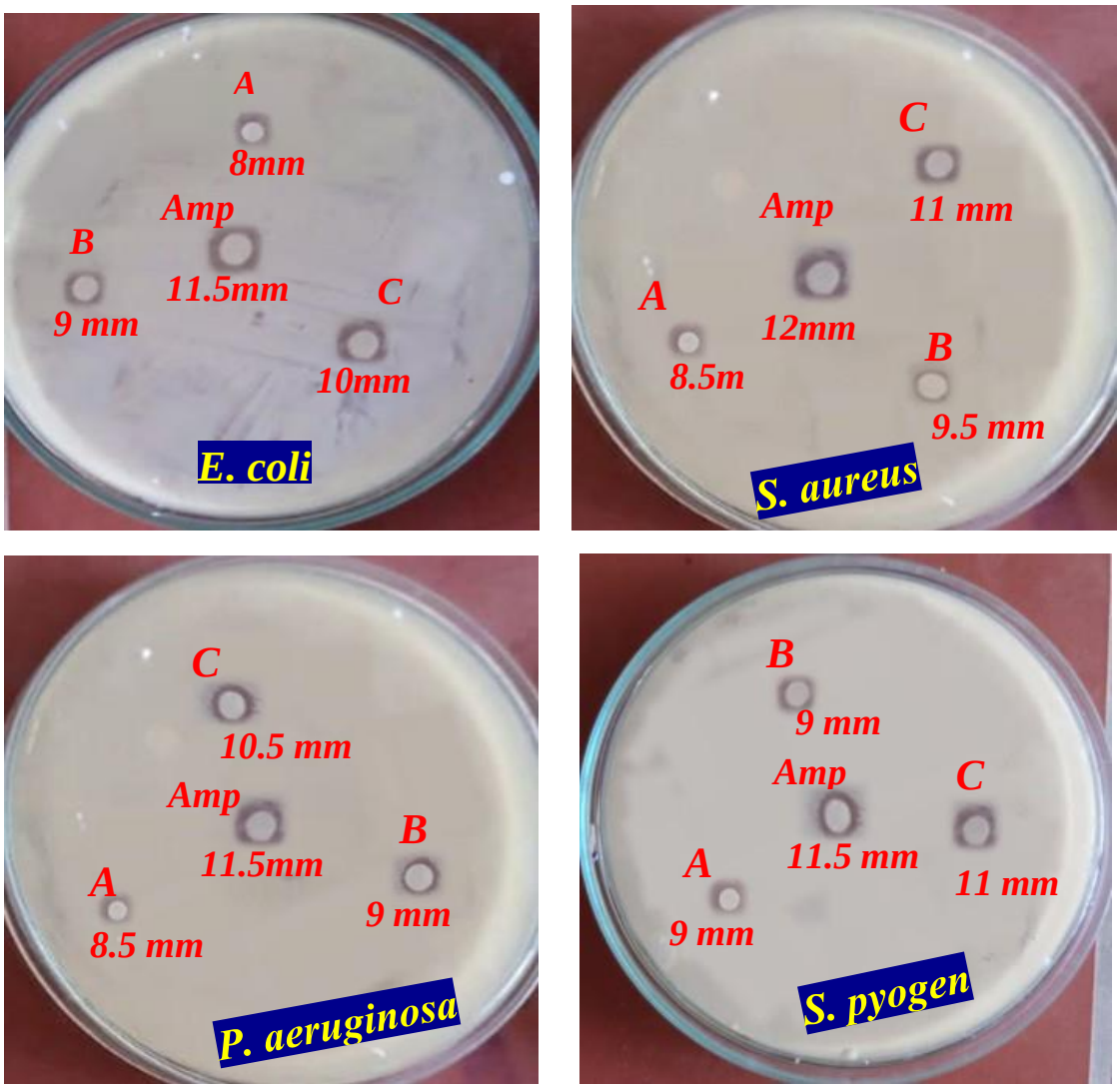

Figure 4.18: Result for anti-bacteria analysis of OLLA-g-GA (3%), PLA-ETML (5%), PLA/master batch

Table 4.10: Antimicrobial activity of OLLA-g-GA (3%), PLA/OLLA-g-ETML (5%), and PLA/master batch

Bacteria Species and Zone of Inhibitions				
	Gram-negative		**Gram-positive**	
SAMPLE NANE	***E.coli*** **ATCC25922**	***S.aureus*** **ATCC2592**	***P.aeruginosa*** **ATCC27853**	***S.pyogen*** **ATCC19615**
A.OLLA-g-GA (3%)	8	8.5	8.5	9
B.PLA-ETML (5%)	9	9.5	9	9
C.PLA/master batch	10.5	11	10.5	11
Ampicillin(+ve control)	11.5	12	11.5	11.5

4.2.5 Mechanical Properties

In order to determine the possibility of using bio composites in packaging for handling and transportation of items, it is crucial to investigate their mechanical properties. Thus, tensile strength, elongation at break and Young's modulus are the three qualities that are most typically assessed in mechanical property analysis. Average values of obtained tensile strength, elongation at break were illustrated in Figure 4.19a-c and on Appendix 1. It can be established from the figure that incorporation of OLLLA-g-GA, OLLA-g-ETML and its master batch in PLA matrix significantly changed the mechanical properties. The addition of 1%OLLA-g GA, 2% OLLA-g GA and 3%OLLA-g-GA increased the tensile strength of PLA from 70.76 ± 0.79 N/mm^2 by 24.37, 34.1, and 38.31%, respectively. The elongation at break was increased from 2.54% by 14.3, 15.7 and 20%, respectively. This due to well adhesion of OLLL-g-GA with PLA matrix, in which OLLA-g-GA chain entanglement effect with PLA interphase entangled into the PLA matrix as revealed in the optical microscope analysis, causes superior load transfer from the PLA matrix to reinforcement preventing the crack progress until the catastrophic failure (Lohrasbi and Yeganeh 2021). Similarly, tensile strength for PLA/OLLA-g-ETML was increased compared neat PLA, however, as the loading of OLLA-g-ETML increased from 3 to 5%, it showed that a decline in tensile strength (18.52 and 10.74%). However, a remarkable enhancement in elongation at break was observed by 34 and 62% for PLA/OLLA-g-ETML (3%), PLA/OLLA-g-ETML (5%) respectively due to elastomeric property of OLLA-g-ETML (Chaiwutthinan et al.2021). This is might be due to elastomer nature of ETML and plasticizing nature OLLA which cause a reduction of chain entanglement effect with PLA interphase (Z. Li et al. 2022). Furthermore, addition of master batch which have synergic effect in PLA matrix enhanced the tensile strength and elongation at break of PLA as shown in Figure 4.19 (c). Different loading has showed of enhancement of tensile strength by 20, 24, 35, 40, 34, 38, 47.1 and 36% for PLA/OLLA-g-GA (1%) -OLLA-g-ETML (3%), PLA/OLLA-g-GA(1%)-OLLA-g-ETML(5%), PLA/OLLA-g-GA(2%)-OLLA-g-ETM (3%) and PLA/OLLA-g-GA (2%)-OLLA-g-ETML(5%), PLA/OLLA-g-GA(2%)-OLLA-g-ETML(10%),PLA/OLLA-g-GA(3%)-OLLA-g-ETML(3%),PLA/OLLA-g-GA(3%)-OLLA-g-ETML(5%)and PLA/OLLA-g-GA(3%)-OLLA-g-ETML(10%), respectively. The result from these biopolymers reveled the developed bio composite used as packaging film as it has comparable mechanical property with conventional polymers (Michelot et al. 2017).

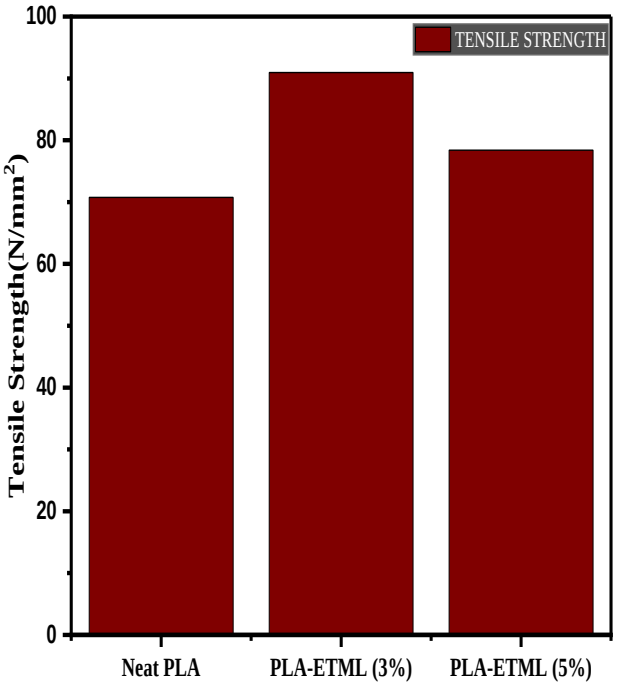
TENSILE STRENGTH
Tensile Strength(N/mm²)
100
80
60
40
20
0
Neat PLA
PLA-ETML (3%)
PLA-ETML (5%)

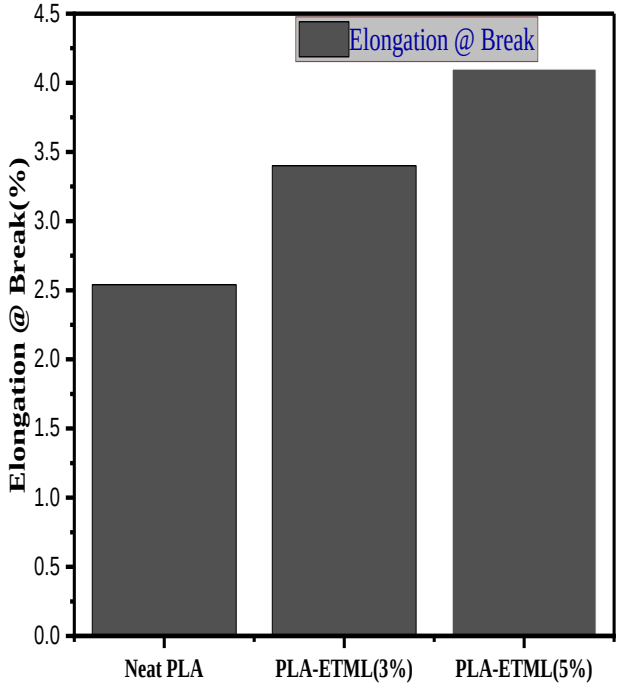
Elongation @ Break
Elongation @ Break(%)
4.5
4.0
3.5
3.0
2.5
2.0
1.5
1.0
0.5
0.0
Neat PLA
PLA-ETML(3%)
PLA-ETML(5%)

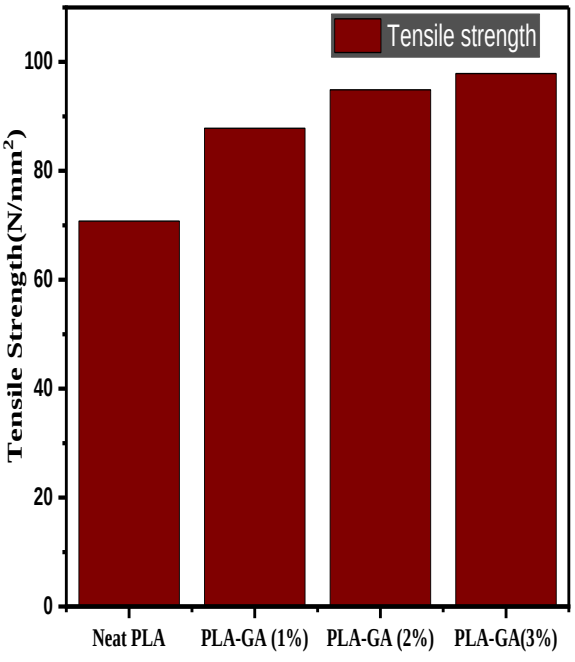
Tensile strength
Tensile Strength(N/mm²)
100
80
60
40
20
0
Neat PLA
PLA-GA (1%)
PLA-GA (2%)
PLA-GA(3%)

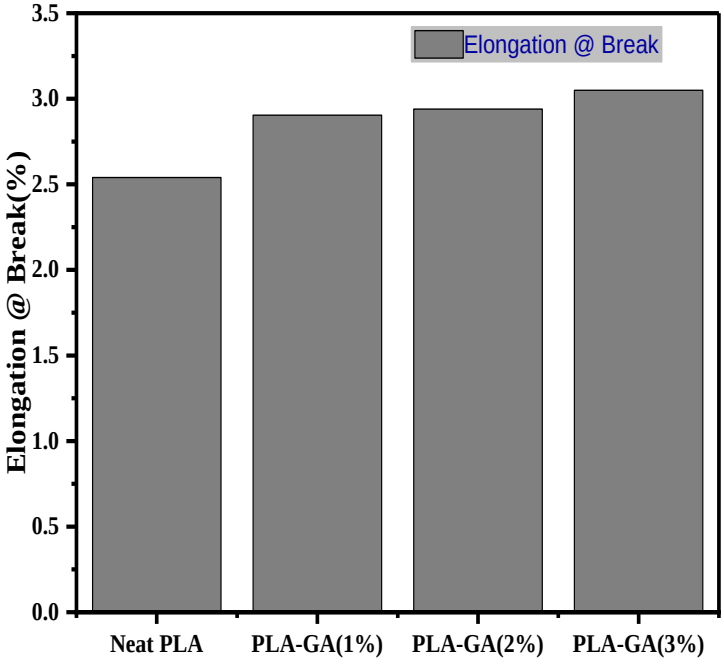
Elongation @ Break
Elongation @ Break(%)
3.5
3.0
2.5
2.0
1.5
1.0
0.5
0.0
Neat PLA
PLA-GA(1%)
PLA-GA(2%)
PLA-GA(3%)

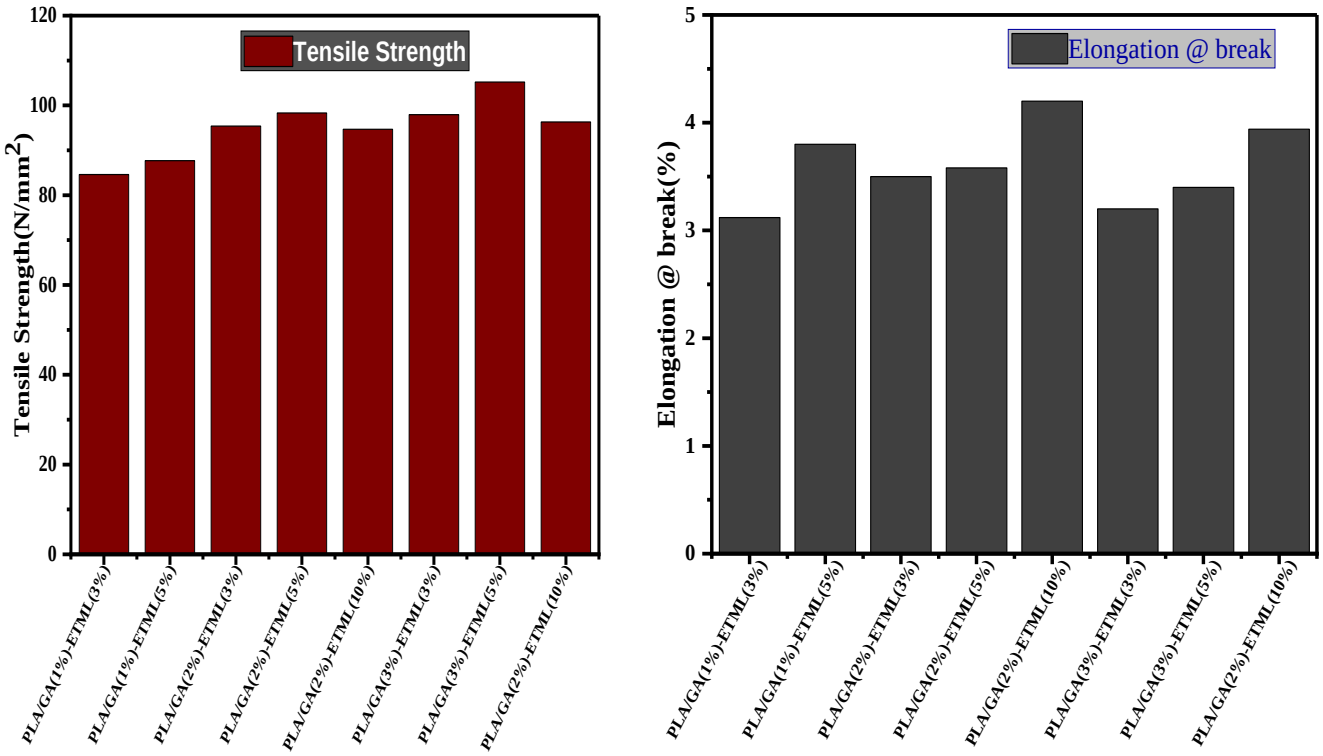

Figure 4.19: Mechanical properties of film samples (a) tensile strength, (b) elongation at break

4.2.6 Differential scanning calorimetry

The no isothermal crystallization behavior of neat polymers and PLA bio composites was studied using differential scanning calorimetry (DSC) to investigate the effect of processing parameters and effect of different nucleating agents in promoting the crystallinity. In this study an investigation was carried out to evaluate effect of incorporation of nucleating agent i.e. OLLA-g-GA, OLLA-g-ETML and master batch on the crystallization property of PLA and other information like glass transition temperature (Tg), melting temperature (Tm), melting enthalpy (ΔH_m), and percentage of crystallinity of PLA at different heating. The percentage of crystallinity of PLA and PLA/OLLA-g-GA, PLA/OLLA-g-ETML and PLA/master batch composite films was calculated by using equation (3.13) (Homklin and Hongsriphan 2013; Jiang et al. 2016; Nagarajan et al. 2015).

$$X_C = \frac{\Delta H_m}{\Delta H_m^{\circ}} * 100$$

Among different nucleating agent, OLLA-g-GA, OLLA-g-ETML and its master batch neculating agent behaves synergetic property, which is it acts as crystallizer as well as plasticizer agent within the PLA polymer matrix due the presence of oligomer which act as plasticizing effect due to enhancement in molecular segmental mobility resulting reduction in Tg values. PLA is a semi-crystalline polymer that has an amorphous and crystalline region, in its amorphous state no crystallization occurs during fast cooling. When the nucleating agent (OLLA-g-GA, OLLA-g-ETML and master batch) was incorporated with PLA, some parts (crystalline region) of PLA become more crystallized by initiating the crystallization of the polymer through initiating nucleation, and also in some parts of PLA (amorphous region), the nucleating agent promotes or increase the tendency of amorphous state by acting as a plasticizer. During thermal annealing the previous thermal history of PLA was erased which means PLA's become completely amorphous from its semi-crystalline so that PLA starts crystallization after incorporation of the nucleating agent from zero (Aliotta et al. 2017). It is well known that PLA molecules seldom crystallize during the cooling process due to their molecular nature. While the both lactic acid grafted GA and ETML and its master batch (OLLA-g-GA, OLLA-g-ETML and master batch) dispersed well and providing relatively higher active sites for polymer molecules to nucleate by forming hydrogen bonding between C=O group in PLA and N-H group in modified GA(OLLA-g-GA) OH group in modified ETML. Additionally, neculating agent the enhance the formation of crystal growth by lowering the barrier energy of crystal formation (Jiang et al. 2016) as shown in Figure 4.20.

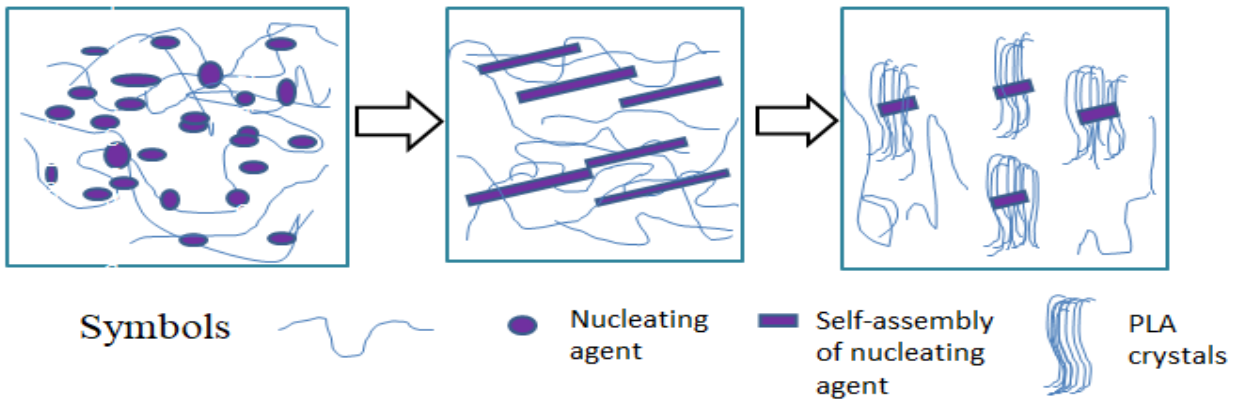

Figure 4.20: Illustrations of the crystallization process of PLA initiated by OLLA-g-GA, OLLA-g-ETML and master batch neculating agent

The impact of the three nucleating agents were compared based on their percentage of the degree of crystallinity on PLA at constant annealing time of 150 minute and annealing temperature of 110^{o}C. The percentage of crystallinity could be used to quantify the effectiveness of those nucleating agents at a given process parameter. DSC thermo grams of the neat PLA and PLA bio composites are shown in Figure 4.21. Thermal parameters with respect to glass transition temperature (Tg), melting temperature (Tm), melting enthalpy (ΔHm) and degree of crystallinity (Xc) were tabulated in Table 4.11.

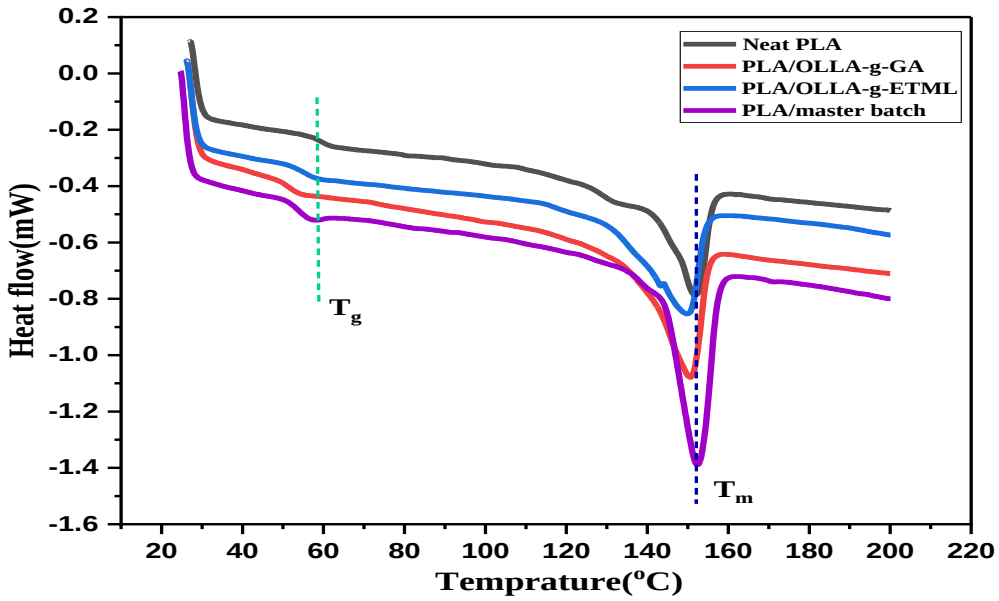

Figure 4.21: DSC thermo grams of neat PLA and PLA/bio composites

The glass transition temperature OLLA-g-GA, OLLA-g-ETML where decreased compared to neat PLA this may be due to the plasticers nature of additives, the decrease glass temperature of PLA helps to improve ductility and draw ability of PLA. However, results from thermal analysis (Table 4.11) show that the addition of the master batches to PLA did not have any significant effects on the glass transition or melting temperature. Any decrease in glass transition temperature would have been unfavorable as this would reduce the effective working temperature of PLA products (Greco and Ferrari 2021). As shown in Table 4.9, improvement of the crystallinity of the PLA polymers with incorporation of neculating agent was observed, incorporation of the nucleating agent significantly enhanced the crystallinity of PLA from 31.36 (without neculating agent) to 39.32,36.3,40.39 for PLA/OLLA-g-GA, PLA/OLLA-g-ETML and

PLA/master respectively. The possible reason for an increment of degree of crystallinity was due to dispersion of neculating agent that interacts with the PLA.

Table 4-11: Calculated degree of crystallinity of neat PLA and PLA based bio composite

Sample	T_g(℃)	$\Delta H_m(J/g)$	T_m(℃)	X_c(%)
Neat PLA	57.43	29.16	151.59	31.36
PLA/OLLA-g-GA	49.72	36.575	150.55	39.32
PLA/ OLLA-g-ETML	52.16	33..72	149.64	36.93
PLA/master batch	51.35	43.1	152.25	45.83

Effects of annealing on neat PLA

Gently heating the material to its glass transition temperature or just above but below its melting temperature had a great impact on the physical and chemical properties of the materials. As shown below in Figure 4.22 and the tabulated numerical values, when the neat PLA was annealed at 110 ℃ isothermal temperatures for 150 minutes, the glass transition temperature was decreased from 61.6 ℃ to 56.71 ℃ which indicates the formation of regularly arranged crystals, therefore due to annealing the T_g became lower which means that the PLA became soften at a lower temperature which was very advantageous to improve the ductility and drawability of PLA and also the melting temperature was also increased from 143℃ to151.59 ℃, which a large amount of energy was required during processing of annealed PLA because of higher crystallinity. Annealing of PLA had improved the chain arrangement of polymer into the regularly ordered matrix and better inter-layer bonding that was why the thermal properties of annealed PLA were improved; the crystallinity of neat PLA without annealing was lower than that of annealed PLA (Nagarajan et al. 2013). This discussion could support by the study of (Diani and Gall 2006) in which the annealing time and temperature impacts were studied on poly(lactic acid) (PLA).

Annealing has a great impact on the end application of PLA by influencing Tg, mechanical property and others (Pérez-Fonseca et al. 2016). By which samples were subjected to thermal annealing (105. 8^{o}C for 1 hr) to modify the crystallinity of the materials.

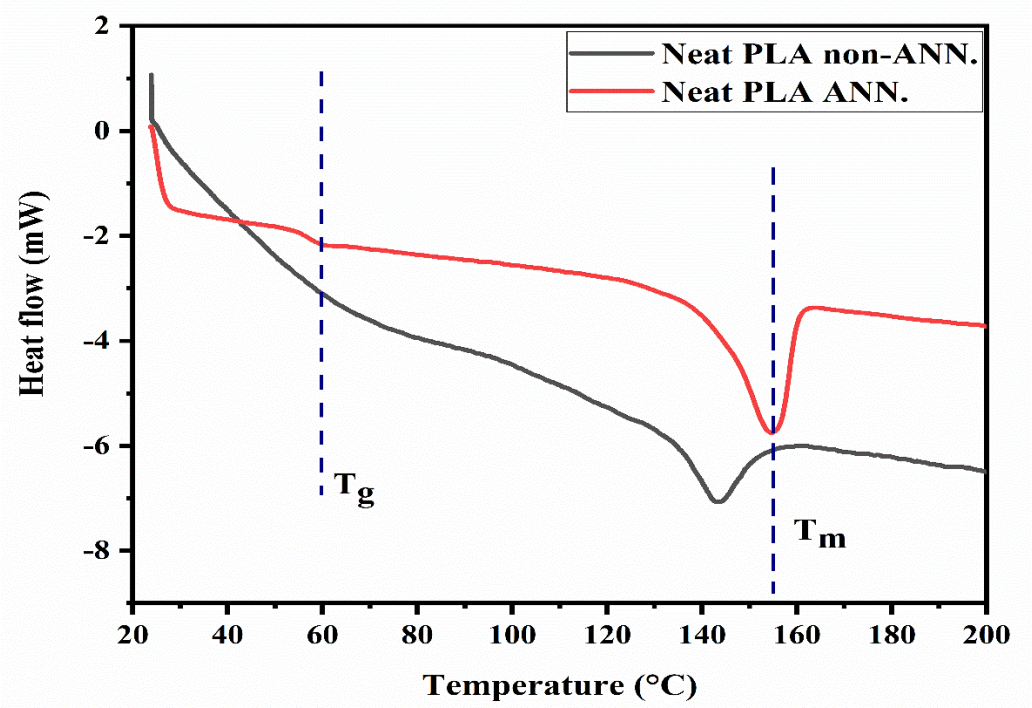

Figure 4.22: DSC thermograms of neat PLA without and without annealing

Table 4.12 Calculated degree of crystallinity of neat PLA with and without annealing

Sample	T_g(℃)	$\Delta H_m(J/g)$	T_m(℃)	X_c(%)
Neat PLA (non-annealed)	65.6 ℃	23.4	143	25.2
Neat PLA (annealed)	57.43	29.16	151.59	31.6

Effects of annealing time on percentage crystallinity

DSC thermos grams of the PLA bio composites are shown in Figure.4.23. The effect of annealing time with respect to glass transition temperature (Tg), melting temperature (Tm), melting enthalpy (ΔHm) and degree of crystallinity (Xc) are tabulated in Table 4.13. Thermal

annealing is the processing step, which can be easily added as an intermediate step during the polymer processing method. Thus, thermal annealing was applied to achieve high degree of crystallinity of neat PLA and PLA/bio composite as only neculating agent improves crystallinity. Treating the sample with heat reduces the surface free energy (volume) and the boundary between PLA chains a chance for nucleation and enables crystallization. The tabulated data in Table 4.13 show degree of crystallinity of PLA bio composite were improved with the increasing annealing time.

Table 4.13: Effects of annealing time on the degree of crystallinity of PLA

Sample	$Time$ (minutes)	T_g(℃)	$\Delta H_m(J/g$	T_m(℃)	X_c(%)
PLA/ OLLA-g-GA	30	48.42	34.2	150.34	38.77
	60	49.2	38.34	152.41	41.22
	90	48.9	39.45	150.55	44.2
PLA/ OLLA-g-ETML	30	46.66	33.71	149.3	37.6
	60	53.784	36.13	150.32	39.84
	90	51.32	34.34	149.64	37.96
PLA/master batch	30	51.095	40.28	152.23	40.3
	60	51.54	33.6	149.74	43.12
	150	51.95	41.7	152.25	45.83

When the annealing time increased from 30 minutes to 150 minutes, the degree of crystallinity also increased from 38.7% to 44.2%, as PLA/OLLA-g-GA gets enough time its sluggish crystallization properties changed to good crystallization, which enhance the mechanical property of PLA/ OLLA-g-GA. While PLA/ OLLA-g-ETML it observes in enhancement form 37.6 to 39.84% but as shown in Table 4.13, but as annealing time increase the percentage of crystallinity become decrease, this due to OLLA-g-ETML act as plasticizing agent rather than

acting as neculating agent Tg was also decrease with an increase of annealing time as plasticizing effect which enhance molecular mobility of resulting in reduction Tg value. The degree of crystallinity was increase with annealing time for PLA/ master batch, well dispersion a master batch into PLA matrix enhance the percentage of crystallinity as annealing time increase from 40.3 to 45.83%(Diani and Gall 2006).

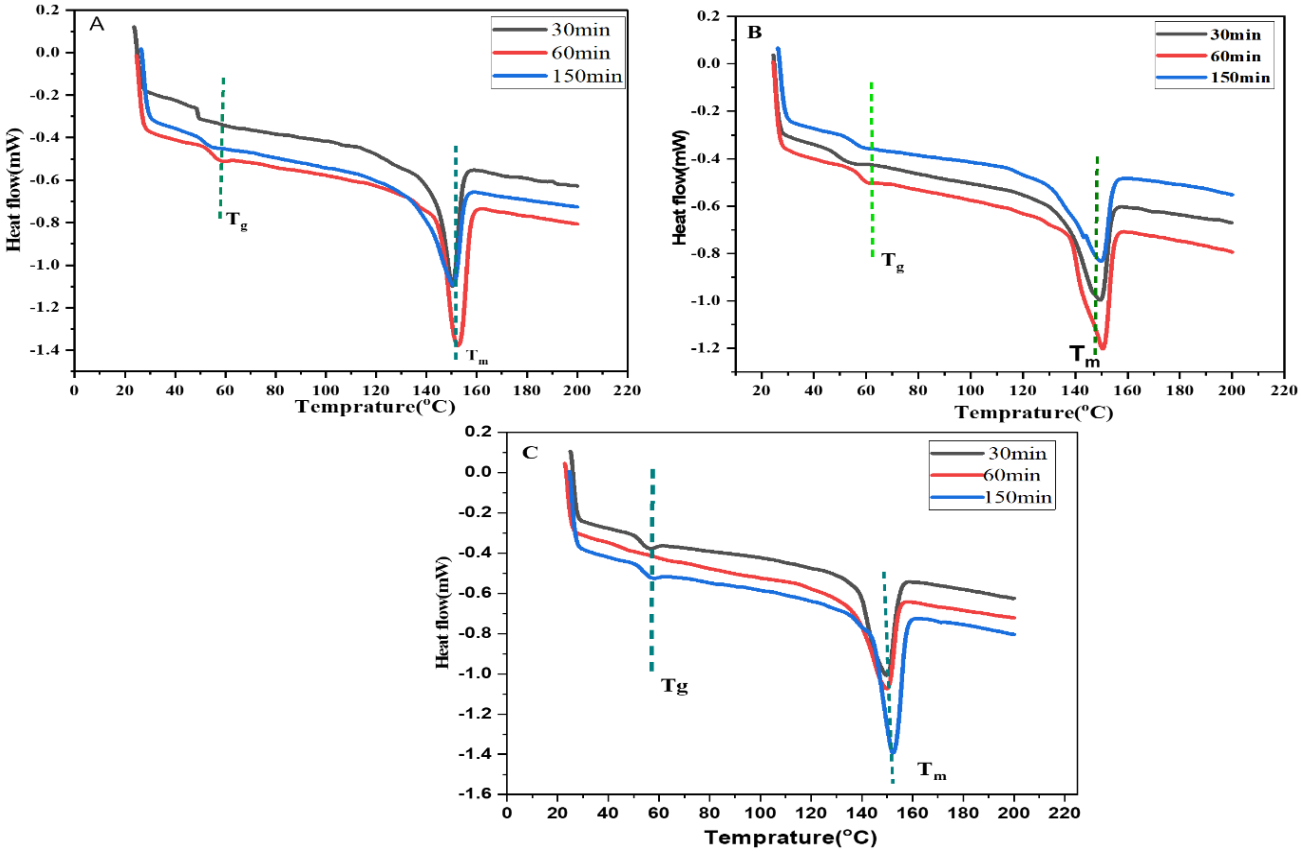

Figure 4.23: DSC thermograms of (a) PLA/OLLA-g-GA, (b) PLA/OLLA-g-ETML and (c) PLA/master batch bio composites.

4.2.7 Thermo gravimetric Analysis (TGA)

The thermal decomposition behavior of pure PLA and composites was studied using TGA and the corresponding TGA curves were illustrated in Figure 4.24. It can clearly be observed that the neat PLA weight loss occurred in three sections. The first weight loss (10.6%) was observed in the 78 –149℃ temperature range and it is attributed to the release of physically adsorbed, volatile components and hydrogen-bonded water that remained in on the end chain of PLA (Ainali et al. 2021). Whereas there is no mass loss in this range of temperature for bio composite.

The second mass loss event in PLA occurs in the temperature ranges 327.26–402.27 ^{o}C with a mass loss of 88%. For bio composite films, this mass loss occurs at lower temperatures which affect thermal stability due to the presence of lower thermally stable *OLLA-g*-GA and *OLLA-g*-ETML. The onset of degradation temperatures for PLA, PLA/OLLA-g-GA (3%), PLA/OLLA-g-ETML (5%), and PLA/OLLA-g-GA (3%) - OLLA-g-GA ETML (5%) are 327.26, 311.5, 321.44, and 288.95^{o}C, respectively as shown in Table 4.14. The maximum degradation temperature (T_{max}) for PLA PLA/OLLA-g-GA (3%), PLA/ OLLA-g-ETML (5%), PLA/ *OLLA-g*-GA (3%) OLLA-g-ETML (5%) (Master batch) are 386.09, 386.667, 392.54, and 361.43^{o}C, respectively and Tendset of PLA and bio composite are 402.22, 407.88, 413.73 and 389.14 ºC. The corresponding percentage weight loss at T_{max} for PLA, PLA/ *OLLA-g*-GA (3%), PLA/OLLA-g-ETML (5%) and PLA/ *OLLA-g*-GA (3%)-OLLA-g-ETML (5%) (Master batch) are 76.42, 64.58, 76.23, and 57.1% respectively. It can be observed that weight loss is higher in bio composite films as compared to neat PLA. These results showed that there was earlier degradation in comparison with neat PLA, because of lower thermal stable with more active end groups have catalytic effect on PLA matrix and finally accelerate the degradation rate of PLA bio-composites (Burgos et al. 2014).

Table 4.14: TGA analysis of PLA and PLA based bio-composite

Sample code	**$T_{10\%}$ weight loss (°C)**	**$T_{50\%}$ weight loss (°C)**	**T_{max} rate of degradation (°C)**	**(°C)**
PLA	321	367	386.09	380.5
PLA/OLLA-*g*-GA (3%)	348	381.5	386.7	392.67
PLA/OLLA-*g*-ETML (5%)	353	384.9	392.51	398
PLA/Master batch	318	354	359	374

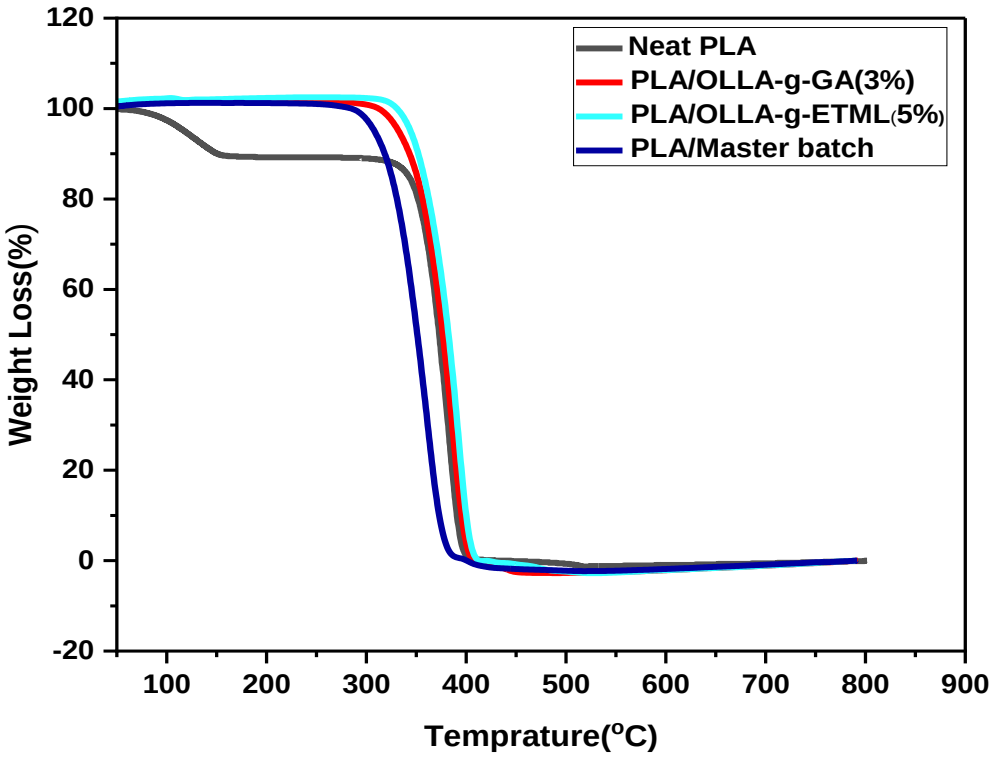

Figure 4.24: Thermal degradation curve of NPLA and PLA/master batch bio composite.

4.2.8 Degradation kinetics analysis

The use of non-isothermal thermogravimetric methods has a high capacity to unravel the mechanisms of chemical and physical processes that occur in the course of the degradation of polymers. It has been revealed that the use model-free evaluation via isoconversional approaches can provide meaningful Ea values in different experimental conditions. The isoconversional methods are powerful and most reliable tools for estimating the activation energies of thermally stimulated reactions (Habibu et al. 2019). Five isoconversional methods which include the Kissinger ,Augis & Bennet, Friedman, F-W-O and K-A-S were selected to analyze the experimental results obtained from the thermal degradation kinetics due to their ability to estimate the kinetic parameters with good accuracy and simplicity (Sergey Vyazovkin et al. 2021). Kissinger method is considered to be a model-free method, and not an isoconversional method as it assumes a constant activation energy, and does not calculate activation energy corresponding to each conversion (Chrissafis 2009; Khosravinezhad and Kazemi 2021). Figure 4.25 a and b shows the typical TGA curves at different β (5,10,15 and 20^{o}C/min) for neat PLA

and PLA/master batch bio composite. It can be seen that the TG curves of both biopolymers samples at different heating rates were qualitatively similar, consisting of one small peak, one pronounced peak and one long tailing. Based on the whole temperature range considered, both samples could be separated into three distinct stages of weight loss in TG curve which each stage had a different primary reaction during thermal decomposition. A circled stage which is in a narrow temperature range within 302–404.45 to 292–405 °C for neat PLA and PLA/master batch bio composite respectively but the highest percentage of weight loss, was caused by the devolatilization. So degradation kinetics study can be taken that there was single-step degradation process for neat PLA and PLA/master batch bio composite film samples as shown Figure 4.25 (a) and (b).

Heating rate was considered for the reason that it had some influence on conversion and product distribution. Heating rate is an important parameter in commercial applications because it can be used to determine the type of reactor used (Mastral et al. 2000). In this experiment, the results clearly showed that increasing heating rate shifted the TGA curves to higher temperatures for both biopolymers. Within the stage selected for this research (circled), at the low heating rate, the shape of TG curve was narrow and shorts (slow pyrolysis), but then becoming broader and higher at higher heating rates. For the characteristic temperatures, increasing heating rate shifted the initial temperature, the peak temperature, and the final temperature to higher values (fast pyrolysis). The initial temperature was increased from 302 to 330 °C for the neat PLA and from 292 to 320 °C for the PLA/master batch bio-composite when the heating rate was raised from 5 to 20 °C/min. The peak temperature (T_{max}) was determined as 349.6, 366,370 and 386.1 °C for the neat PLA and 350, 369, 379 and 381 °C for the PLA/master batch bio composite respectively, at 5, 10, 15 and 20 °C/min of the heating rates. The final reaction temperature was shifted from 374 to 404 °C for the neat PLA and 369–406 °C for the PLA/master batch bio composite when the heating rate of 5 °C/min was changed to 20 °C/min. Those behaviors were most probably because of increased thermal lag. At a given temperature, a higher heating rate implies that the material reaches the temperature in a shorter time (Liang and Kozinski 2000; Vamvuka et al. 2003). Additionally, increased heating rates, there is a faster release of gaseous products, thus resulting in elevated peak temperatures and rates curves (Patwa, et al. 2019).

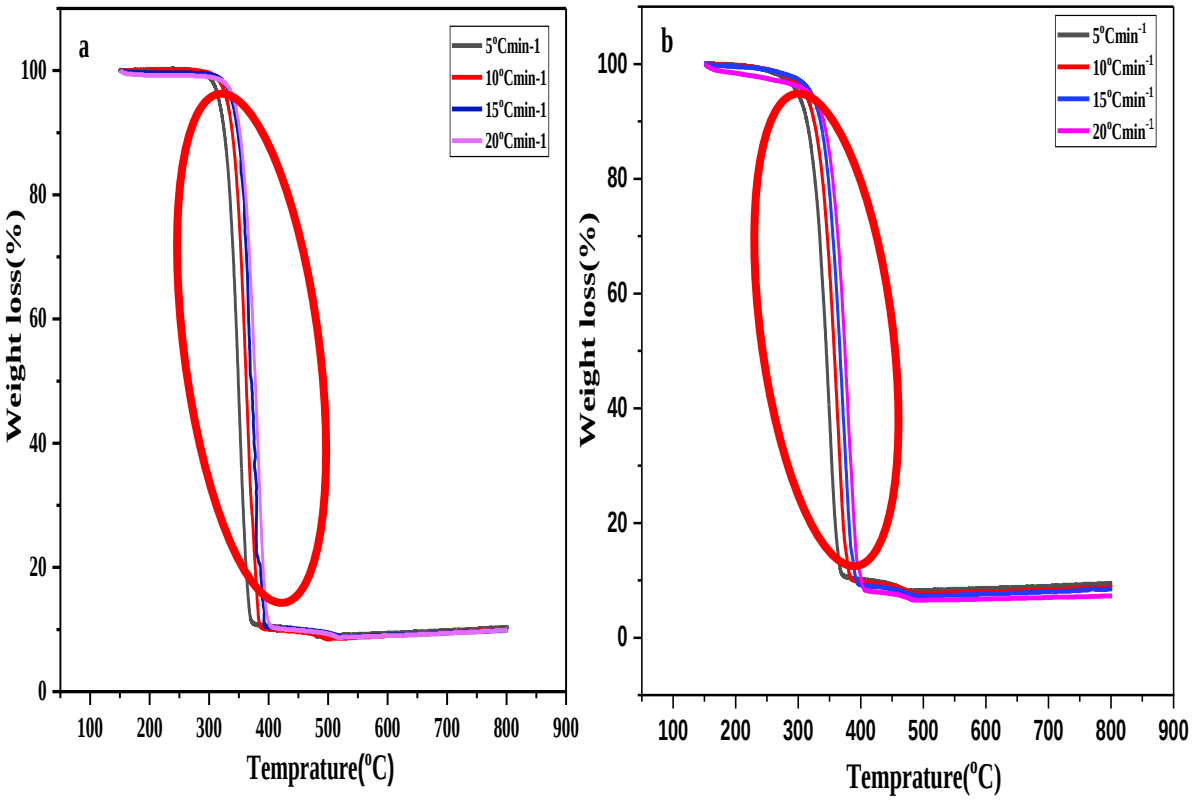

Figure 4.25: TGA plots at different heating rates for (a) Neat PLA and (b) PLA/master batch bio composite.

The results from the TGA were elaborated by the chosen isoconversional and modeling fitting method to estimate the kinetic parameters. In primary stage, the activation energies for NPLA and PLA/master batch bio composite was analyzed by Kissinger method because it was independent of thermal degradation mechanism. The method needs non-isothermal TGA measurement to obtain a constant degradation rate. The Kissinger plot is based on equation (3.5) and thermograms of inflection point temperatures. In this method, Ea. can be obtained from the slope of the line between $\ln\left[\frac{\beta}{Tmax}\right]$ vs $\frac{1}{Tmax}$ without the precise knowledge of reaction mechanism and intercept of the line can be used to determine the pre-exponential factor (A)(Al-Salem 2018). The Kissinger plot for PLA and PLA/master batch bio-composite been presented in Figure 4.26. The activation energy obtained for PLA, PLA/master batch bio composite film samples were obtained to be 105.76 and 103.8 kJ/mol respectively with the correlation coefficient in the range of 0.98697 and 0.96 which suggests that the data fit in the straight line. It could seen that all the fitted lines are almost parallel, which suggests that Kissinger method can be well applied in this system studied through this investigation.

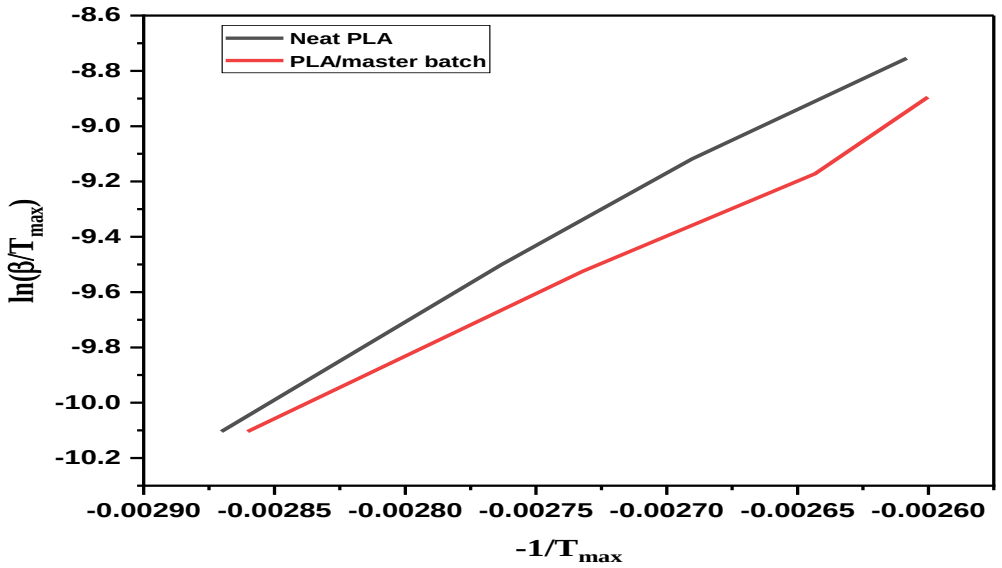

Figure 4.26: Kissinger plot for Neat PLA and PLA/master batch bio-composite films

The Augis & Bennett method was also used to determine E_a as explained in equation (3.4) from the slope of the straight line in the plot of ln $[\frac{\beta}{Tmax-Tonset}]$ vs $\frac{1}{Tmax}$. Figure 4.27 was used to determine the E_a values from the slope of the straight lines. The activation energy obtained for PLA, PLA/master batch bio composite film samples were obtained to be 109.89 and 104.43. The correlation coefficient obtained were 0.9854 and 0.98876 respectively which implies that the straight line fits the data (Wako et al.2018).

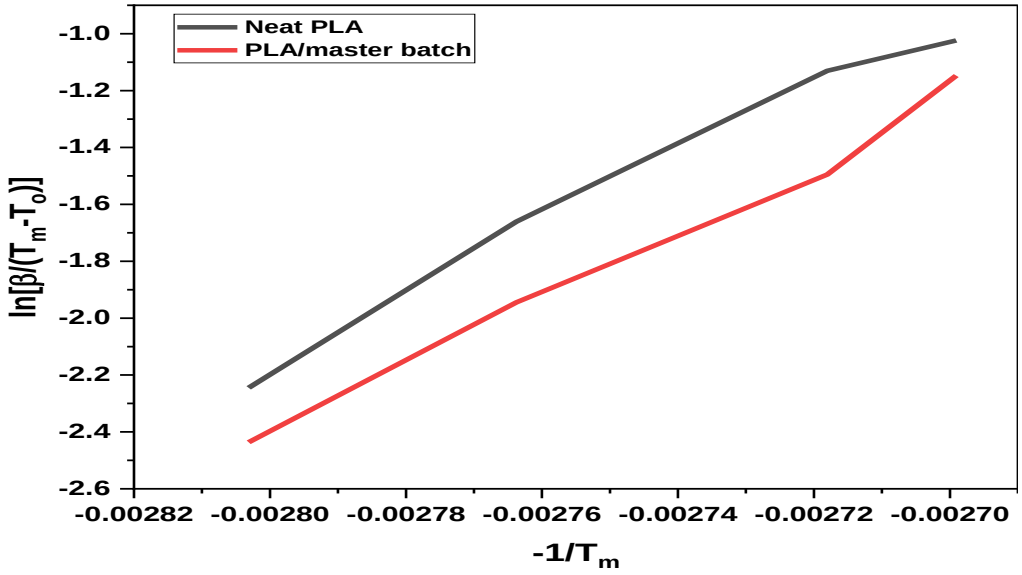

Figure 4.27: Augis & Bennett plot for Neat PLA, PLA/master batch bio composite films

The third method was FD, which is a derivative method and the most commonly used differential isoconversional process was first employed to obtain the kinetic information of the both polymer. This method was used by plotting ln (dα/dT) vs.1/T for a specified conversion and the activation energy was calculated (Figure.4.28). The fluctuation in the activation energy value was observed in FM method for both PLA and PLA/master batch bio composite which might be because of mathematical errors associated with the method and also it can be seen that all the fitted straight lines was not parallel, which suggests the non-applicability of the present system with FD model. The average activation energies for the PLA/master batch bio composite were lower compared with the one obtained for the neat PLA, this was maybe due to the presence of master batch which increases the chain mobility and intermolecular distance of the polymers similar effect was reported (Habibu et al. 2019,Woo et al. 2012).

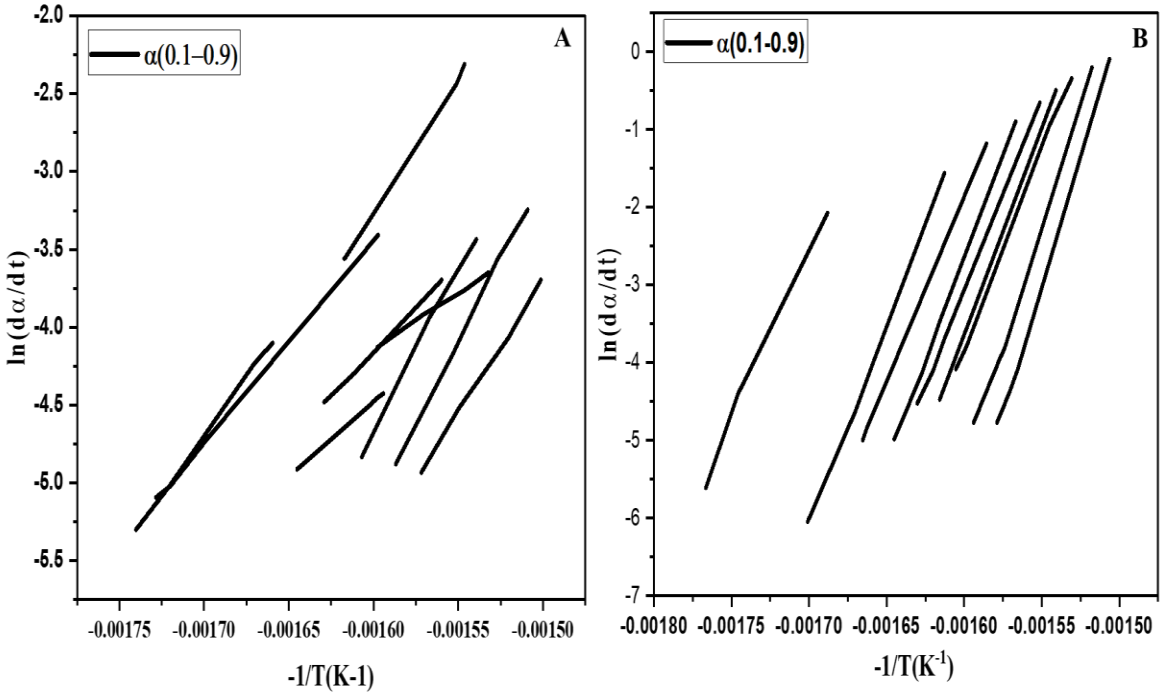

Figure 4.28: Friedman plots for Neat PLA, PLA/master batch bio composite films

The fourth method was the F-W-O which is an integral and model-free method. This technique correlates the conversion rate (α) with various heating rates at a specified conversion. Equation (3.6) was employed, and the Ea was obtained from the plots of *log* β against 1/T for a fixed conversion (α). The Ea was obtained from the slope which equals to − 0.4567 Ea/R. The

conversion values taken for the study were 0.1, 0.2, 0.3, 0.4, 0.5, 0.6, 0.7, 0.8 and 0.9 to determine the values of activation energy. The activation energy and correlation coefficient obtained for the different samples have been presented in Table 4.15. The main advantage of F-W-O method is that apart from the Arrhenius temperature-dependence, no assumptions regarding the form of the kinetic model equations are required (Venkatesh et al.2013). It was also observed that the straight lines for both PLA and P L A /master batch bio composite film samples shifted to lower 1/T values with respect to neat PLA film which suggested that the filler is causing an increase in the degradability of PLA. Similar result was reported (Valapa et al.2014). Figure 4.29 displays the straight lines that fit the data, are almost parallel to each other for each sample at higher conversion values which suggests that F-W-O model is also applicable to this system.

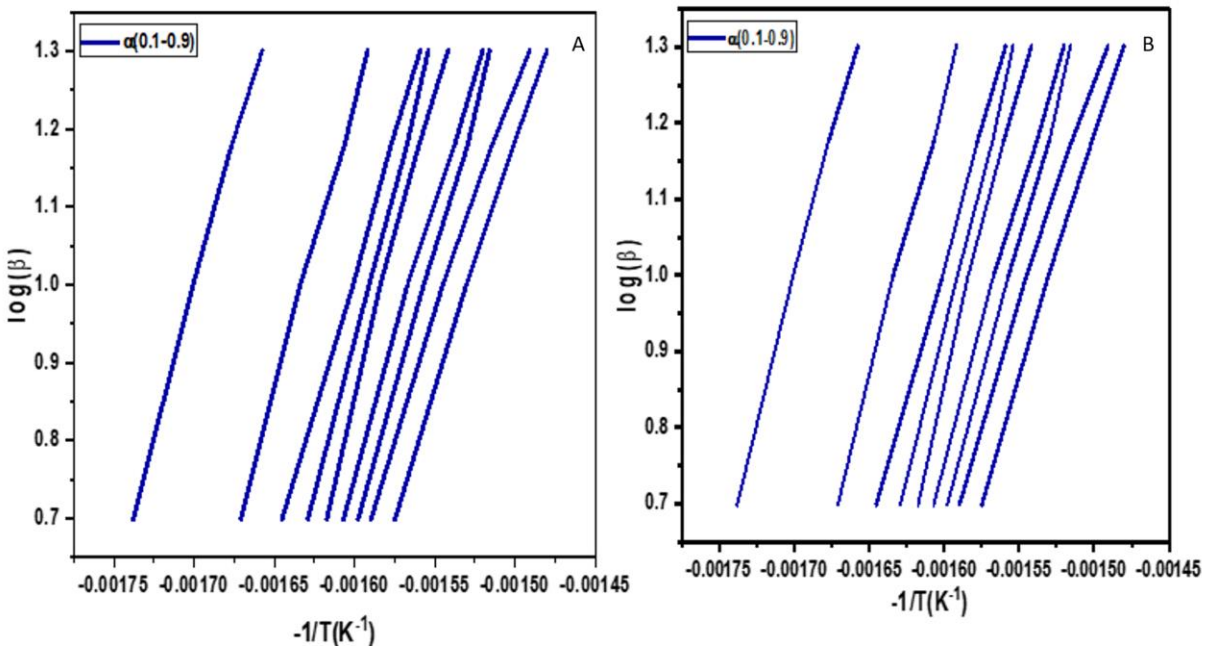

Figure 4.29: Flynn-Wall-Ozawa plots of (a) Neat PLA and (b) PLA/master batch bio composite

The fifth method used was the K-A-S method in which equation (4.9) relates the temperature (T) and the heating rate for a given conversion (α)(Peres, et al. 2021). By this method, the activation energies of decomposition were calculated from for all the values of α, straight line plot of ln (β/Tα) against 1/T is attained at various β as shown in Figure 4.30. Well linearity was observed for E_a data at these conversion values with correlation coefficient above 0.99. The average Ea values for the neat PLA and PLA/master batch bio composite given in Table 4.15. These values

are comparable to the values achieved via the F-W-O techniques. However, value of Ea in K–A–S is slightly lower than those of F–W–O method. The difference in the Ea value calculated by the two methods due to different approximations used to solve the analytical equation. It is well known that the F–W–O method is based on Doyle's linear approximation, while for K–A–S, Murray and white approximation is used (Das and Tiwari 2017)

The average activation energies for the PLA/master batch bio composite were lower compared with the one obtained for the neat PLA, for all isoconversional model this was maybe due to the presence of master batch which increases the chain mobility and intermolecular distance of the PLA matrix, similar effect was reported (Habibu et al. 2019).

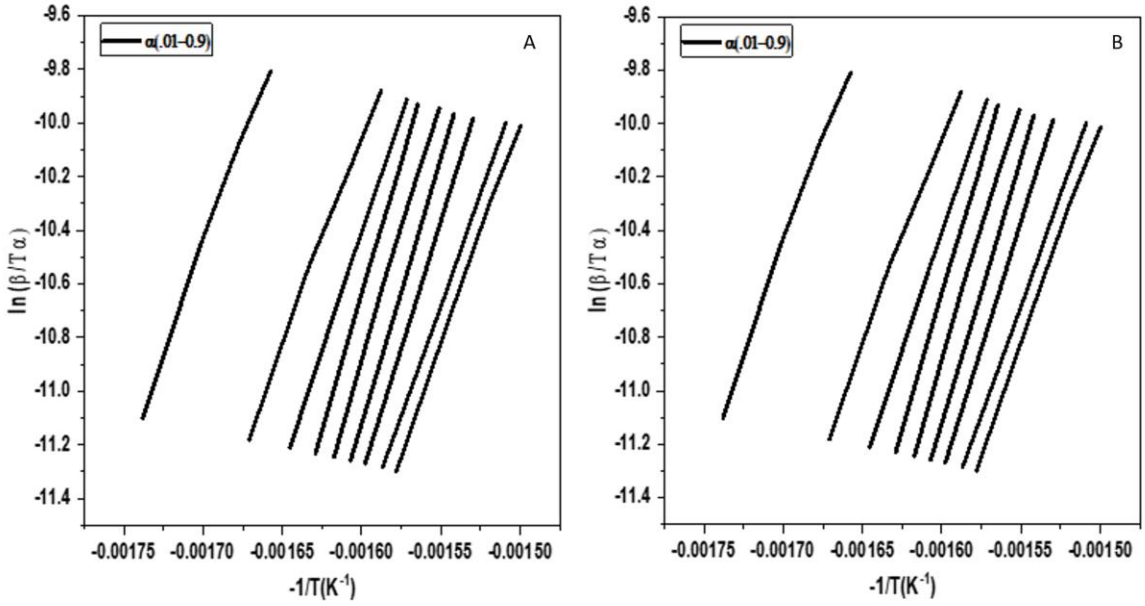

Figure 4.30: Kissinger-Akhira-Sunose plots of (a) Neat PLA, (b) PLA/master batch

The Ea values obtained from for above methods were found to follow similar trend with respect to neat PLA and PLA/ bio composite. However, the Ea values obtained from kissiger and Augis & Bennett was not close with other isoconversional (FD K-A-S and F-W-O). This is because the Kissinger and Augis & Bennett technique only applies to the maximum rate of conversion T_{max} and T_{max} -T_o (just one data point), whereas the FD,K-A-S and F-W-O method provides activation energies for various conversion levels. The regression coefficients (R^2) values achieved for all techniques in the range of 0.95-1 further demonstrate their suitability for predicting the thermal decomposition behavior of PLA and PLA/master batch composites.

It was observed from the Figure 4.22 that the curves show constant pattern behavior at different heating rates for both neat PLA and PLA/bio composite. A quick thermal decomposition is observed in the range of T_{on} to T_{end} (Figure 4.22 a & b).After this quick increase, the solid continues to decompose smoothly and slowly until the end of the experiment. Higher heating rate finishes the decomposition phenomenon faster. The thermal decomposition behavior of all of samples is almost similar, with different T_{max}. The identical reaction mechanism, was attributed to the fact of similar reaction mechanism, which is the basis of multi-heating rate approach for kinetics analysis (Mamleev et al. 2000; Saha et al.2008; S. Vyazovkin and Goryachko 1992).

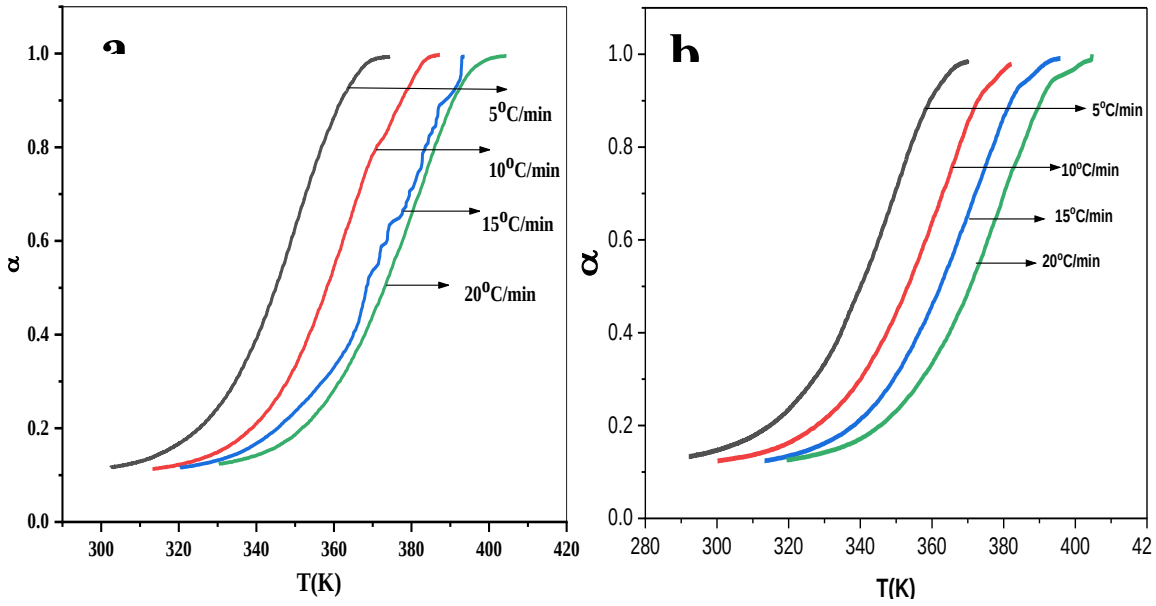

Figure 4.32: Conversion, (α) versus temperature (T) at different heating rates

The correlation between Ea and α could be estimated via the isoconversional methods without prior assumptions of the model of reaction. Moreover, the isoconversional methods allow for the detection of the multi-step kinetic relationship between the activation energy and the extent of conversion which may not be revealed by other methods such as the model fitting method (Alade et al. 2018). According to Figure 4. 23, with increase in degree of conversion, an increase the activation energy ($E_{a)}$ values occurred for neat PLA and PLA/master batch bio-composite film for KAS and FWO which was also found by (E. C. Chen and Wu 2007; Tesfaye et al. 2016;

Valapar et al. 2014), but the some fluctuation in the activation energy value was observed in FM method which might be because of mathematical errors associated with the method which was also found by (Mandal et al.2019). This indicates that activation energy of PLA was dependent of the conversion values which indicates that degradation stage of PLA therefore, from the kinetic mechanism point of view it could be predicted that, the thermal degradation process of NPLA and PLA /master batch bio composite governed by complex reaction mechanism including cis-elimination, intra and inter-molecular transesterification, unzipping de-polymerization, random scission, hydrolytic and radical degradation followed one-dimensional diffusion or unification of multiple-reaction mechanism (Gutierrez et al. 2017; Valapa et al.2014). The activation of neat PLA was higher than the bio composite.

In PLA/master batch bio-composite films, the oligomer molecules in filler (due to grafting) resulted in creating the weak link sites in the matrix by enhancing molecular chain mobility and generating intermolecular distance by small chain segment molecules of the filler. These weak bonds attributed to initiate the thermal degradation. The results also proved that the kinetic models such as Kissinger, Augis & Bennett, F-W-O and K-A-S are in good agreement, and the models have been found to be complementary to each other.

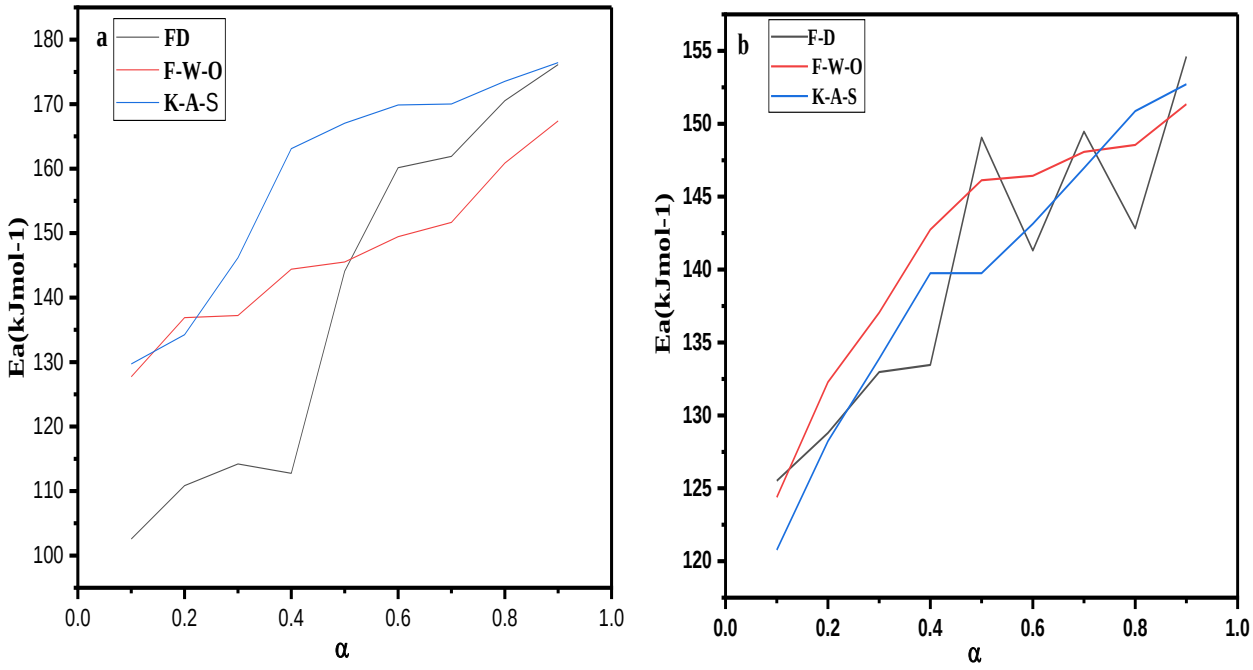

Figure 4.33: Activation energy versus conversion plot obtained from FD, FWO and KAS model

Table 4.15 Values of activation energies obtained using FM, FWO and KAS methods

Sample name	Model type								
	FM			**FWO**			**KAS**		
	α	E/kJ mol-1	R^2	α	E(kJ mol-1)	R^2	α	E/kJmol-1	R^2
	0.1	102.5602	0.999	0.1	127.737	0.9978	0.1	129.7146	0.996
	0.2	110.84	0.999	0.2	136.9	0.994	0.2	134.242	0.997
	0.3	114.1994	0.999	0.3	137.236	0.999	0.3	136.19	1
	0.4	119.76	0.999	0.4	144.417	0.999	0.4	142.1	0.9998
	0.5	144.096	0.999	0.5	145.52	0.9955	0.5	145.04	0.9998
	0.6	160.144	0.995	0.6	149.454	0.99795	0.6	147.86	0.
	0.7	161.9	0.998	0.7	151.67	0.999	0.7	150.03	1
	0.8	170.654	0.998	0.8	160.847	0.9966	0.8	156.531	1
	0.9	176.14	0.998	0.9	163.23	0.998	0.9	166.44	0.9985

		Average=140			Ave=146.7			Average=145.4	
PLA/master batch		186.42							
	0.1	125.513	0.99	0.1	124.38	0.997	0.1	120.77	0.99
	0.2	128.798	0.998	0.2	132.28	0.99734	0.2	128.23	0.9936
	0.3	132.9687	0.999	0.3	137.05	0.99	0.3	133.89	0.989
	0.4	133.46	0.999	0.4	142.739	0.9934	0.4	139.31	0.9923
	0.5	149.059	0.999	0.5	146. 128	0.99368	0.5	139.75	0.9925
	0.6	141.3	1	0.6	146. 427	0.9934	0.6	143.14	0.9934
	0.7	149.46	0.999	0.7	148.076	0.9958	0.7	146.96	0.9926
	0.8	142.825	0.996	0.8	148.547	0.985	0.8	150.872	0.9823
	0.9	154.61	0.998	0.9	151.34	0.993	0.9	152.71	0.9919
		Ave =139.78			Av=141.89			Aav=139.55	

Coats–Redfern method

The Coats–Redfern (CR) technique was chosen to explore the mechanism for the thermal decomposition of these polymers since the activation energy, Ea could be obtained using this approach in the absence of prior information about the nature of the degradation. The activation energy was calculated based on the f(α) functions according to equation (4.12). For the kinetic description of the polymer degradation, two kinds of reaction models are mainly used at the literature (Al-Salem 2018; Arora et al. 2011;Hawkins 1984; Persenaire et al. 2001; Wielage et al. 1999), the first order (F1) and the n th reaction model (Fn), due to their simplicity. For each model (F1 and Fn), the Ea was acquired from the slope of the plot of $ln\frac{g(\alpha)}{T2}$ against 1/T. The values of the activation energy E, the pre-exponential factor A and the reaction order n for the three reaction models (F1, Fn) and the regression coefficients for every fitting curve are presented in Table 4.16. The activation energy values obtained from reaction order Fn=0.5(128.79 E/ kJ mol–1) was relatively close to the values obtained from the isoconversional methods. The quality of the fitting with Fn = 0.5 models was very good for both neat PLA and PLA/ master batch. As reaction order increase for both polymers the fitting become decrease, which indicated that the degradation reaction was not corresponding to it.

Table 4:16 Activation energy, log A and R^2 for neat PLA (a) and PLA/bio-composite films (b) pyrolysis by Coats–Red fern method @10 ^{o}C/min

Kinetic model	Reaction order	E(kJ mol–1)	Aα (min−1)	Regr. coef. R
(a)	n = 0.5	128.79	1.857×10^{14}	0.97
	n =1	145.825	1.08×10^{13}	0.95
Kinetic model	n =1.5	177.11	8.377×10^{18}	0.922
	n = 2	207.1	3.97×10^{21}	0.891
	n = 3	276.32	4.965×10^{28}	0.833
	n = 4	354.27	4.168×10^{34}	0.785

Kinetic model	Reaction order	E(kJ mol–1)	Aα (min−1)	Regr. coef. R
(b)	n =0.5	106.667	2.201×10^{13}	0.972
	n =1	119.7	6.42×10^{11}	0.94
Kinetic model	n =1.5	146.02	1.999×10^{17}	0.91
(n-order reactions)	n = 2	170.3	3.36×10^{19}	0.87
	n = 3	226.32	4.12×10^{24}	0.81
	n = 4	289.4	2.1×10^{30}	0.72

5. Conclusion and Recommendation

5.1 Conclusion

In this study, gum arabica and euphorbia trigon mill latex based filler were synthesized by using lactic acid, euphorbia trigon mill latex and gum arabic as precursors. The synthesis was conducted by poly-condensation reaction without using any catalyst or additive. The effect of different operational parameters like mixing ratio, temperature and grafting time for GA were optimized by using design expert software by applying the box-behnken design. The grafting occurred at -OH and -NH_2 groups which were confirmed by FTIR and NMR analysis. The PLA, PLA/OLLA-g-GA, PLA/OLLA-g-ETML and PLA/master batch bio-composite films were prepared by solution casting method. FTIR of prepared films suggested successful preparation of PLA/OLLA-g-GA,PLA/OLLA-g-ETML,PLA/master-batch bio-composite films while dispersion of fillers studied by optical microscope that helped the determine maximum loading . The effect of reinforcing agent of OLLA-g-GA, OLLA-g-ETML and master batch in the PLA matrix on its transmittance, mechanical properties, degree of crystallization, thermal stability, and antimicrobial properties was investigated. Tensile testing of the films established improved ductility of films with the incorporation of OLLA-g-GA, OLLA-g-ETML and mater batch. Addition of OLLA-g-GA improved tensile strength and elongation at break of neat PLA by 38.3 and 20%, respectively with 3% loading of OLLA-g-GA. The elongation at break increased by 62% with 5% OLLA-g-ETML in comparison to PLA films. Additionally, tensile strength and elongation at break of neat PLA improved by 47.1 and 34% with addition of mater batch (OLLA-g-GA (3%)-OLLA-g-ETML (5%). The transmittance of PLA was decreased after incorporating the fillers. The neat PLA has the highest transmittance with a value of 55.63% while the transmittance of PLA bio-composite incorporated with master batch at 600 nm is 46.76% which shows the decrement in transmittance, but it is good when compared to other reinforced composite materials (OLLA-g-GA, OLLA-g-ETML). Addition of OLLA-g-GA, OLLA-g-ETML and ,master batch as a nucleating agent at different thermal annealing time changes the melting glass transition temperature and crystallization behavior of PLA, even though the temperatures of glass transition and melting (Tg and Tm) respectively changes insignificantly. The degree of crystallinity increased from 29.16% for neat PLA to 44.20, 37.96 and 45.83 % with addition of OLLA-g-GA (3%), OLLA-g-ETML (5%) and master batch, respectively. The thermal stability of PLA after incorporating master was reduced, and this

arouses from the lower thermal stability of the filler than PLA polymer. Thermal degradation of neat PLA and PLA/master batch bio-composites was investigated using thermal gravimetric analysis. A single step decomposition behavior was assumed from the observed single pattern TGA thermograph for all the heating rates which reveals master batch were effectively dispersed in the PLA matrix. Degradation kinetics of PLA and PLA/master batch bio composites were investigated using five different model free (isoconversional (Kissinger, Augis & Bennett, FD, F-W-O and K-A-S)) and model fitting (Coats-Redfern) method. Activation energy E_a of neat PLA was higher than PLA/master batch bio composite. Coates Redfern method helped in elucidating the thermal degradation mechanism for both neat PLA and bio-composite, which was found to follow 1/2 order kinetics. The activation energy obtained by Coats-Redfern was smoothly consistent with isoconversional values. E_a versus conversion plot indicated that the degradation stage of PLA and PLA/master batch bio-composite followed one- dimensional diffusion mechanism or unification of multiple-reaction mechanism. The increase in activation energy with increase in conversion indicates complex reaction in neat PLA, PLA/master batch bio-composite films. The results also proved that the kinetic models are in good agreement,and the models are complementary to each other. Hence, the results can provide valuable information for researchers in order to predict kinetic model and optimization of the process conditions for the system. The antibacterial activities of PLA/OLLA-g-GA, PLA/OLLA-g-ETML and PLA/master batch bio-composite film were examined against Gram-negative bacteria (*E. coli* and *P. aeruginosa*) and Gram-positive bacteria species (*S.pyogen* and *S. aureus*) bacteria. The zone of inhibition larger for PLA/master batch bio- composite for all species of bacteria, this exhibits strong potential for development as active packaging film.

5.2 Scope for Future Work

In this research work, both bio-conjugate (OLLA-g-GA and OLLA-g-ETML) were successfully synthesized. Bio-degradable, ecofriendly, sustainable and biocompatible nature make best candidate for properties enhancing agent for PLA, because of the potential of products; their interesting physical and chemical property, and their good compatibility with each other, a few recommendations for carrying out future research in this field are as follows:-

- Detailed studies on toxicity, migration, biodegradation and recycling of PLA/ bio-composite films can be undertaken.
- Detailed study can be done on morphology of the films using SEM and TEM.
- Due to the good antibacterial of both OLLA-g-GA, OLLA-g-ETML and master batch in the films, it is good if the Anti-fungal activities and shelf life in the food packaging application may be investigated in detail.
- Permeability tests Water at different relative humidity and oxygen transmission rate can be tested for packaging applications.
- Estimation of activation energy and pre-exponential factor using Coats and Redfern method for fourteen different models.
- Analysis of thermal decomposition products by using thermogravimetry coupled Fourier transform infrared spectroscopy (TG-FTIR).

Reference

A. Ibrahim, Buthaina, and Karrer M.Kadum. 2010. “Influence of Polymer Blending on Mechanical and Thermal Properties.” *Modern Applied Science* 4(9): 157–61.

Aaliya, Basheer, Kappat Valiyapeediyekkal Sunooj, and Maximilian Lackner. 2021. “Biopolymer Composites: A Review.” *International Journal of Biobased Plastics* 3(1): 40–84.

Abdullah, Nur A S et al. 2019. “Thermal and Toughness Enhancement of Poly (Lactic Acid).” 7(September 2018): 427–32.

Ai, Informativa, and Sensi Della. 2003. “192 193 192 194.” : 2003.

Ainali, Nina Maria et al. 2021. “Thermal Stability and Decomposition Mechanism of Pla Nanocomposites with Kraft Lignin and Tannin.” *Polymers* 13(16).

Al-akayleh, Faisal et al. 2014. “In Controlled Release Formulations of Ambroxol HCl - in Vitro.” 5(June): 140–48.

Al-Salem, Sultan M. 2018. Plastics to Energy: Fuel, Chemicals, and Sustainability Implications *Kinetic Studies Related to Polymer Degradation and Stability*. Elsevier Inc. http://dx.doi.org/10.1016/B978-0-12-813140-4.00009-1.

Alade, Olalekan S. et al. 2018. “Kinetics of Thermal Degradation of a Japanese Oil Sand.” *Egyptian Journal of Petroleum* 27(4): 505–12. https://doi.org/10.1016/j.ejpe.2017.08.001.

Alang, MB, JT Barminas, BA Aliyu, and SA Osemeahon. 2012. “Synthesis and Optimization of Polyacrylamide and Gum Arabic Graft Copolymer.” *International Journal of Biological and Chemical Sciences* 5(4): 1694–1702.

Ali, Asgar, Mehdi Maqbool, Senthil Ramachandran, and Peter G. Alderson. 2010. “Gum Arabic as a Novel Edible Coating for Enhancing Shelf-Life and Improving Postharvest Quality of Tomato (Solanum Lycopersicum L.) Fruit.” *Postharvest Biology and Technology* 58(1): 42–47. http://dx.doi.org/10.1016/j.postharvbio.2010.05.005.

Aliotta, Laura et al. 2017. “Effect of Nucleating Agents on Crystallinity and Properties of Poly (Lactic Acid) (PLA).” *European Polymer Journal* 93: 822–32.

Almuslet, Nafie A., Elfatih Ahmed Hassan, Al Sayed Abd El Magied Al-Sherbini, and Mohamed Gusm Alla Muhgoub. 2012. “Diode Laser (532 Nm) Induced Grafting of Polyacrylamide onto Gum Arabic.” *Journal of Physical Science* 23(2): 43–53.

Appolonia Ibekwe, Chinenye, Grace Modupe Oyatogun, Temitope Ayodeji Esan, and Kunle

Michael Oluwasegun. 2017. “Synthesis and Characterization of Chitosan/Gum Arabic Nanoparticles for Bone Regeneration.” *American Journal of Materials Science and Engineering* 5(1): 28–36.

Arrieta, M. P. et al. 2014. “PLA-PHB/Cellulose Based Films: Mechanical, Barrier and Disintegration Properties.” *Polymer Degradation and Stability* 107: 139–49. http://dx.doi.org/10.1016/j.polymdegradstab.2014.05.010.

Arrieta, M P, and M D Samper. 2020. “‘Improvement of PLA Film Ductility by Plasticization with Epoxidized Karanja Oil.’” *Polymer Degradation and Stability*: 109259.

Avinc, Ozan, and Akbar Khoddami. 2009. “Overview of Poly Lactid Acid (PLA) Fibre Part I : Production , Properties , Performance , Environmental Impact , and End-Use Applications of Poly (Lactic Acid) Fibres.” *Fibre Chemistry* 41(6): 16–25. https://link.springer.com/content/pdf/10.1007/s10692-010-9213-z.pdf.

Baien, Shima Hassan et al. 2020. “Antimicrobial and Immunomodulatory Effect of Gum Arabic on Human and Bovine Granulocytes Against Staphylococcus Aureus and Escherichia Coli.” *Frontiers in Immunology* 10(January): 1–18.

Bajpai, Pramendra Kumar, Inderdeep Singh, and Jitendra Madaan. 2014. “Development and Characterization of PLA-Based Green Composites: A Review.” *Journal of Thermoplastic Composite Materials* 27(1): 52–81.

Balakrishnan, Harintharavimal et al. 2010. “Novel Toughened Polylactic Acid Nanocomposite: Mechanical, Thermal and Morphological Properties.” *Materials and Design* 31(7): 3289–98.

Balakrishnan, Harintharavimal, Azman Hassan, Muhammad Imran, and Mat Uzir Wahit. 2012. “Toughening of Polylactic Acid Nanocomposites: A Short Review.” *Polymer - Plastics Technology and Engineering* 51(2): 175–92.

Balakrishnan, Harintharavimal, Azman Hassan, and Mat Uzir Wahit. 2010. “Mechanical, Thermal, and Morphological Properties of Polylactic Acid/Linear Low Density Polyethylene Blends.” *Journal of Elastomers and Plastics* 42(3): 223–39.

Balla, Evangelia et al. 2021. “Poly(Lactic Acid): A Versatile Biobased Polymer for the Future with Multifunctional Properties-from Monomer Synthesis, Polymerization Techniques and Molecular Weight Increase to PLA Applications.” *Polymers* 13(11).

“BASED NANOCOMPOSITES BY ENHANCED DISPERSION OF MODIFIED

CELLULOSE North Dakota State University." 2018. (October).

Basu, Arijit et al. 2017. "Poly(Lactic Acid)-Based Nanocomposites." *Polymers for Advanced Technologies* 28(8): 919–30.

Bautista-Hernández, Israel et al. 2021. "Antioxidant Activity of Polyphenolic Compounds Obtained from Euphorbia Antisyphilitica By-Products." *Heliyon* 7(4).

Bax, Benjamin, and Jörg Müssig. 2008. "Impact and Tensile Properties of PLA/Cordenka and PLA/Flax Composites." *Composites Science and Technology* 68(7–8): 1601–7.

Bhattacharya, A., and B. N. Misra. 2004. "Grafting: A Versatile Means to Modify Polymers: Techniques, Factors and Applications." *Progress in Polymer Science (Oxford)* 29(8): 767–814.

Bhattarai, Narayan, Hassna R. Ramay, Shinn Huey Chou, and Miqin Zhang. 2006. "Chitosan and Lactic Acid-Grafted Chitosan Nanoparticles as Carriers for Prolonged Drug Delivery." *International Journal of Nanomedicine* 1(2): 181–87.

Bitinis, N. et al. 2012. "Physicochemical Properties of Organoclay Filled Polylactic Acid/Natural Rubber Blend Bionanocomposites." *Composites Science and Technology* 72(2): 305–13.

Bonilla, J. et al. 2013. "Effects of Chitosan on the Physicochemical and Antimicrobial Properties of PLA Films." *Journal of Food Engineering* 119(2): 236–43.

Bucheery, Raja Ali M. 2001. "In the Name of Allah , the Most Beneficent , the Most Merciful."

Burgos, Nuria, Daniel Tolaguera, Stefano Fiori, and Alfonso Jiménez. 2014. "Synthesis and Characterization of Lactic Acid Oligomers: Evaluation of Performance as Poly(Lactic Acid) Plasticizers." *Journal of Polymers and the Environment* 22(2): 227–35.

Carrasco, F. et al. 2010. "Processing of Poly(Lactic Acid): Characterization of Chemical Structure, Thermal Stability and Mechanical Properties." *Polymer Degradation and Stability* 95(2): 116–25.

Chaiwutthinan, Phasawat, Naruedee Phutfak, and Amnouy Larpkasemsuk. 2021. "Effects of Thermoplastic Poly(Ether-Ester) Elastomer and Bentonite Nanoclay on Properties of Poly(Lactic Acid)." *Journal of Applied Polymer Science* 138(20): 8–11.

Chen, Erh Chiang, and Tzong Ming Wu. 2007. "Isothermal Crystallization Kinetics and Thermal Behavior of Poly(ε-Caprolactone)/Multi-Walled Carbon Nanotube Composites." *Polymer Degradation and Stability* 92(6): 1009–15.

Chen, Weijun et al. 2019. "Preparation of Modified Whey Protein Isolate with Gum Acacia by

Ultrasound Maillard Reaction." *Food Hydrocolloids* 95: 298–307.

Chrissafis, K. 2009. "Kinetics of Thermal Degradation of Polymers : CComplementary Use of Isoconversional and Model-Fitting Methods." *Journal of Thermal Analysis and Calorimetry* 95(1): 273–83.

Chung, Pooi Yin. 2020. "Novel Targets of Pentacyclic Triterpenoids in Staphylococcus Aureus: A Systematic Review." *Phytomedicine* 73(July 2018): 152933.

Čolnik, Maja, Maša Knez Hrnčič, Mojca Škerget, and Željko Knez. 2020. "Biodegradable Polymers, Current Trends of Research and Their Applications, a Review." *Chemical Industry and Chemical Engineering Quarterly* 26(4): 401–18.

Crozier, Alan, Indu B. Jaganath, and Michael N. Clifford. 2007. "Phenols, Polyphenols and Tannins: An Overview." *Plant Secondary Metabolites: Occurrence, Structure and Role in the Human Diet* (April 2016): 1–24.

Das, Pallab, and Pankaj Tiwari. 2017. "Thermal Degradation Kinetics of Plastics and Model Selection." *Thermochimica Acta* 654(June): 191–202. http://dx.doi.org/10.1016/j.tca.2017.06.001.

van Deenen, N., D. Prüfer, and C. Schulze Gronover. 2011. "A Latex Lectin from Euphorbia Trigona Is a Potent Inhibitor of Fungal Growth." *Biologia Plantarum* 55(2): 335–39.

Di, Y., Salvatore Iannace, Ernesto Di Maio, and Luigi Nicolais. 2005. "Poly(Lactic Acid)/Organoclay Nanocomposites: Thermal, Rheological Properties and Foam Processing." *Journal of Polymer Science, Part B: Polymer Physics* 43(6): 689–98.

Diani, Julie, and Ken Gall. 2006. "Finite Strain 3D Thermoviscoelastic Constitutive Model." *Society*: 1–10.

Donate, Ricardo, Mario Monzón, and Mariá Elena Alemán-Domínguez. 2020. "Additive Manufacturing of PLA-Based Scaffolds Intended for Bone Regeneration and Strategies to Improve Their Biological Properties." *E-Polymers* 20(1): 571–99.

Dong, Xinyi et al. 2021. "Toughening Polylactide Using Epoxy-Functionalized Core-Shell Starch Nanoparticles." *Polymer Testing* 93(October 2020): 106926. https://doi.org/10.1016/j.polymertesting.2020.106926.

Dünnhaupt, S. et al. 2015. "Thiolated Nanocarriers for Oral Delivery of Hydrophilic Macromolecular Drugs." *Carbohydrate Polymers* 117: 577–84.

Ecker, Josef Valentin et al. 2019. "Mechanical Properties and Water Absorption Behaviour of

PLA and PLA/Wood Composites Prepared by 3D Printing and Injection Moulding." *Rapid Prototyping Journal* 25(4): 672–78.

Emam, Hossam E. 2019. "Arabic Gum as Bio-Synthesizer for Ag–Au Bimetallic Nanocomposite Using Seed-Mediated Growth Technique and Its Biological Efficacy." *Journal of Polymers and the Environment* 27(1): 210–23. http://dx.doi.org/10.1007/s10924-018-1331-3.

Eng, Chern Chiet et al. 2013. "Enhancement of Mechanical and Thermal Properties of Polylactic Acid/Polycaprolactone Blends by Hydrophilic Nanoclay." *Indian Journal of Materials Science* 2013: 1–11.

Enyew, Abiyu, Zemede Asfaw, Ensermu Kelbessa, and Raja Nagappan. 2014. "Ethnobotanical Study of Traditional Medicinal Plants in and Around Fiche District , Central Ethiopia." 6(4): 154–67.

Espartero, J. L. et al. 1996. "NMR Analysis of Low Molecular Weight Poly(Lactic Acid)S." *Macromolecules*.

Farah, Shady, Daniel G. Anderson, and Robert Langer. 2016. "Physical and Mechanical Properties of PLA, and Their Functions in Widespread Applications — A Comprehensive Review." *Advanced Drug Delivery Reviews* 107: 367–92.

Fattahi, Farnaz Sadat, Akbar Khoddami, and Ozan Avinc. 2019. "Poly (Lactic Acid) Nano-Fibers as Drug-Delivery Systems: Opportunities and Challenges." *Nanomedicine Research Journal* 4(3): 130–40.

Feng, Yongqi et al. 2017. "The Crystallization Behavior of Poly(Lactic Acid) with Different Types of Nucleating Agents." *International Journal of Biological Macromolecules*.

Fitri Rahmafitria, 2014. 1999. "No 主観的健康感を中心とした在宅高齢者における 健康関連指標に関する共分散構造分析Title." (19): 1–5.

Fortunati, E. et al. 2015. "Processing of PLA Nanocomposites with Cellulose Nanocrystals Extracted from Posidonia Oceanica Waste: Innovative Reuse of Coastal Plant." *Industrial Crops and Products* 67: 439–47.

Frone, Adriana Nicoleta et al. 2016. "The Effect of Cellulose Nanofibers on the Crystallinity and Nanostructure of Poly(Lactic Acid) Composites." *Journal of Materials Science* 51(21): 9771–91.

Ganie, Showkat A., Akbar Ali, and Nasreen Mazumdar. 2015. "Iodine Derivatives of Chemically Modified Gum Arabic Microspheres." *Carbohydrate Polymers* 129: 224–31.

http://dx.doi.org/10.1016/j.carbpol.2015.04.044.

Gao, Yu et al. 2017. “Preparation and Properties of Novel Thermoplastic Vulcanizate Based on Bio-Based Polyester/Polylactic Acid, and Its Application in 3D Printing.” *Polymers* 9(12).

Garlotta, Donald. 2019. “A Literature Review of Poly (Lactic Acid) A Literature Review of Poly (Lactic Acid).” *Journal of Polymers and the Environment* 9(2): 63–84.

Gironi, F., S. Frattari, and V. Piemonte. 2016. “PLA Chemical Recycling Process Optimization: PLA Solubilization in Organic Solvents.” *Journal of Polymers and the Environment* 24(4): 328–33.

Glycol, Polyethylene. 2015. “Thermo-Mechanical Properties of Poly ε-Caprolactone / Poly L-Lactic Acid Blends : Addition of Nalidixic Acid and Polyethylene Glycol Additives Journal of the Mechanical Behavior of Biomedical Materials Thermo-Mechanical Properties of Poly ε -Caprolactone .”

Gneshin, Keith W, Æ Andrew M Herring, and J Thomas Mckinnon. 2008. “Renewable Cellulose Derived Carbon Nanospheres as Nucleating Agents for Polylactide and Polypropylene.” : 131–40.

Greco, Antonio, and Francesca Ferrari. 2021. “Thermal Behavior of PLA Plasticized by Commercial and Cardanol-Derived Plasticizers and the Effect on the Mechanical Properties.” *Journal of Thermal Analysis and Calorimetry* 146(1): 131–41. https://doi.org/10.1007/s10973-020-10403-9.

Gu, Jin, and Jeffrey M. Catchmark. 2013. “Polylactic Acid Composites Incorporating Casein Functionalized Cellulose Nanowhiskers.” *Journal of Biological Engineering* 7(1).

Gunasekera, Deshani H.A.T. et al. 2016. “Three Dimensional Ink-Jet Printing of Biomaterials Using Ionic Liquids and Co-Solvents.” *Faraday Discussions* 190: 509–23.

Gutierrez-Villarreal, Mario, Helia Bibiana León-Molina, and Ricardo Acosta. 2017. “Kinetic Study on the Thermal Degradation of Ethylene–Norbornene Copolymers under the Effect of Fe and Mn Stearates.” *Reaction Kinetics, Mechanisms and Catalysis* 122(2): 995–1010.

Habibu, Shehu, Norazilawati Muhamad Sarih, Nor Asrina Sairi, and Muzafar Zulkifli. 2019. “Rheological and Thermal Degradation Properties of Hyperbranched Polyisoprene Prepared by Anionic Polymerization.” *Royal Society Open Science* 6(11).

Han, Jung H., and John D. Floros. 1997. “Casting Antimicrobial Packaging Films and Measuring Their Physical Properties and Antimicrobial Activity.” *Journal of Plastic Film and Sheeting*

13(4): 287–98.

Hao, Mingyang, Hongwu Wu, and Zhihua Zhu. 2017. “In Situ Reactive Interfacial Compatibilization of Polylactide/Sisal Fiber Biocomposites via Melt-Blending with an Epoxy-Functionalized Terpolymer Elastomer.” *RSC Advances* 7(51): 32399–412. http://dx.doi.org/10.1039/C7RA03513F.

Hao, Xiaoqiong et al. 2015. “Entanglement Network Formed in Miscible PLA/PMMA Blends and Its Role in Rheological and Thermo-Mechanical Properties of the Blends.” *Polymer* 80: 38–45.

Hao, Yuhua, and Zhen Huang. 2018. “Effects of Different Zeolites on Poly(L-Lactide) Thermal Degradation.” *Lecture Notes in Electrical Engineering* 477(January): 849–55.

Harshe, Yogesh M. et al. 2007. “Polycondensation Kinetics of Lactic Acid.” *Macromolecular Reaction Engineering* 1(6): 611–21.

Hawkins, W. Lincoln. 1984. “Polymer Degradation.” : 3–34.

Hindi, S S Z et al. 2017. “Synthesis, Characterization and Biodegradation of Gum Arabic-Based Bioplastic Membranes.” *Synthesis Nanoscience and Nanotechnology Research* 4(2): 32–42.

Homklin, Rungsima, and Nattakarn Hongsriphan. 2013. “Mechanical and Thermal Properties of PLA/PBS Cocontinuous Blends Adding Nucleating Agent.” *Energy Procedia* 34: 871–79.

Hu, Huan et al. 2020. “High-Toughness Poly(Lactic Acid) / Starch Blends Prepared through Reactive Blending Plasticization and Compatibilization.”

Hua, Juan et al. 2017. “Chemical Profile and Defensive Function of the Latex of Euphorbia Peplus.” *Phytochemistry* 136: 56–64.

Ilyas, R. A. et al. 2021. “Polylactic Acid (Pla) Biocomposite: Processing, Additive Manufacturing and Advanced Applications.” *Polymers* 13(8).

Indah Sari, Tuti, Asep Handaya Sa, Dadi R. Maspang, and Setijo Bismo. 2017. “Modification of Natural Rubber as a Resistant Material to Dimethyl Ether.” *Journal of Applied Sciences* 17(2): 53–60.

Jang, Woo Yeul, Boo Young Shin, Tae Jin Lee, and Ramani Narayan. 2007. “Thermal Properties and Morphology of Biodegradable PLA/Starch Compatibilized Blends.” *Journal of Industrial and Engineering Chemistry* 13(3): 457–64.

Jiang, Long et al. 2016. “Crystallization Modification of Poly(Lactide) by Using Nucleating Agents and Stereocomplexation.” *E-Polymers* 16(1): 1–13.

Jin, Fan Long, Rong Rong Hu, and Soo Jin Park. 2019. “Improvement of Thermal Behaviors of Biodegradable Poly(Lactic Acid) Polymer: A Review.” *Composites Part B: Engineering* 164(November 2018): 287–96.

Jonoobi, Mehdi, Jalaluddin Harun, Aji P. Mathew, and Kristiina Oksman. 2010. “Mechanical Properties of Cellulose Nanofiber (CNF) Reinforced Polylactic Acid (PLA) Prepared by Twin Screw Extrusion.” *Composites Science and Technology* 70(12): 1742–47.

Kaith, Balbir Singh, Amar Singh Singha, and Shabnam Ranjta. 2010. “Synthesis, Characterization, and Swelling Studies of Gum Arabic-Grafted Methacrylic Acid Polymeric Network.” *International Journal of Polymer Analysis and Characterization* 15(4): 222–34.

Kamthai, Suthaphat, and Rathanawan Magaraphan. 2015. “Thermal and Mechanical Properties of Polylactic Acid (PLA) and Bagasse Carboxymethyl Cellulose (CMCB) Composite by Adding Isosorbide Diesters.” *AIP Conference Proceedings* 1664(2015).

Kang, Hailan et al. 2018. “An Environmentally Sustainable Plasticizer Toughened Polylactide.” *RSC Advances* 8(21): 11643–51.

Kang, Kyung Su et al. 2008. “Effect of Biobased and Biodegradable Nucleating Agent on the Isothermal Crystallization of Poly (Lactic Acid).” 25(3): 599–608.

Kangwansupamonkon, Wiyong, Robert G. Gilbert, and Suda Kiatkamjornwong. 2005. “Modification of Natural Rubber by Grafting with Hydrophilic Vinyl Monomers.” *Macromolecular Chemistry and Physics* 206(24): 2450–60.

Kanmani, Paulraj, and Jong Whan Rhim. 2014. “Properties and Characterization of Bionanocomposite Films Prepared with Various Biopolymers and ZnO Nanoparticles.” *Carbohydrate Polymers* 106(1): 190–99.

Kaseem, Mosab, Kotiba Hamad, Fawaz Deri, and Young Gun Ko. 2017. “A Review on Recent Researches on Polylactic Acid/Carbon Nanotube Composites.” *Polymer Bulletin* 74(7): 2921–37.

Kaur, Loveleenpreet, and G. D. Gupta. 2020. “Gum Karaya-g-Poly (Acrylamide): Microwave Assisted Synthesis, Optimisation and Characterisation.” *International Journal of Applied Pharmaceutics* 12(5): 143–52.

Ke, Tianyi, and Xiuzhi Sun. 2003. “Melting Behavior and Crystallization Kinetics of Starch and Poly(Lactic Acid) Composites.” *Journal of Applied Polymer Science* 89(5): 1203–10.

Khoo, R Z, H Ismail, and W S Chow. 2016. “Thermal and Morphological Properties of Poly (

Lactic Acid)/ Nanocellulose Nanocomposites." *Procedia Chemistry* 19: 788–94.

Khosravinezhad, Maryam, and Masoumeh Kazemi. 2021. "Study on Kinetics of Thermal Degradation of Polymethyl Methacrylate / Cyclic Olefin Copolymer Blend." (May).

Koh, J. Justin, Xiwen Zhang, and Chaobin He. 2018. "Fully Biodegradable Poly(Lactic Acid)/Starch Blends: A Review of Toughening Strategies." *International Journal of Biological Macromolecules* 109(December): 99–113.

Konno, Kotaro. 2011. "Plant Latex and Other Exudates as Plant Defense Systems: Roles of Various Defense Chemicals and Proteins Contained Therein." *Phytochemistry* 72(13): 1510–30.

Kumar Vangala, Sai Phani. 2014. "Thermal Degradation Kinetics of Poly (3-Hydroxybutyrate)/Cellulose Nanocrystals Based Nanobiocomposite." *Journal of Biofertilizers & Biopesticides* 05(01): 3–10.

Kumari, Minashree, and Sunil Kumar Gupta. 2019. "Response Surface Methodological (RSM) Approach for Optimizing the Removal of Trihalomethanes (THMs) and Its Precursor's by Surfactant Modified Magnetic Nanoadsorbents (SMNP) - An Endeavor to Diminish Probable Cancer Risk." *Scientific Reports* 9(1): 1–11.

De La Rosa-Ramírez, Harrison et al. 2020. "Modification of Poly (Lactic Acid) through the Incorporation of Gum Rosin and Gum Rosin Derivative: Mechanical Performance and Hydrophobicity." *Journal of Applied Polymer Science* 137(44): 1–15.

Lee, Carmen et al. 2020. "Talc Filled Polylactic - Acid Biobased Polymer Composites : Tensile , Thermal and Morphological Properties." (1).

Li, Chenglang, Qiang Dou, Zhifei Bai, and Quliang Lu. 2015. "Non-Isothermal Crystallization Behaviors and Spherulitic Morphology of Poly(Lactic Acid) Nucleated by a Novel Nucleating Agent." *Journal of Thermal Analysis and Calorimetry* 122(1): 407–17.

Li, Fei et al. 2013. "Tunable Green Oxygen Barrier through Layer-by-Layer Self-Assembly of Chitosan and Cellulose Nanocrystals." *Carbohydrate Polymers* 92(2): 2128–34.

Li, Luyao et al. 2019. "Preparation of Polylactic Acid/TEMPO-Oxidized Bacterial Cellulose Nanocomposites for 3D Printing via Pickering Emulsion Approach." *Composites Communications* 16(October): 162–67.

Li, Zhao Qian, Xiao Dong Zhou, and Chong Hua Pei. 2010. "Synthesis of PLA-Co-PGMA Copolymer and Its Application in the Surface Modification of Bacterial Cellulose."

International Journal of Polymeric Materials and Polymeric Biomaterials 59(9): 725–37.

Li, Zheng et al. 2022. “Suppression of Eucommia Ulmoides Gum / Natural.” : 21704–12.

Liang, X. H., and J. A. Kozinski. 2000. “Numerical Modeling of Combustion and Pyrolysis of Cellulosic Biomass in Thermogravimetric Systems.” *Fuel* 79(12): 1477–86.

Lin, Ling, Cong Deng, and Yu Zhong Wang. 2015. “Improving the Impact Property and Heat-Resistance of PLA/PC Blends through Coupling Molecular Chains at the Interface.” *Polymers for Advanced Technologies* 26(10): 1247–58.

Liu, Junshao, Huihua Jiang, and Liangbi Chen. 2012. “Grafting of Glycidyl Methacrylate onto Poly(Lactide) and Properties of PLA/Starch Blends Compatibilized by the Grafted Copolymer.” *Journal of Polymers and the Environment* 20(3): 810–16.

Lohrasbi, Pardis, and Jafar Khademzadeh Yeganeh. 2021. “Synergistic Toughening of Poly(Lactic Acid)/Poly(Ethylene Vinyl Acetate) (PLA/EVA) by Dynamic Vulcanization and Presence of Hydrophobic Nanoparticles.” *Polymers for Advanced Technologies* 32(11): 4326–39.

Lu, Fangfang, Houyong Yu, Chenfeng Yan, and Juming Yao. 2016. “Polylactic Acid Nanocomposite Films with Spherical Nanocelluloses as Efficient Nucleation Agents: Effects on Crystallization, Mechanical and Thermal Properties.” *RSC Advances* 6(51): 46008–18.

Lunt, James. 1998. “Large-Scale Production, Properties and Commercial Applications of Poly Lactic Acid Polymers.” *Polymer Degradation and Stability* 59(1–3): 145–52.

Machrafi, Hatim. 2012. Green Energy and Technology *Green Energy and Technology*.

Madhavan Nampoothiri, K., Nimisha Rajendran Nair, and Rojan Pappy John. 2010. “An Overview of the Recent Developments in Polylactide (PLA) Research.” *Bioresource Technology* 101(22): 8493–8501.

Maga, Daniel, Markus Hiebel, and Nils Thonemann. 2019. “Life Cycle Assessment of Recycling Options for Polylactic Acid.” *Resources, Conservation and Recycling* 149(October 2018): 86–96. https://doi.org/10.1016/j.resconrec.2019.05.018.

Maharana, T., B. Mohanty, and Y. S. Negi. 2009. “Melt-Solid Polycondensation of Lactic Acid and Its Biodegradability.” *Progress in Polymer Science (Oxford)* 34(1): 99–124.

Malek, N. S.A. et al. 2021. “Preparation and Characterization of Biodegradable Polylactic Acid (PLA) Film for Food Packaging Application: A Review.” *Journal of Physics: Conference*

Series 1892(1).

Mamleev, V. et al. 2000. “Modelling of Nonisothermal Kinetics in Thermogravimetry.” *Physical Chemistry Chemical Physics* 2(20): 4708–16.

Mandal, Dev K., Haripada Bhunia, and Pramod K. Bajpai. 2019. “Thermal Degradation Kinetics of PP/PLA Nanocomposite Blends.” *Journal of Thermoplastic Composite Materials* 32(12): 1714–30.

Masek, Anna, and Stefan Cichosz. 2021. “Biocomposites of Epoxidized Natural Rubber/Poly(Lactic Acid) Modified with Natural Substances: Influence of Biomolecules on the Aging Properties (Part Ii).” *Polymers* 13(11).

Mastral, A. M. et al. 2000. “Influence of Process Variables on Oils from Tire Pyrolysis and Hydropyrolysis in a Swept Fixed Bed Reactor.” *Energy and Fuels* 14(4): 739–44.

Mclauchlin, Andy R., and Noreen L. Thomas. 2012. “Biodegradable Polymer Nanocomposites.” *Advances in Polymer Nanocomposites: Types and Applications*: 398–430.

Michelot, Harmonie et al. 2017. “The Mechanical Properties of Plastic Evidence Bags Used for Collection and Storage of Drug Chemicals Relevant to Clandestine Laboratory Investigations.” *Forensic Sciences Research* 2(4): 198–202. https://doi.org/10.1080/20961790.2017.1335459.

Mihai, Mihaela. 2017. “Novel Bio-Nanocomposite Hybrids Made from Polylactide / Nanoclay Nanocomposites and Short Flax Fibers.”

Mokhena, T. C. et al. 2018. “Thermoplastic Processing of PLA/Cellulose Nanomaterials Composites.” *Polymers* 10(12).

Mullapudi, S. S., K. Pandey, S. N. Maiti, and Sampa Saha. 2018. “PLA/EVA/Teak Wood Flour Biocomposites for Packaging Application: Evaluation of Mechanical Performance and Biodegradation Properties.” *Journal of Packaging Technology and Research* 2(3): 191–201. https://doi.org/10.1007/s41783-018-0037-2.

Nagarajan, Vidhya, Amar K. Mohanty, and Manjusri Misra. 2013. “Sustainable Green Composites: Value Addition to Agricultural Residues and Perennial Grasses.” *ACS Sustainable Chemistry and Engineering* 1(3): 325–33.

Nagarajan, Vidhya, Kunyu Zhang, Manjusri Misra, and Amar K. Mohanty. 2015. “Overcoming the Fundamental Challenges in Improving the Impact Strength and Crystallinity of PLA Biocomposites: Influence of Nucleating Agent and Mold Temperature.” *ACS Applied*

Materials and Interfaces 7(21): 11203–14.

Nagy, Bianka, Norbert Miskolczi, and Zoltán Eller. 2021. "Improving Mechanical Properties of Pla/Starch Blends Using Masterbatch Containing Vegetable Oil Based Active Ingredients." *Polymers* 13(17).

Nair, Nimisha R, and K Madhavan Nampoothiri. 2012. "Preparation of Poly (L -Lactide) Blends and Biodegradation by Lentzea Waywayandensis." : 2031–35.

Nandiyanto, Asep Bayu Dani, Rosi Oktiani, and Risti Ragadhita. 2019. "How to Read and Interpret Ftir Spectroscope of Organic Material." *Indonesian Journal of Science and Technology* 4(1): 97–118.

Nashikkar, N et al. 2011. "Inhibition of Swarming Motility, Biofilm Formation and Virulence Factor Expression of Urinary Pathogens by Euphorbia Trigona Latex Extracts." *International Journal of Pharmaceutical and Research* 2(3): 558–66.

Norazlina, H., and Y. Kamal. 2015. 72 Polymer Bulletin *Graphene Modifications in Polylactic Acid Nanocomposites: A Review*.

Nz-j, Okereke. 2012. "Improving the Film Forming Ability of Gum Arabic." *J. Nat. Prod. Plant Resour* 2(2): 314–17.

Olalere, Olusegun Abayomi, and Chee Yuen Gan. 2021. "Microwave-Assisted Extraction of Phenolic Compounds from Euphorbia Hirta Leaf and Characterization of Its Morphology and Thermal Stability." *Separation Science and Technology (Philadelphia)* 56(11): 1853–65.

Omar, Anis Ainaa et al. 2021. "A Best-Evidence Review of Bio-Based Plasticizer and the Effects on the Mechanical Properties of PLA." *Chemical Engineering Transactions* 89(2): 241–46.

Pal, Akhilesh Kumar, and Vimal Katiyar. 2017a. "Theoretical and Analyzed Data Related to Thermal Degradation Kinetics of Poly (L-Lactic Acid)/Chitosan-Grafted-Oligo L-Lactic Acid (PLA/CH-g-OLLA) Bionanocomposite Films." *Data in Brief* 10: 304–11.

. 2017b. "Thermal Degradation Behaviour of Nanoamphiphilic Chitosan Dispersed Poly (Lactic Acid) Bionanocomposite Films." *International Journal of Biological Macromolecules* 95: 1267–79.

Pan, Pengju, Zhichao Liang, Amin Cao, and Yoshio Inoue. 2009. "Layered Metal Phosphonate Reinforced Poly(L-Lactide) Composites with a Highly Enhanced Crystallization Rate." *ACS*

Applied Materials and Interfaces 1(2): 402–11.

Pastorek, Miroslav, and Adriana Kovalcik. 2018. “Effects of Thermal Annealing as Polymer Processing Step on Poly(Lactic Acid).” *Materials and Manufacturing Processes* 33(15): 1674–80.

Patel. 2019. “**済無**No Title No Title No Title.” 4(1): 9–25.

Patwa, Rahul, Nabanita Saha, Petr Sáha, and Vimal Katiyar. 2019. “Biocomposites of Poly(Lactic Acid) and Lactic Acid Oligomer-Grafted Bacterial Cellulose: It’s Preparation and Characterization.” *Journal of Applied Polymer Science* 136(35): 1–13.

Patwa, Rahul, Monika Singh, Amit Kumar, and Vimal Katiyar. 2019. 76 Polymer Bulletin *Kinetic Modelling of Thermal Degradation and Non-Isothermal Crystallization of Silk Nano-Discs Reinforced Poly (Lactic Acid) Bionanocomposites*. Springer Berlin Heidelberg. https://doi.org/10.1007/s00289-018-2434-7.

Peres, Christiano Bruneli, André Henrique Rosa, and Leandro Cardoso de Morais. 2021. “Investigation of Pyrolysis Kinetics Parameters and Thermal Behavior of Thermochemically Modified Bagasse for Bioenergy Potential.” *SN Applied Sciences* 3(3).

Pérez-Fonseca, A. A., J. R. Robledo-Ortíz, R. González-Núñez, and D. Rodrigue. 2016. “Effect of Thermal Annealing on the Mechanical and Thermal Properties of Polylactic Acid–Cellulosic Fiber Biocomposites.” *Journal of Applied Polymer Science* 133(31): 1–10.

Perry, Mitchell R., and Michael P. Shaver. 2011. “Flexible and Rigid Core Molecules in the Synthesis of Poly(Lactic Acid) Star Polymers.” *Canadian Journal of Chemistry* 89(4): 499–505.

Persenaire, O., M. Alexandre, P. Degée, and P. Dubois. 2001. “Mechanisms and Kinetics of Thermal Degradation of Poly(ε-Caprolactone).” *Biomacromolecules* 2(1): 288–94.

Phomrak, Sirilak, and Muenduen Phisalaphong. 2020. “Lactic Acid Modified Natural Rubber-Bacterial Cellulose Composites.” *Applied Sciences (Switzerland)* 10(10).

Properties, Physical. 2003. “Part V.”

Rasal, Rahul M., Amol V. Janorkar, and Douglas E. Hirt. 2010. “Poly(Lactic Acid) Modifications.” *Progress in Polymer Science (Oxford)* 35(3): 338–56.

Ravi, Valapa, Central Electrochemical, and Technology Guwahati. 2015. “Poly (Lactic Acid) Nanocomposites Reinforced with Different Additives.” 7(May 2017): 495–522.

Rhim, Jong Whan, Seok In Hong, and Chang Sik Ha. 2009. “Tensile, Water Vapor Barrier and

Antimicrobial Properties of PLA/Nanoclay Composite Films." *LWT - Food Science and Technology* 42(2): 612–17. http://dx.doi.org/10.1016/j.lwt.2008.02.015.

Rhim, Jong Whan, Seok In Hong, Hwan Man Park, and Perry K.W. Ng. 2006. "壳聚糖基纳米复合抗菌膜的制备与表征." *Journal of Agricultural and Food Chemistry* 54(16): 5814–22.

Rudnik, E., and D. Briassoulis. 2011. "Degradation Behaviour of Poly(Lactic Acid) Films and Fibres in Soil under Mediterranean Field Conditions and Laboratory Simulations Testing." *Industrial Crops and Products* 33(3): 648–58.

Ruz-Cruz, M. A. et al. 2022. "Thermal and Mechanical Properties of PLA-Based Multiscale Cellulosic Biocomposites." *Journal of Materials Research and Technology* 18: 485–95.

Saha, B., A. K. Maiti, and A. K. Ghoshal. 2006. "Model-Free Method for Isothermal and Non-Isothermal Decomposition Kinetics Analysis of PET Sample." *Thermochimica Acta* 444(1): 46–52.

Saha, B., P. Karthik Reddy, and A. K. Ghoshal. 2008. "Hybrid Genetic Algorithm to Find the Best Model and the Globally Optimized Overall Kinetics Parameters for Thermal Decomposition of Plastics." *Chemical Engineering Journal* 138(1–3): 20–29.

Salehi, Bahare, Marcello Iriti, Sara Vitalini, and Hubert Antolak. 2019. "Euphorbia -Derived Natural Products with Potential for Use in Health Maintenance." : 1–22.

Sanivada, Usha Kiran, Gonzalo Mármol, F. P. Brito, and Raul Fangueiro. 2020. "Pla Composites Reinforced with Flax and Jute Fibers—a Review of Recent Trends, Processing Parameters and Mechanical Properties." *Polymers* 12(10): 1–29.

Saraswat, Shipra, Neeraj Mehta, and Surendra Dutt Sharma. 2016. "Applicability of Augis-Bennett Relation for Determination of Activation Energy of Glass Transition in Some Se Rich Chalcogenide Glasses." *Journal of Materials Research and Technology* 5(2): 111–16.

Sayyar, Sepidar, David L. Officer, and Gordon G. Wallace. 2017. "Fabrication of 3D Structures from Graphene-Based Biocomposites." *Journal of Materials Chemistry B* 5(19): 3462–82.

Series, Conference. 2021. "Preparation and Characterization of Biodegradable Polylactic Acid (PLA) Film for Food Packaging Application : A Review Preparation and Characterization of Biodegradable Polylactic Acid (PLA) Film for Food Packaging Application : A Review."

Sha, Lili et al. 2016. "Polylactic Acid Based Nanocomposites: Promising Safe and Biodegradable Materials in Biomedical Field." *International Journal of Polymer Science* 2016.

Shaik, Shameem Akthar, Jens Schuster, Yousuf Pasha Shaik, and Monis Kazmi. 2022. "Manufacturing of Biocomposites for Domestic Applications Using Bio-Based Filler Materials." *Journal of Composites Science* 6(3).

Shojaeiarani, Jamileh, Dilpreet S. Bajwa, and Nicole M. Stark. 2018. "Spin-Coating: A New Approach for Improving Dispersion of Cellulose Nanocrystals and Mechanical Properties of Poly (Lactic Acid) Composites." *Carbohydrate Polymers* 190: 139–47.

da Silva, Dana et al. 2018. "Biocompatibility, Biodegradation and Excretion of Polylactic Acid (PLA) in Medical Implants and Theranostic Systems." *Chemical Engineering Journal* 340: 9–14.

Sinha Ray, Suprakas, and Masami Okamoto. 2003. "Polymer/Layered Silicate Nanocomposites: A Review from Preparation to Processing." *Progress in Polymer Science (Oxford)* 28(11): 1539–1641.

Snegirev, A. Yu et al. 2017. "Autocatalysis in Thermal Decomposition of Polymers." *Polymer Degradation and Stability* 137: 151–61. http://dx.doi.org/10.1016/j.polymdegradstab.2017.01.008.

Sohn, Yu Jung et al. 2020. "Recent Advances in Sustainable Plastic Upcycling and Biopolymers." *Biotechnology Journal* 15(6): 1–16.

Solomon-Wisdom, G. O., and G. A. Shittu. 2010. "In Vitro Antimicrobial and Phytochemical Activities of Acacia Nilotica Leaf Extract." *Journal of Medicinal Plants Research* 4(12): 1232–34.

Su Shen, Kopitzky Rodion, Tolga Sengül, Kabasci Stephan. 2019. "Polylactide (PLA) and Its Blends with Poly (Butylene." *Polymers*: 1–21.

Swaroop, Chetan, and Mukul Shukla. 2018. "Mechanical, Optical and Antibacterial Properties of Polylactic Acid/Polyethylene Glycol Films Reinforced with MgO Nanoparticles." *Materials Today: Proceedings* 5(9): 20711–18. https://doi.org/10.1016/j.matpr.2018.06.455.

Syed Mustafa, Sharifah Nurul Inani et al. 2020. "Mechanical and Thermal Properties of Polylactic Acid/Liquid Epoxidized Natural Rubber Blends." *Chemical Engineering Transactions* 78: 103–8.

Tesfaye, Melakuu et al. 2016. "Silk Nanocrystals Stabilized Melt Extruded Poly (Lactic Acid) Nanocomposite Films: Effect of Recycling on Thermal Degradation Kinetics and Optimization Studies." *Thermochimica Acta* 643: 41–52.

Thomas, Ananya, Khalid Moinuddin, Svetlana Tretsiakova-McNally, and Paul Joseph. 2020. “A Kinetic Analysis of the Thermal Degradation Behaviours of Some Bio-Based Substrates.” *Polymers* 12(8).

Tripathi, Neelima, and Vimal Katiyar. 2016. “PLA/Functionalized-Gum Arabic Based Bionanocomposite Films for High Gas Barrier Applications.” *Journal of Applied Polymer Science* 133(21): 1–8.

2018. “Lactic Acid Oligomer (OLLA) Grafted Gum Arabic Based Green Adhesive for Structural Applications.” *International Journal of Biological Macromolecules* 120: 711–20. https://doi.org/10.1016/j.ijbiomac.2018.07.199.

Tripathi, Neelima, Manjusri Misra, and Amar K. Mohanty. 2021. “Durable Polylactic Acid (PLA)-Based Sustainable Engineered Blends and Biocomposites: Recent Developments, Challenges, and Opportunities.” *ACS Engineering Au* 1(1): 7–38.

Tumeh, Paul C. et al. 2014. “PD-1 Blockade Induces Responses by Inhibiting Adaptive Immune Resistance.” *Nature* 515(7528): 568–71.

Tyler, Betty et al. 2016. “Polylactic Acid (PLA) Controlled Delivery Carriers for Biomedical Applications.” *Advanced Drug Delivery Reviews* 107: 163–75. http://dx.doi.org/10.1016/j.addr.2016.06.018.

Valapa, Ravibabu, Gopal Pugazhenthi, and Vimal Katiyar. 2014. 65 International Journal of Biological Macromolecules *Thermal Degradation Kinetics of Sucrose Palmitate Reinforced Poly(Lactic Acid) Biocomposites*. Elsevier B.V.

Vamvuka, D., E. Kakaras, E. Kastanaki, and P. Grammelis. 2003. “Pyrolysis Characteristics and Kinetics of Biomass Residuals Mixtures with Lignite.” *Fuel* 82(15–17): 1949–60.

Venkatesh, M., P. Ravi, and Surya P. Tewari. 2013. “Isoconversional Kinetic Analysis of Decomposition of Nitroimidazoles: Friedman Method vs Flynn-Wall-Ozawa Method.” *Journal of Physical Chemistry A* 117(40): 10162–69.

Villanueva, Judith, Luis Manuel Quirós, and Sonia Castañón. 2015. “Purification and Partial Characterization of a Ribosome-Inactivating Protein from the Latex of Euphorbia Trigona Miller with Cytotoxic Activity toward Human Cancer Cell Lines.” *Phytomedicine* 22(7–8): 689–95.

Vyazovkin, S., and V. Goryachko. 1992. “Potentialities of Software for Kinetic Processing of Thermoanalytical Data by the Isoconversion Method.” *Thermochimica Acta* 194(C): 221–

30.

Vyazovkin, Sergey et al. 2011. “ICTAC Kinetics Committee Recommendations for Performing Kinetic Computations on Thermal Analysis Data.” *Thermochimica Acta* 520(1–2): 1–19.

2021. “ICTAC Kinetics Committee Recommendations for Analysis of Multi-Step Kinetic To Cite This Version : HAL Id : Emse-03107652 ICTAC Kinetics Committee Recommendations for Analysis of Multi-Step Kinetics.”

Wako, Fekadu Mosisa, Ali Shemshedin Reshad, and Vaibhav V. Goud. 2018. “Thermal Degradation Kinetics Study and Thermal Cracking of Waste Cooking Oil for Biofuel Production.” *Journal of Thermal Analysis and Calorimetry* 131(3): 2157–65.

Wang, Hong Bing et al. 2015. “Tigliane Diterpenoids from the Euphorbiaceae and Thymelaeaceae Families.” *Chemical Reviews* 115(9): 2975–3011.

Wen-Dong, Tang et al. 2021. “The Reactive Compatibilization of PLA/PP Blends and Improvement of PLA Crystallization Properties Induced Byin SituUV Irradiation.” *CrystEngComm* 23(4): 864–75.

Wielage, B. et al. 1999. “Thermogravimetric and Differential Scanning Calorimetric Analysis of Natural Fibres and Polypropylene.” *Thermochimica Acta* 337(1–2): 169–77.

Woldegiorgis., YohannesF. 2017. “Economic and Environmental Impacts of Plastic Waste: A Case Study in Addis Ababa City, Ethiopia.” *International Journal of Advanced Research* 5(6): 1624–30.

Woo, Claire H. et al. 2012. “A Quantitative Correlation between the Mobility and Crystallinity of Photo-Cross-Linkable P3HT.” *Macromolecules* 45(7): 3057–62.

Xie, Guangqiang, Yanhua Zhang, and Wenshu Lin. 2017. “Plasticizer Combinations and Performance of Wood Flour-Poly(Lactic Acid) 3D Printing Filaments.” *BioResources* 12(3): 6736–48.

Xu, Linqiong et al. 2021. “Green-Plasticized Poly(Lactic Acid)/Nanofibrillated Cellulose Biocomposites with High Strength, Good Toughness and Excellent Heat Resistance.” *Composites Science and Technology* 203(August 2020): 108613.

Xu, Yuewen et al. 2015. “Reactive Compatibilization of Polylactide/Polypropylene Blends.” *Industrial and Engineering Chemistry Research* 54(23): 6108–14.

Yadav, Pushpendra, Ankit Sahai, and Rahul Swarup Sharma. 2021. “Strength and Surface Characteristics of FDM-Based 3D Printed PLA Parts for Multiple Infill Design Patterns.”

Journal of The Institution of Engineers (India): Series C 102(1): 197–207.

Yang, W et al. 2016. "Synergic Effect of Cellulose and Lignin Nanostructures in PLA Based Systems for Food Antibacterial Packaging." *EUROPEAN POLYMER JOURNAL* 79: 1–12.

Yang, Zhe, Hongdan Peng, Weizhi Wang, and Tianxi Liu. 2010. "Crystallization Behavior of Poly(ε-Caprolactone)/Layered Double Hydroxide Nanocomposites." *Journal of Applied Polymer Science* 116(5): 2658–67.

Yener, İsmail et al. 2018. "A Detailed Study on Chemical and Biological Profile of Nine Euphorbia Species from Turkey with Chemometric Approach: Remarkable Cytotoxicity of E. Fistulasa and Promising Tannic Acid Content of E. Eriophora." *Industrial Crops and Products* 123(July): 442–53.

Yiga, Vianney Andrew et al. 2021. "Optimization of Tensile Strength of PLA/Clay/Rice Husk Composites Using Box-Behnken Design." *Biomass Conversion and Biorefinery* (0123456789).

Yu, Long, Katherine Dean, and Lin Li. 2006. "Polymer Blends and Composites from Renewable Resources." *Progress in Polymer Science (Oxford)* 31(6): 576–602.

Yu, Meihong, Yongjie Zheng, and Jingzhi Tian. 2020. "Study on the Biodegradability of Modified Starch/Polylactic Acid (PLA) Composite Materials." *RSC Advances* 10(44): 26298–307.

Zahir, Lamya et al. 2021. "Synthesis of Thermoplastic Elastomers with High Biodegradability in Seawater." *Polymer Degradation and Stability* 184.

Zeng, Jian Bing, Kun Ang Li, and An Ke Du. 2015. "Compatibilization Strategies in Poly(Lactic Acid)-Based Blends." *RSC Advances* 5(41): 32546–65.

Zhang, Haichen et al. 2015. "Preparation, Characterization and Properties of PLA/TiO2 Nanocomposites Based on a Novel Vane Extruder." *RSC Advances* 5(6): 4639–47.

Zhang, Kunyu, Vidhya Nagarajan, Manjusri Misra, and Amar K. Mohanty. 2014. "Supertoughened Renewable PLA Reactive Multiphase Blends System: Phase Morphology and Performance." *ACS Applied Materials and Interfaces* 6(15): 12436–48.

Zotti, Aldobenedetto et al. 2018. "Effects of 1D and 2D Nanofillers in Basalt/Poly(Lactic Acid) Composites for Additive Manufacturing." *Composites Part B: Engineering* 153: 364–75.

APPENDIXES

Appendix-1 Mechanical properties of PLA and PLA/bio-composite

S.N	Sample name	Tensile strength (N/mm^2)	Elongation @ Break
1	Neat PLA	70.76 ±0.1	2.54±0.11
2	PLA/OLLA-g-GA (1%)	87.82 ±0.301	2.904±0.023
3	PLA/OLLA-g-GA (2%)	94.89±0.32	2.94±0.051
4	PLA-OLLA-g-GA (3%)	97.87±0.23	3.05±0.041
5	PLA/OLLA-g-ETML (3%)	90.94 ± 0.43	3.41±0.022
6	PLA/OLLA-g-ETML (5%)	78.39±0.24	4.1±0.047
7	PLA/OLLA-g-GA (1%)-OLLA-g-ETML (3%)	84.6±0.630	3.12±0.12
8	PLA/OLLA-g-GA (1%)-OLLA-g-ETML (5%)	87.7±0.331	3.8±0.084
9	PLA/OLLA-g-GA (2%)-OLLA-g-ETML (3%)	95.47. ±810	3.5±0.056
10	PLA/OLLA-g-GA (2%)-OLLA-g-ETML (5%)	98.39±0.68	3.58±0.24
11	PLA/OLLA-g-GA (2%)-OLLA-g-ETML (10%)	94.72±0.87	4.2±0.014
12	PLA/OLLA-g-GA (3%)-OLLA-g-ETML (3%)	97.93±0.89	3.2±0.076
13	PLA/OLLA-g-GA (3%)-OLLA-g-ETML (5%)	105.23±0.65	3.4±0.059
14	PLA/OLLA-g-GA (3%)-OLLA-g-ETML (10%)	96.32±0.85	3.94±0.804

Appendix-2 Letter from the Ethiopian conformity assessment enterprise

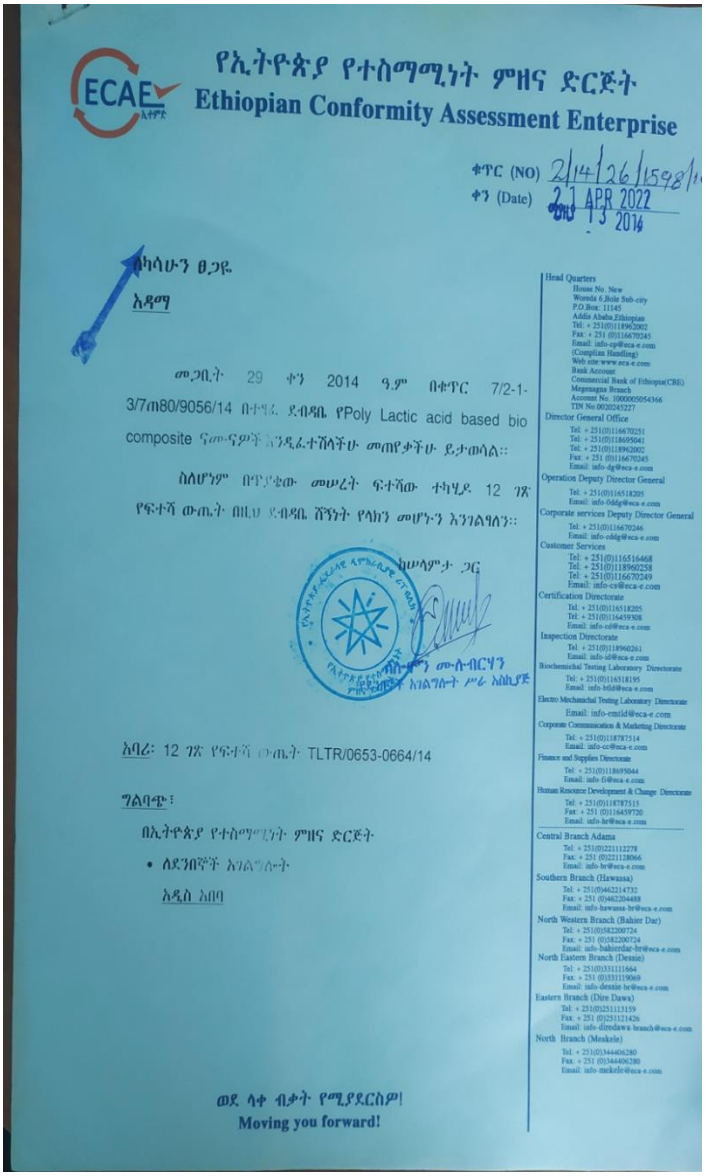

የኢትዮጵያ የተስማሚነት ምዘና ድርጅት
Ethiopian Conformity Assessment Enterprise

ቁጥር (NO) 2/14/26/1598/1
ቀን (Date) 21 APR 2022 / 13 2014

ለካሳሁን ፀጋዬ
አዳማ

መጋቢት 29 ቀን 2014 ዓ.ም በቁጥር 7/2-1-3/7m80/9056/14 በተፃፈ ደብዳቤ የPoly Lactic acid based bio composite ናሙናዎች እንዲፈተሽላችሁ መጠየቃችሁ ይታወሳል።

ስለሆነም በጥያቄው መሠረት ፍተሻው ተካሂዶ 12 ገጽ የፍተሻ ውጤት በዚህ ደብዳቤ ሸኝነት የላክን መሆኑን እንገልፃለን።

ከሠላምታ ጋር

ሙሉብርሃን
አገልግሎት ሥራ አስኪያጅ

አባሪ፡ 12 ገጽ የፍተሻ ውጤት TLTR/0653-0664/14

ግልባጭ፣
በኢትዮጵያ የተስማሚነት ምዘና ድርጅት
• ለደንበኞች አገልግሎት
አዲስ አበባ

Head Quarters
House No. New
Woreda 6,Bole Sub-city
P.O.Box: 11145
Addis Ababa,Ethiopian
Tel: + 251(0)118962002
Fax: + 251 (0)116670245
Email: info-cp@eca-e.com
(Complian Handling)
Web site:www.eca-e.com
Bank Account
Commercial Bank of Ethiopia(CBE)
Megenagna Branch
Account No. 1000005054366
TIN No 0020245227

Director General Office
Tel: + 251(0)116670251
Tel: + 251(0)118695041
Tel: + 251(0)118962002
Fax: + 251 (0)116670245
Email: info-dg@eca-e.com

Operation Deputy Director General
Tel: + 251(0)116518205
Email: info-0ddg@eca-e.com

Corporate services Deputy Director General
Tel: + 251(0)116670246
Email: info-cddg@eca-e.com

Customer Services
Tel: + 251(0)116516468
Tel: + 251(0)118960258
Tel: + 251(0)116670249
Email: info-cs@eca-e.com

Certification Directorate
Tel: + 251(0)116518205
Tel: + 251(0)116459308
Email: info-cd@eca-e.com

Inspection Directorate
Tel: + 251(0)118960261
Email: info-id@eca-e.com

Biochemichal Testing Laboratory Directorate
Tel: + 251(0)116518195
Email: info-btld@eca-e.com

Electro Mechanichal Testing Laboratory Directorate
Email: info-emtld@eca-e.com

Corporate Communication & Marketing Directorate
Tel: + 251(0)118787514
Email: info-cc@eca-e.com

Finance and Supplies Directorate
Tel: + 251(0)118695044
Email: info-fi@eca-e.com

Human Resource Development & Change Directorate
Tel: + 251(0)118787515
Fax: + 251 (0)116459720
Email: info-hr@eca-e.com

Central Branch Adama
Tel: + 251(0)221112278
Fax: + 251 (0)221128066
Email: info-br@eca-e.com

Southern Branch (Hawassa)
Tel: + 251(0)462214732
Fax: + 251 (0)462204488
Email: info-hawassa-br@eca-e.com

North Western Branch (Bahier Dar)
Tel: + 251(0)582200724
Fax: + 251 (0)582200724
Email: info-bahierdar-br@eca-e.com

North Eastern Branch (Dessie)
Tel: + 251(0)331111664
Fax: + 251 (0)331119069
Email: info-dessie-br@eca-e.com

Eastern Branch (Dire Dawa)
Tel: + 251(0)251113159
Fax: + 251 (0)251121426
Email: info-diredawa-branch@eca-e.com

North Branch (Mekele)
Tel: + 251(0)344406280
Fax: + 251 (0)344406280
Email: info-mekele@eca-e.com

ወደ ላቀ ብቃት የሚያደርስዎ!
Moving you forward!

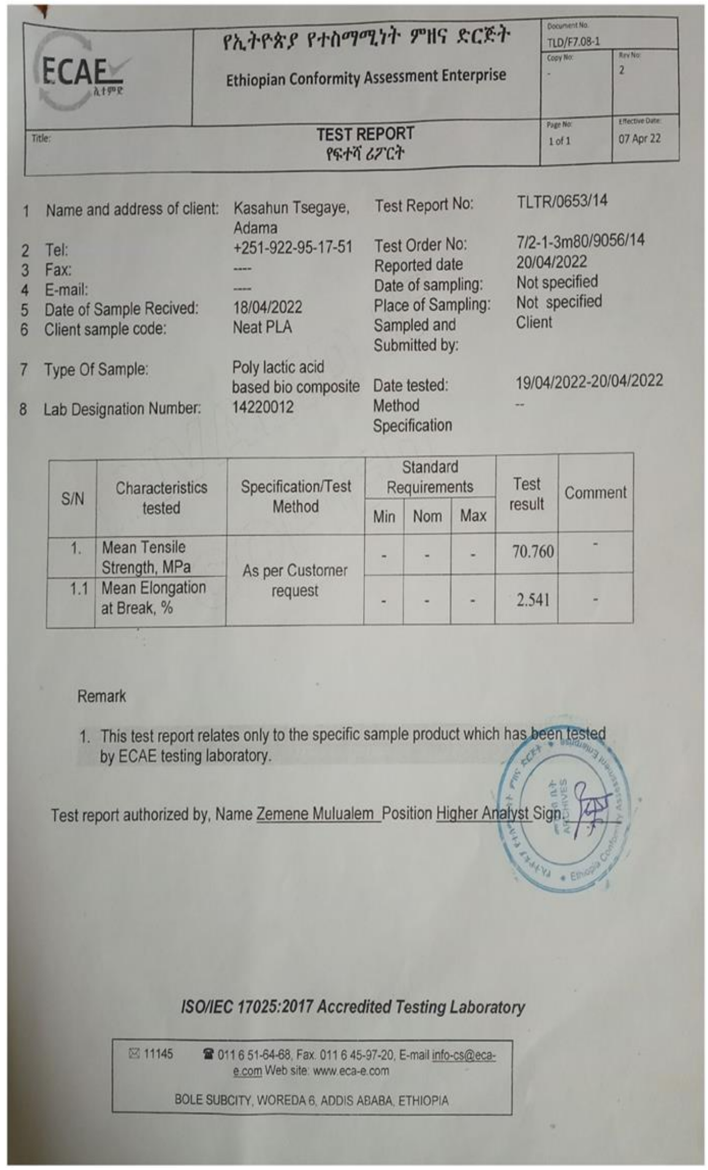

ECAE	የኢትዮጵያ የተስማሚነት ምዘና ድርጅት Ethiopian Conformity Assessment Enterprise	Document No. TLD/F7.08-1 Copy No: -	Rev No: 2
Title:	TEST REPORT የፍተሻ ሪፖርት	Page No: 1 of 1	Effective Date: 07 Apr 22

1	Name and address of client:	Kasahun Tsegaye, Adama	Test Report No:	TLTR/0653/14
2	Tel:	+251-922-95-17-51	Test Order No:	7/2-1-3m80/9056/14
3	Fax:	----	Reported date	20/04/2022
4	E-mail:	----	Date of sampling:	Not specified
5	Date of Sample Recived:	18/04/2022	Place of Sampling:	Not specified
6	Client sample code:	Neat PLA	Sampled and Submitted by:	Client
7	Type Of Sample:	Poly lactic acid based bio composite	Date tested:	19/04/2022-20/04/2022
8	Lab Designation Number:	14220012	Method Specification	--

S/N	Characteristics tested	Specification/Test Method	Standard Requirements			Test result	Comment
			Min	Nom	Max		
1.	Mean Tensile Strength, MPa	As per Customer request	-	-	-	70.760	-
1.1	Mean Elongation at Break, %		-	-	-	2.541	-

Remark

1. This test report relates only to the specific sample product which has been tested by ECAE testing laboratory.

Test report authorized by, Name Zemene Mulualem Position Higher Analyst Sign.

ISO/IEC 17025:2017 Accredited Testing Laboratory

✉ 11145 ☎ 011 6 51-64-68, Fax 011 6 45-97-20, E-mail info-cs@eca-e.com Web site: www.eca-e.com
BOLE SUBCITY, WOREDA 6, ADDIS ABABA, ETHIOPIA

ECAE

የኢትዮጵያ የተስማሚነት ምዘና ድርጅት

Ethiopian Conformity Assessment Enterprise

Document No. TLD/F7.08-1 | Copy No. - | Rev No. 2 | Page No. 1 of 1 | Effective Date: 07 Apr 22

Title: **TEST REPORT** የፍተሻ ሪፖርት

1	Name and address of client:	Kasahun Tsegaye, Adama	Test Report No:	TLTR/0654/14
2	Tel:	+251-922-95-17-51	Test Order No:	7/2-1-3m80/9056/14
3	Fax:	----	Reported date	20/04/2022
4	E-mail:	----	Date of sampling:	Not specified
5	Date of Sample Recived:	18/04/2022	Place of Sampling:	Not specified
6	Client sample code:	PLA 1% GA	Sampled and Submitted by:	Client
7	Type Of Sample:	Poly lactic acid based bio composite	Date tested:	19/04/2022-20/04/2022
8	Lab Designation Number:	14220013	Method Specification	--

S/N	Characteristics tested	Specification/Test Method	Standard Requirements			Test result	Comment
			Min	Nom	Max		
1.	Mean Tensile Strength, MPa	As per Customer request	-	-	-	87.823	-
1.1	Mean Elongation at Break, %		-	-	-	2.904	-

Remark

1. This test report relates only to the specific sample product which has been tested by ECAE testing laboratory.

Test report authorized by, Name Zemene Mulualem Position Higher Analyst Sign.

ISO/IEC 17025:2017 Accredited Testing Laboratory

☒ 11145 ☎ 011 6 51-64-68, Fax. 011 6 45-97-20, E-mail info-cs@eca-e.com Web site: www.eca-e.com

BOLE SUBCITY, WOREDA 6, ADDIS ABABA, ETHIOPIA

ECAE

የኢትዮጵያ የተስማሚነት ምዘና ድርጅት

Ethiopian Conformity Assessment Enterprise

Document No. TLD/F7.08-1 | Copy No. - | Rev No. 2 | Page No. 1 of 1 | Effective Date: 07 Apr 22

Title: **TEST REPORT** የፍተሻ ሪፖርት

	Name and address of client:	Kasahun Tsegaye, Adama	Test Report No:	TLTR/0655/14
2	Tel:	+251-922-95-17-51	Test Order No:	7/2-1-3m80/9058/14
3	Fax:	----	Reported date	20/04/2022
4	E-mail:	----	Date of sampling:	Not specified
5	Date of Sample Recived:	18/04/2022	Place of Sampling:	Not specified
6	Client sample code:	PLA 2% GA	Sampled and Submitted by:	Client
7	Type Of Sample:	Poly lactic acid based bio composite	Date tested:	19/04/2022-20/04/2022
8	Lab Designation Number:	14220014	Method Specification	--

S/N	Characteristics tested	Specification/Test Method	Standard Requirements			Test result	Comment
			Min	Nom	Max		
1.	Mean Tensile Strength, MPa	As per Customer request	-	-	-	94.892	-
1.1	Mean Elongation at Break, %		-	-	-	2.941	-

Remark

1. This test report relates only to the specific sample product which has been tested by ECAE testing laboratory.

Test report authorized by, Name Zemene Mulualem Position Higher Analyst Sign.

ISO/IEC 17025:2017 Accredited Testing Laboratory

☒ 11145 ☎ 011 6 51-64-68, Fax. 011 6 45-97-20, E-mail info-cs@eca-e.com Web site: www.eca-e.com

BOLE SUBCITY, WOREDA 6, ADDIS ABABA, ETHIOPIA

ECAE	የኢትዮጵያ የተስማሚነት ምዘና ድርጅት Ethiopian Conformity Assessment Enterprise	Document No: TLD/F7.08-1 Copy No: - Rev No: 2
Title:	TEST REPORT የፍተሻ ሪፖርት	Page No: 1 of 1 Effective Date: 07 Apr 22

1	Name and address of client:	Kasahun Tsegaye, Adama	Test Report No:	TLTR/0656/14
2	Tel:	+251-922-95-17-51	Test Order No:	7/2-1-3m80/9056/14
3	Fax:	----	Reported date	20/04/2022
4	E-mail:	----	Date of sampling:	Not specified
5	Date of Sample Recived:	18/04/2022	Place of Sampling:	Not specified
6	Client sample code:	PLA 3% GA	Sampled and Submitted by:	Client
7	Type Of Sample:	Poly lactic acid based bio composite	Date tested:	19/04/2022-20/04/2022
8	Lab Designation Number:	14220015	Method Specification	--

S/N	Characteristics tested	Specification/Test Method	Standard Requirements			Test result	Comment
			Min	Nom	Max		
1.	Mean Tensile Strength, MPa	As per Customer request	-	-	-	97.871	-
1.1	Mean Elongation at Break, %		-	-	-	3.054	-

Remark

1. This test report relates only to the specific sample product which has been tested by ECAE testing laboratory.

Test report authorized by, Name Zemene Mulualem Position Higher Analyst Sign.

ISO/IEC 17025:2017 Accredited Testing Laboratory

✉ 11145 ☎ 011 6 51-64-68, Fax. 011 6 45-97-20, E-mail info-cs@eca-e.com Web site: www.eca-e.com

BOLE SUBCITY, WOREDA 6, ADDIS ABABA, ETHIOPIA

ECAE AIPE

የኢትዮጵያ የተስማሚነት ምዘና ድርጅት

Ethiopian Conformity Assessment Enterprise

Document No.	Copy No.	Rev No.
TLD/F7.08-1	-	2

Title: **TEST REPORT** የፍተሻ ሪፖርት

Page No.	Effective Date:
1 of 1	07 Apr 22

1	Name and address of client:	Kasahun Tsegaye, Adama	Test Report No:	TLTR/0657/14
2	Tel:	+251-922-95-17-51	Test Order No:	7/2-1-3m80/9056/14
3	Fax:	----	Reported date	20/04/2022
4	E-mail:	----	Date of sampling:	Not specified
5	Date of Sample Recived:	18/04/2022	Place of Sampling:	Not specified
6	Client sample code:	PLA 3%EUTM	Sampled and Submitted by:	Client
7	Type Of Sample:	Poly lactic acid based bio composite	Date tested:	19/04/2022-20/04/2022
8	Lab Designation Number:	14220016	Method Specification	--

S/N	Characteristics tested	Specification/Test Method	Standard Requirements			Test result	Comment
			Min	Nom	Max		
1.	Mean Tensile Strength, MPa	As per Customer request	-	-	-	90.941	-
1.1	Mean Elongation at Break, %		-	-	-	3.411	-

Remark

1. This test report relates only to the specific sample product which has been tested by ECAE testing laboratory.

Test report authorized by, Name Zemene Mulualem Position Higher Analyst Sign.

ISO/IEC 17025:2017 Accredited Testing Laboratory

☒ 11145 ☎ 011 6 51-64-68, Fax. 011 6 45-97-20, E-mail info-cs@eca-e.com Web site: www.eca-e.com

BOLE SUBCITY, WOREDA 6, ADDIS ABABA, ETHIOPIA

5

ECAE AIPE

የኢትዮጵያ የተስማሚነት ምዘና ድርጅት

Ethiopian Conformity Assessment Enterprise

Document No.	Copy No.	Rev No.
TLD/F7.08-1	-	2

Title: **TEST REPORT** የፍተሻ ሪፖርት

Page No.	Effective Date:
1 of 1	07 Apr 22

1	Name and address of client:	Kasahun Tsegaye, Adama	Test Report No:	TLTR/0658/14
2	Tel:	+251-922-95-17-51	Test Order No:	7/2-1-3m80/9056/14
3	Fax:	----	Reported date	20/04/2022
4	E-mail:	----	Date of sampling:	Not specified
5	Date of Sample Recived:	18/04/2022	Place of Sampling:	Not specified
6	Client sample code:	PLA 5% EUTM	Sampled and Submitted by:	Client
7	Type Of Sample:	Poly lactic acid based bio composite	Date tested:	19/04/2022-20/04/2022
8	Lab Designation Number:	14220017	Method Specification	--

S/N	Characteristics tested	Specification/Test Method	Standard Requirements			Test result	Comment
			Min	Nom	Max		
1.	Mean Tensile Strength, MPa	As per Customer request	-	-	-	78.390	-
1.1	Mean Elongation at Break, %		-	-	-	4.108	-

Remark

1. This test report relates only to the specific sample product which has been tested by ECAE testing laboratory.

Test report authorized by, Name Zemene Mulualem Position Higher Analyst Sign.

ISO/IEC 17025:2017 Accredited Testing Laboratory

☒ 11145 ☎ 011 6 51-64-68, Fax. 011 6 45-97-20, E-mail info-cs@eca-e.com Web site: www.eca-e.com

BOLE SUBCITY, WOREDA 6, ADDIS ABABA, ETHIOPIA

6

ECAE

የኢትዮጵያ የተስማሚነት ምዘና ድርጅት

Ethiopian Conformity Assessment Enterprise

Document No. TLD/F7.08-1 | Copy No. - | Rev No. 2

Title: **TEST REPORT** የፍተሻ ሪፖርት

Page No: 1 of 1 | Effective Date: 07 Apr 22

1	Name and address of client:	Kasahun Tsegaye, Adama	Test Report No:	TLTR/0659/14
2	Tel:	+251-922-95-17-51	Test Order No:	7/2-1-3m80/9056/14
3	Fax:	----	Reported date	20/04/2022
4	E-mail:	----	Date of sampling:	Not specified
5	Date of Sample Recived:	18/04/2022	Place of Sampling:	Not specified
6	Client sample code:	PLA 1% GA 3% EUTM	Sampled and Submitted by:	Client
7	Type Of Sample:	Poly lactic acid based bio composite	Date tested:	19/04/2022-20/04/2022
8	Lab Designation Number:	14220018	Method Specification	--

S/N	Characteristics tested	Specification/Test Method	Standard Requirements			Test result	Comment
			Min	Nom	Max		
1.	Mean Tensile Strength, MPa	As per Customer request	-	-	-	84.610	-
1.1	Mean Elongation at Break, %		-	-	-	3.122	-

Remark

1. This test report relates only to the specific sample product which has been tested by ECAE testing laboratory.

Test report authorized by, Name Zemene Mulualem Position Higher Analyst Sign.

ISO/IEC 17025:2017 Accredited Testing Laboratory

☒ 11145 ☎ 011 6 51-64-68, Fax. 011 6 45-97-20, E-mail info-cs@eca-e.com Web site: www.eca-e.com

BOLE SUBCITY, WOREDA 6, ADDIS ABABA, ETHIOPIA

ECAE

የኢትዮጵያ የተስማሚነት ምዘና ድርጅት

Ethiopian Conformity Assessment Enterprise

Document No. TLD/F7.08-1 | Copy No. - | Rev No. 2

Title: **TEST REPORT** የፍተሻ ሪፖርት

Page No: 1 of 1 | Effective Date: 07 Apr 22

1	Name and address of client:	Kasahun Tsegaye, Adama	Test Report No:	TLTR/0660/14
2	Tel:	+251-922-95-17-51	Test Order No:	7/2-1-3m80/9056/14
3	Fax:	----	Reported date	20/04/2022
4	E-mail:	----	Date of sampling:	Not specified
5	Date of Sample Recived:	18/04/2022	Place of Sampling:	Not specified
6	Client sample code:	PLA 1% GA 5% EUTM	Sampled and Submitted by:	Client
7	Type Of Sample:	Poly lactic acid based bio composite	Date tested:	19/04/2022-20/04/2022
8	Lab Designation Number:	14220019	Method Specification	--

S/N	Characteristics tested	Specification/Test Method	Standard Requirements			Test result	Comment
			Min	Nom	Max		
1.	Mean Tensile Strength, MPa	As per Customer request	-	-	-	87.701	-
1.1	Mean Elongation at Break, %		-	-	-	3.810	-

Remark

1. This test report relates only to the specific sample product which has been tested by ECAE testing laboratory.

Test report authorized by, Name Zemene Mulualem Position Higher Analyst Sign.

ISO/IEC 17025:2017 Accredited Testing Laboratory

☒ 11145 ☎ 011 6 51-64-68, Fax. 011 6 45-97-20, E-mail info-cs@eca-e.com Web site: www.eca-e.com

BOLE SUBCITY, WOREDA 6, ADDIS ABABA, ETHIOPIA

ECAE

የኢትዮጵያ የተስማሚነት ምዘና ድርጅት

Ethiopian Conformity Assessment Enterprise

Document No.	Rev No.
TLD/F7.08-1	2
Copy No.	
-	

Title: **TEST REPORT** የፍተሻ ሪፖርት

Page No:	Effective Date:
1 of 1	07 Apr 22

1	Name and address of client:	Kasahun Tsegaye, Adama	Test Report No:	TLTR/0661/14
2	Tel:	+251-922-95-17-51	Test Order No:	7/2-1-3m80/9056/14
3	Fax:	----	Reported date	20/04/2022
4	E-mail:	----	Date of sampling:	Not specified
5	Date of Sample Recived:	18/04/2022	Place of Sampling:	Not specified
6	Client sample code:	PLA 2% GA 3% EUTM	Sampled and Submitted by:	Client
7	Type Of Sample:	Poly lactic acid based bio composite	Date tested:	19/04/2022-20/04/2022
8	Lab Designation Number:	14220020	Method Specification	--

S/N	Characteristics tested	Specification/Test Method	Standard Requirements			Test result	Comment
			Min	Nom	Max		
1.	Mean Tensile Strength, MPa	As per Customer request	-	-	-	95.405	-
1.1	Mean Elongation at Break, %		-	-	-	3.530	-

Remark

1. This test report relates only to the specific sample product which has been tested by ECAE testing laboratory.

Test report authorized by, Name Zemene Mulualem Position Higher Analyst Sign.

ISO/IEC 17025:2017 Accredited Testing Laboratory

☒ 11145 ☎ 011 6 51-64-68, Fax. 011 6 45-97-20, E-mail info-cs@eca-e.com Web site: www.eca-e.com

BOLE SUBCITY, WOREDA 6, ADDIS ABABA, ETHIOPIA

የኢትዮጵያ የተስማሚነት ምዘና ድርጅት

Ethiopian Conformity Assessment Enterprise

TEST REPORT የፍተሻ ሪፖርት

Name and address of client:	Kasahun Tsegaye, Adama	Test Report No:	TLTR/0662/14
Tel:	+251-922-95-17-51	Test Order No:	7/2-1-3m80/9056/14
Fax:	----	Reported date	20/04/2022
E-mail:	----	Date of sampling:	Not specified
Date of Sample Recived:	18/04/2022	Place of Sampling:	Not specified
Client sample code:	PLA 2% GA 5% EUTM	Sampled and Submitted by:	Client
Type Of Sample:	Poly lactic acid based bio composite	Date tested:	19/04/2022-20/04/2022
Lab Designation Number:	14220021	Method Specification	--

S/N	Characteristics tested	Specification/Test Method	Standard Requirements			Test result	Comment
			Min	Nom	Max		
1.	Mean Tensile Strength, MPa	As per Customer request	-	-	-	98.331	-
1.1	Mean Elongation at Break, %		-	-	-	3.584	-

Remark

1. This test report relates only to the specific sample product which has been tested by ECAE testing laboratory.

Test report authorized by, Name Zemene Mulualem Position Higher Analyst Sign.

ISO/IEC 17025:2017 Accredited Testing Laboratory

☒ 11145 ☎ 011 6 51-64-68, Fax. 011 6 45-97-20, E-mail info-cs@eca-e.com Web site: www.eca-e.com

BOLE SUBCITY, WOREDA 6, ADDIS ABABA, ETHIOPIA

ECAE

የኢትዮጵያ የተስማሚነት ምዘና ድርጅት

Ethiopian Conformity Assessment Enterprise

Document No.	Rev No.
TLD/F7.08-1	2
Copy No.	
-	
Page No.	Effective Date
1 of 1	07 Apr 22

Title: **TEST REPORT** የፍተሻ ሪፖርት

1	Name and address of client:	Kasahun Tsegaye, Adama	Test Report No:	TLTR/0663/14	
2	Tel:	+251-922-95-17-51	Test Order No:	7/2-1-3m80/9056/14	
3	Fax:	----	Reported date	20/04/2022	
4	E-mail:	----	Date of sampling:	Not specified	
5	Date of Sample Recived:	18/04/2022		Not specified	
6	Client sample code:	PLA 3% GA 3% EUTM	Place of Sampling: Sampled and Submitted by:	Client	
7	Type Of Sample:	Poly lactic acid based bio composite	Date tested:	19/04/2022-20/04/2022	
8	Lab Designation Number:	14220022	Method Specification	--	

S/N	Characteristics tested	Specification/Test Method	Standard Requirements			Test result	Comment
			Min	Nom	Max		
1.	Mean Tensile Strength, MPa	As per Customer request	-	-	-	97.937	-
1.1	Mean Elongation at Break, %		-	-	-	3.213	-

Remark

1. This test report relates only to the specific sample product which has been tested by ECAE testing laboratory.

Test report authorized by, Name Zemene Mulualem Position Higher Analyst Sign.

ISO/IEC 17025:2017 Accredited Testing Laboratory

✉ 11145 ☎ 011 6 51-64-68, Fax. 011 6 45-97-20, E-mail info-cs@eca-e.com Web site: www.eca-e.com

BOLE SUBCITY, WOREDA 6, ADDIS ABABA, ETHIOPIA

ECAE

የኢትዮጵያ የተስማሚነት ምዘና ድርጅት

Ethiopian Conformity Assessment Enterprise

Document No.	Rev No.
TLD/F7.08-1	2
Copy No.	
-	
Page No.	Effective Date
1 of 1	07 Apr 22

Title: **TEST REPORT** የፍተሻ ሪፖርት

1	Name and address of client:	Kasahun Tsegaye, Adama	Test Report No:	TLTR/0664/14	
2	Tel:	+251-922-95-17-51	Test Order No:	7/2-1-3m80/9056/14	
3	Fax:	----	Reported date	20/04/2022	
4	E-mail:	----	Date of sampling:	Not specified	
5	Date of Sample Recived:	18/04/2022		Not specified	
6	Client sample code:	PLA 3%GA 5% EUTM	Place of Sampling: Sampled and Submitted by:	Client	
7	Type Of Sample:	Poly lactic acid based bio composite	Date tested:	19/04/2022-20/04/2022	
8	Lab Designation Number:	14220023	Method Specification	--	

S/N	Characteristics tested	Specification/Test Method	Standard Requirements			Test result	Comment
			Min	Nom	Max		
1.	Mean Tensile Strength, MPa	As per Customer request	-	-	-	105.220	-
1.1	Mean Elongation at Break, %		-	-	-	3.434	-

Remark

1. This test report relates only to the specific sample product which has been tested by ECAE testing laboratory.

Test report authorized by, Name Zemene Mulualem Position Higher Analyst Sign.

ISO/IEC 17025:2017 Accredited Testing Laboratory

✉ 11145 ☎ 011 6 51-64-68, Fax. 011 6 45-97-20, E-mail info-cs@eca-e.com Web site: www.eca-e.com

BOLE SUBCITY, WOREDA 6, ADDIS ABABA, ETHIOPIA